UNIVERSITÀ POLITECNICA DELLE MARCHE

FACOLTÀ DI INGEGNERIA

Corso di Laurea Magistrale in Biomedical Engineering

HYPERSPECTRAL IMAGING SYSTEM IN FORENSIC SCIENCE: DEFINITION OF THE TEST BENCH AND AGE ESTIMATION OF BLOODSTAINS ON DIFFERENT SUBSTRATES

Relatore:
Prof. Lorenzo Scalise

Tesi di Laurea di:
Delia Iafelice

Correlatore:
Prof. Paolo Castellini

Matricola:
1096225

ANNO ACCADEMICO 2020/2021

ABSTRACT

In the last years hyperspectral imaging system has been used in different fields, and recently it has been taken in consideration as a potential tool for forensic science. Hyperspectral imaging system is both an imaging and spectroscopy technique and is considered to be useful in forensic science as it is a fast, portable, and non-destructive technique, able to maintain the integrity of the biological traces found at the crime scene. In general, several traces can be found at the crime scene; the most important is blood since several information can be obtained from it. In fact, visual inspection of the bloodstains gives information about the motion of the victims and the suspects, the DNA analysis performed on the stain is useful for the identification of the suspects, and the determination of the age of the bloodstains gives insight about the temporal aspect of the crime. Haemoglobin spectrum dominates the visible spectrum of a bloodstain, and it is the main blood chromophore. When haemoglobin is found outside the human body, i.e., in a bloodstain, it undergoes a series of degradation processes which lead to the formation of the haemoglobin derivatives. The changes in the haemoglobin and haemoglobin derivatives concentration lead to the colour change of the bloodstains, from red to dark brown, according to the fact that the derivatives are characterised by different absorption spectra. Consequently, the bloodstain spectrum changes over time, hence the temporal analysis of the bloodstain spectrum can be used for age estimation purposes since the temporal behaviour of the spectrum relates to the chemical changes occurring in the bloodstain. In this study, hyperspectral imaging system has been used to perform the temporal analysis of bloodstains deposited on different substrates to determine a set of temporal parameters related to the age of the stain. Moreover, since the characteristics of the illumination system affect the performance and reliability of the hyperspectral imaging system, the test bench has been defined to obtain the spectral data for the temporal analysis. Subsequently, the curves, expressing the relation between the age of the bloodstain on different substrates and the temporal parameters defined, have been determined. After the correction of the bloodstain spectra, which are influenced by the substrate colour and texture, via a Neural Network model, it has been possible to obtain a general curve for each defined temporal parameters with optimal RMSE and R^2 values which

could be used to perform the age estimation of the bloodstain when the substrate is not known.

INDEX

1. INTRODUCTION

Forensic science is the application of the methods of natural and physical sciences to the subject of criminal and civil law; in other words, it is the application of the scientific analysis in a legal context with the purpose of solving crimes. [1][2] Forensic science deals with the recognition, identification, individualization, and evaluation of evidence material, in a true crime casework. [3] With the aim of solving crimes or convicting the offender, the tools and the skills used by crime scene investigators and lab technicians are extremely important; moreover, due to the continuous scientific developments and to the advancement in technological equipment, forensic science is becoming a rapidly evolving speciality comprising many sciences and law. [4][2] Part of forensic science is the forensic engineering, that uses the concept of mechanical, chemical, civil and electric engineering tools for the reconstruction of crimes and for the determination of their causes. [1]

Many biological traces can be found in a crime scene, and each one of them is important since it could be a potential carrier of information for the investigation. The most common biological material found in a crime scene, and in general in a violent crime scene, is blood: it is an excellent information carrier and commonly it is analysed in many ambits, such as in forensic science, in toxicology and diagnostic. [5] The age determination of the bloodstain and the visual inspection of the bloodstain pattern (in terms of size and shape) are of important interest for the forensic work. [6] The determination of the age of the bloodstain is very important in order to determine the time in which the crime has been committed, also giving the possibility to verify if the bloodstain is related or not to the crime. [7] The visual inspection of the shape and the size of the bloodstains carries important information about the position and the motion of the suspects and the victims. [8] Moreover, other information can be obtained from the blood when it is subjected to another analysis: the DNA analysis; in fact, the suspect can be identified by means of the DNA analysis. However, the DNA analysis is extremely time consuming, and for this reason it is important to perform it only on real bloodstains, hence, not on blood-like substances. [6] For this reason, the first step to perform in a crime scene is blood identification. In fact, in this way it is possible to avoid waste of resources and time, performing the analyses and the examinations only on real bloodstains. One of the simplest methods that can be used to perform blood identification is

the visual inspection, but it is extremely difficult to carry out, since blood could be similar to other substances in terms of appearance and colour. [6] This is why, during the years several presumptive tests, capable to identify blood with respect other confusing substances, have been developed. [6] Presumptive blood identification tests are therefore used to prove the presence of blood in a stain, and most of them are based on the use of chemicals that in contact with blood change colour, fluoresce or luminesce. [9] Kastle-Mayer (KM), Leucmalachite Green (LMG), Benzidine and Luminol are examples of chemical based presumptive blood identification tests. [6] KM test is based on the use of phenolphthalein chemical that reacts with hydrogen peroxide in presence of haemoglobin, producing a bright pink colour; it has a high sensitivity, but false positive can occur with certain vegetables, excluding it from the application in a crime scene. [10] LMG test is also based on colour change occurring when it enters in contact with real bloodstains, but several experiments have demonstrated DNA damages; consequently, the samples, after the application of the LMG test, are no longer suitable for the DNA analysis. [10] Luminol is a more sensitive test compared to the KM one [6] and it is made up of a spray alkaline solution that produces a bluish luminescence in presence of blood; it requires a dark environment for its application. [6][10] However, detail loss can occur in case of excessive spraying and false positive have been observed. [10] In general, chemical presumptive blood identification tests are sensitive and fast, but require contact with samples, hence the samples are more exposed to destruction, and this is against the goal of forensic science which instead wants to maintain their integrity. [9][10] Moreover, the chemicals used to perform these tests can be also harmful for the users. [9] After the performing of the presumptive tests, confirmatory tests, including spectroscopic, chromatographic, microscopic, and crystal tests, are required; unfortunately, all these tests are characterized by samples preparation or based on the use of chemicals that can destroy the samples, going again against the goal of forensic science. [6] Therefore, forensic science is fascinated by non-destructive, non-contact, user-friendly and rapid techniques for blood detection and identification. [10] Different non-contact techniques have been investigated, like the spectroscopic techniques, as the Raman, the reflectance, and the infrared (IR) spectroscopies, as the attenuated total reflectance Fourier transform IR spectroscopy. [6] All these techniques focalize on the spectral information, but

the spatial information, in terms of location and distribution within the scene of the blood evidence, is completely lost. [6][7]

After the correct identification of the presence of the blood in a stain, it is possible to perform different analysis and to obtain different information from the blood, as reported before. Of important interest is the age determination of the blood, because, as briefly discussed before, it helps the investigators in the determination of when the crime has been committed. This is one of the fundamental aims of the forensic research. [11] Age estimation for bloodstains is defined as the time that has passed from the moment of its creation [5]; it may help the investigators to determine the temporal aspects of a crime [5], to verify the witnesses, to adjust the direction of the investigation [7], to reduce the pool of the suspect [8][12], and to understand if the stain is crime related or not.[7] Despite the potential of the age estimation of the bloodstain to determine the temporal features of a crime, it has not yet been used in forensic science; however, several techniques have been investigated. [12][13] Oxygen electrodes have been used to understand the effect that the time has on bloodstains: this technique is used to see the changes occurring to the oxy-haemoglobin - haemoglobin ratio. [11] Other methods for age determination include: the analysis of RNA degradation, spectroscopy methods, electron paramagnetic resonance and high-performance liquid chromatography. [7] Spectroscopic methods comprise the atomic force microscopy and the electron spin resonance spectroscopy; the former is used to explore the elasticity of bloodstains on glass slides through coagulation over time, while the latter sets up a connection between the electron paramagnetic resonance of the non-ferric heme species and the age. [11] The previous cited methods are not yet applied in forensic procedure, and the majority part of them requires sample preparation and needs to be executed in the laboratory [7], meaning that they do not offer the possibility of an analysis being performed at the crime scene. [14] Moreover, it is known that the colour of blood changes from red to brown over time, showing that optical methods could be used to measure bloodstains colour, hence they could be used for the estimation of the blood age, and this leads to the application of the reflectance spectroscopy. [11] However, the main disadvantage of spectroscopy is that the precise measurement of all the suspected bloodstains at the crime scene is time consuming [7], and more important, the spatial information, in terms of location and distribution within the scene of the blood evidence, is lost.

A solution for both the problems connected to the identification and the age estimation of blood could be represented by the hyperspectral imaging, which integrates conventional spectroscopy and imaging. [7] In fact, the hyperspectral imaging provides both the spectral and the spatial information of all the elements present in the field of view; in this way the spectral properties are recorded together with the information of their location in the scene. [7] Hyperspectral imaging is a fast and non-destructive technique; [5] moreover, the current hyperspectral imaging systems are also portable, thus they can be carried to the crime scene and used to analyse the traces in their original context, reducing the work of forensic laboratories and giving instant information to the investigators.[7] Hyperspectral imaging is a reflectance spectroscopy technique that provides the reflectance spectrum of each point of the analysed sample; the outcomes are given in the form of a *hyperspectral cube*, meaning that the data are three-dimensional, with two spatial dimensions and one spectral dimension. [5] Furthermore, being the hyperspectral imaging also an imaging system, where for imaging system it is intended a system able to create a picture or an image that represents the object under investigation [15], it also provides the image of the bloodstain, that is the spatial information. Originally, hyperspectral imaging was developed for remote sensing applications based on satellite imaging data of the Earth; since then, it has been used in different fields, like food science, pharmaceutical and medical diagnosis, and it is an emerging tool in the forensic practice. [16] In fact, identification of bloodstains can be done based on the spectral features of the blood, while the analysis of the temporal behaviour of the spectra can be used for age estimation purposes, because it is connected with the chemical changes occurring in blood when outside of the body. [16] In addiction, the spatial information provided by the hyperspectral camera gives the investigators the possibility to examine the shape and the size of the bloodstain together with its location and distribution within the scene, from which information about the position and the motion of the suspects and the victims can be retrieved. [8]

In the present study, the hyperspectral camera has been used to acquire the image of bloodstains deposited over different substrates, in order to perform the temporal analysis, in a qualitative and quantitative manner, according to the fact that the temporal analysis can be used for age estimation purposes since the temporal behaviour of the spectra is connected with chemical changes occurring in the bloodstain. [16] Moreover, the illumination system

is the most important part for the hyperspectral imaging system, since its performance and reliability depend on the characteristics (illumination system source, properties of the light, arrangement of the illumination system) of the illumination system chosen. [16] For this reason, the first thing that has been considered, has been the definition of the test bench to be used to get spectral data for the temporal analysis. Subsequently, after the definition of the test bench, the temporal analysis of the spectra has been performed. In the end, the aim of the present work is to estimate the age of the bloodstains on different substrates, by determining the relation existing between a set of temporal parameters, obtained performing the temporal analysis, and the age of the stain.

STATE OF THE ART

Over the years, several authors have investigated the use of hyperspectral imaging for the identification of bloodstains and, specifically, for age estimation purposes. Li et al. [17] have been the first to report the use of the visible hyperspectral imaging technique for the identification and age estimation of horse bloodstains, as testbed research. Age estimation has been performed by means of linear discriminant analysis, according to the fact that since the composition of blood changes over time, relative changes in the absorption spectra are found. [17] Testing and training dataset comes from the same stains thus the level of accuracy reaches high values, and therefore, applying the same approach to different stains lowers the level of the accuracy. [17] However, this study has demonstrated the feasibility of using hyperspectral imaging technique to perform age estimation of bloodstains in a non-destructive manner. [17] More recently, the same group research of Li et al. [14][18] have introduced a new method for the identification and the age estimation of bloodstains based on the Soret band absorption of haemoglobin, which differs from the previous mentioned method that instead considers the changes of the bloodstains spectra in the wavelength range from 442 nm to 585 nm. The new method has shown a higher sensitivity and specificity for detection and identification respect the previous cited method. [18] Moreover, for what concern the age estimation, the research group of Li et al. [14] have used visible wavelength hyperspectral imaging for the age estimation of bloodstains up to 30 days; after the spectral

pre-processing of the reflectance spectra coming from selected area of the hyperspectral image, a linear discriminant classification model has been applied, allowing the age estimation with an error of ± 0.27 days for the first seven days and an average error of ± 1.17 days up to 30 days. Furthermore, this is also the first study to report the age determination of fresh bloodstains, specifically the stains with less than one day old, with an error of ± 0.09 h. The research group of Li et al. [14] have performed the study under controlled condition for what concern the environmental variables (type of blood, substrate and sample preparation, thickness of the bloodstain, temperature, and humidity), and the results obtained for the age estimation are the most accurate for measurements performed between 0 to 30 days. Another study for the age estimation has been performed by Edelman et al. [7], that have derived from the visible reflectance spectra of the bloodstains the relative amount of oxyhaemoglobin, methaemoglobin and hemichrome. By means of the comparisons of the previous haemoglobin derivatives with a reference dataset, the age of bloodstains up to 200 days has been estimated with an absolute error increasing with the age and a median relative error of 13.4% the real age. Cadd et al. [11] have performed both the identification and the age estimation of blood-stained fingerprints, based on the features of the absorption spectrum of the haemoglobin between 400 nm and 680 nm. The stained-fingerprints have been analysed for over 30 days and false colour aging scales have been realized from a 30-day scale and a 24-hour scale, giving the possibility to realize a clear visual method for the age estimation. Finally, a total of nine blood-stained fingerprints of different ages, deposited on white ceramic tiles, have been distinguish using the 30-day false colour scale.

2. HYPERSPECTRAL IMAGING

Hyperspectral imaging provides three-dimensional dataset, containing both spatial and spectral information. [16] Furthermore, it is known that the optical properties of the sample and the incident light determine the interactions between sample and light; moreover, since hyperspectral imaging measures the interaction within light and sample, it can be used to characterize the sample itself. [16] This also underline the fact that to use a hyperspectral imaging system it is necessary the correct illumination of the sample. [16] For these reasons in the following section is reported briefly the description of the electromagnetic spectrum and the interaction between light and matter; furthermore, being hyperspectral imaging an imaging spectroscopy technique, a brief description of spectroscopy is done. Moreover, since hyperspectral imaging is a spectroscopy technique, it can be applied in different regions of the electromagnetic spectrum. [16] Finally, a brief review of the use of the hyperspectral imaging for forensic traces analysis is reported and an in deep descriptions of the hyperspectral imaging technique, the dataset along with the acquisition techniques, the hyperspectral system, and the calibration procedure, are going to be reported.

2.1 THE ELECTROMAGNETIC SPECTRUM AND THE INTERACTIONS BETWEEN LIGHT AND MATTER

Electromagnetic radiation, defined as the emission or the transfer of energy in the form of photons or electromagnetic waves, is a wave-like phenomenon and can be divided with respect to the wavelength, where for wavelength is intended the length of its waves. [19][20] It has sometimes as its synonym the term light and comprises the ultraviolet, the visible, the infrared, the X- and gamma-ray ranges and the radio range. [19] In the context of hyperspectral imaging techniques, and in general in the case of different methods based on the use of electromagnetic radiation, electromagnetic radiations are considered in terms of their wavelengths. The graphical representation of the electromagnetic radiations, organized with respect to their wavelengths, takes the name of electromagnetic spectrum. [19] The electromagnetic spectrum covers all the electromagnetic radiations that can be generated physically, from the shortest to the longest wavelength, from zero to near infinite. [19] The

electromagnetic spectrum can be divided in different regions and each of it correspond to a wavelength or a frequency range; however, there is not an exact division between the different regions, because there is a gradual transition from one region to the other. [19] Electromagnetic radiations comprise within 400 nm and 700 nm take the name of visible light, and they are the only wavelengths correlated with a sensory impression of a particular colour in human eyes. [19] The visible region of the electromagnetic spectrum is divided in three bands: blue band (400 nm-500 nm), green band (500 nm-600 nm) and red band (600 nm-700 nm). [20] The other wavebands are characterized by wavelengths that are not perceived by human eyes, and these are the X-rays, gamma-rays, and the ultraviolet radiation that present wavelengths shorter than the visible region, together with infrared radiation, micro-waves, and radio-waves, which instead present a wavelength longer than the visible radiations. [20] In Table 1 are reported all the wavebands with the relative name and the associated wavelength and frequency ranges. Figure 1 represents the electromagnetic spectrum with the different regions in which it is subdivided, and a detailed representation of the visible region of the spectrum.

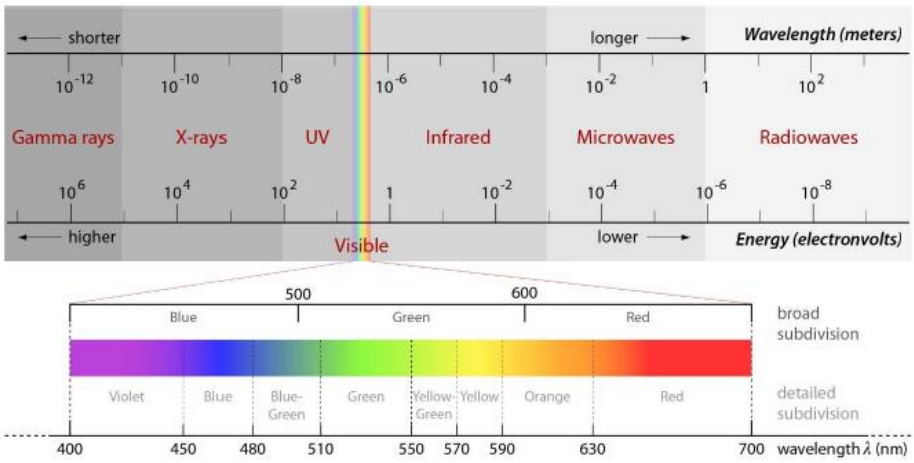

Figure 1 Electromagnetic spectrum; in red are represented the regions in which it is divided and the wavelength ranges. The visible region is represented in the bottom part of the figure; taken from [20].

Table 1 Regions of the electromagnetic spectrum, both the wavebands name, the wavelength and the frequency ranges are reported. Taken and adapted from [19]

Wavelength range (nm)	**Frequency range (s^{-1})**	**Type of electromagnetic radiation**
< 0.1	10^{20}-10^{23}	Gamma rays
0.1-10	10^{17}-10^{20}	X-rays
10-400	10^{15}-10^{17}	Ultraviolet
400-700	10^{14}-10^{15}	Visible
700-1 mm	10^{11}-10^{14}	Infrared
1 mm-1 cm	10^{10}-10^{11}	Microwaves
1 cm-100 km	10^{3}-10^{10}	Radio waves

It is important to point out that the only thing that changes between electromagnetic radiations in the different regions of the spectrum is the wavelength; this means that when light interacts with matter, the phenomena occurring will depend on the relationship between the wavelength of light and the physical size of the matter itself. [19] In general, three different phenomena can occur when light is incident on a material: part of the light will be reflected by the material, part could be transmitted through the material and part will be absorbed by the material. [21] Moreover, the degrees of which these phenomena will take place depend also on the nature of the material: in opaque materials no transmission of lights occurs, while for translucent material both transmission, absorption and reflection of light occurs. [21] More in detail, when light interacts with a sample, the first interaction occurring is on the surface of the sample, where part of the light is reflected. [16] In general, there are two ways in which light can be reflected from a surface: specular (or regular) reflection and diffuse reflection. [22] Specular reflection occurs when light is incident on smooth, polished surfaces, like mirrors, where the surface will reflect the light with the same angle of the incident light; on the contrary, diffuse reflection occurs in case of mat or dull surfaces, as

powders, or more in general in case of not smooth surfaces, where the surface will reflect the light with an angle independent from the angle of the incident light. [22][23] The specular reflected light contains no or little information about the internal part of the medium and it is controlled by the difference of the refraction index between the two media. [16] Figure 2 shows the two different reflections that can occur when light is incident on a material.

Figure 2 The two-reflection mechanisms occurring when light is incident on a material. Taken from [24].

Moreover, before entering the medium and being transmitted, light can be absorbed or scattered. Scattering occurs when light interacts with the structures found in the sample, causing a variation of the direction of propagation of the incident light. [16] The changing of the direction of propagation depends on several factors, including the wavelength of the incident light, the dimension of the particles and the differences of the index of refraction. [16] Scattering presents different names, with respect the changes of the direction of propagation; elastic scattering occurs when light is scattered at the same wavelength of the incident light, inelastic scattering, or *Raman scattering*, occurs when the wavelength shifts occurring correspond to the vibrational states of the molecules in the sample. [16] For what concern the absorption, the absorption occurs when the incident light is absorbed by the matter and converted into energy. [25] In details, the electrons in an atom vibrate with a specific frequency, known as *natural frequency*, and in the case in which matter is hit by a wave whose frequency is the same as the frequency of vibration of the electrons, the electron will absorb the energy converting it into vibrational motion, and it will be promoted to a

higher energy level, and the electron will be in the so called *exited state*. [25] Figure 3 represents the promoting of the electron to a high energy level, in case of light energy (photon) absorption. Furthermore, knowing that the properties of absorption of the matter depend on the wavelength of the incident light, it is possible to say that the absorption occurring in the visible wavebands corresponds to the electronic state of the molecule, while the one occurring in the near-infrared and infrared are determined by the vibrational modes. [16] Thus, when absorption occurs, light energy is absorbed and in general, as the electron falls back into its original energy level, known as the *ground state*, it releases a packet of energy, called *photon*. [25] The energy can be hence released in the form of a radiation, which can be heat or photoluminescence, or can be transferred to another molecule. [16][21] Finally, starting from the knowledge that hyperspectral imaging system measures the interaction between light and matter, it is hence possible to use the hyperspectral imaging system to measure the spectral absorption and the induced photoluminescence, if present, in order then to identify the chemical contents of the sample under study. [16] Figure 4 represents the different ways in which light can interact with a specimen.

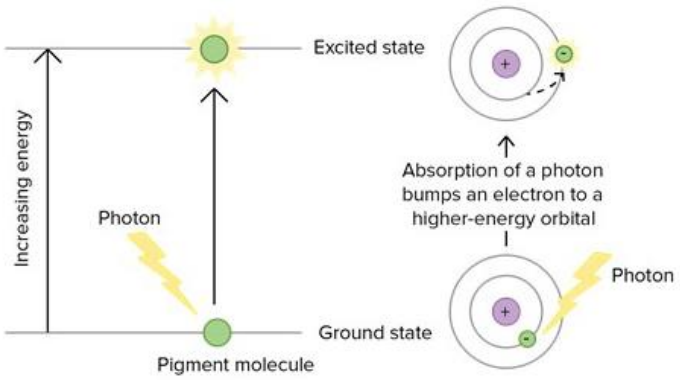

Figure 3 Absorption of incident light: the electron absorbs the energy, being promoted to a high energy level. Taken from [15].

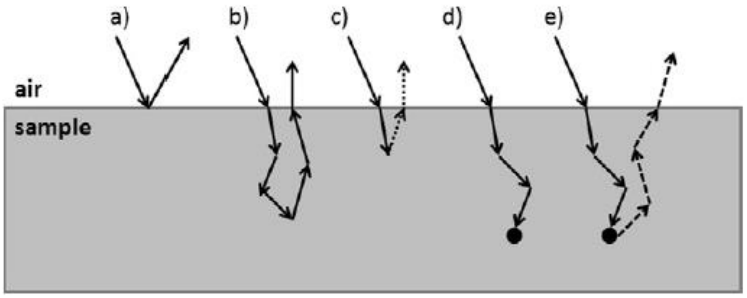

Figure 4 Interaction of light with matter: a) specular reflection, b) elastic scattering followed by diffuse reflection, c) inelastic scattering, d) absorption, e) absorption followed by photoluminescence emission; taken from [16].

2.2 SPECTROSCOPY

The interaction between electromagnetic waves, i.e., light, and substances, is a matter of study of spectroscopy. [26] As already said in the previous section, when light is incident on an object, various phenomena occur, for example, some of the light is reflected, and some is absorbed by the matter; moreover, a part of the absorbed light is subsequently emitted as light of a different colour or of a different wavelength. [26] Hence, spectroscopy is the science that seeks to determine what type of energy and how much incident light is absorbed by the substance under study, along with what type of energy and how much of it will subsequently be re-emitted by the substance. [26] What spectroscopy provides are acquisitions, which takes the name of *spectra*, from which relevant information about the atomic and molecular structure of the substance are retrieved. [26] In this way, these spectra provide the so-called *fingerprints* that represent in a uniquely way the different substances, thus allowing to perfectly distinguish one substance from another. [26] By means of a spectroscope, which is the instrument used for the spectral analysis of the light emitted by a source [27], it is hence possible to characterize a material, determining the type of elements contained and the proportions of them. [26] Furthermore, it is possible to perform not only the identification of the elements that make up a material, the so called spectrochemical or elements analysis, but information about the constituents of these elements, in terms of electrons and atomic nuclei, atoms and molecules, can be also obtained; this type of spectroscopy analysis is referred to as atomic or molecular spectroscopy. [26] In general,

there are two types of spectra that can be considered: the continuous and the discrete spectra. [28] The continuous spectra are characterized by the light that is a continuous set of energies, i.e., colors, and they are generated by solid objects or dense gases, such as stars, light bulbs, electric stove filaments, which emit heat due to light production. [28] The spectrum looks continuous because these sources generate light over a wide spectrum of wavelengths. [28] The discrete spectra, instead, are characterized by dark or bright bands of light at specific energies and they originate from the atom. [28] Two types of discrete spectra are of important interest for spectroscopy: the emission spectrum, the spectrum with bright bands, and the absorption spectrum, the spectrum with dark bands. [28] Moreover, the light emitted by a radiation source generates the emission spectrum, while the light that is partially absorbed by a medium generates the absorption spectrum. [29] In detail, the emission spectrum for a substance occurs when the substance receives energy from an external source, hence it absorbs energy exciting the atoms, which are raised to a higher energy level, then emitting a characteristic amount of energy as the atoms return to the previous energy level. [29] The absorption spectrum, instead, occurs when light is incident on a material and part of the wavelengths of the light are absorbed by means of internal energy excitations. [29] Figure 5 reports the different spectra previously described together with the sources from which the spectra are obtained.

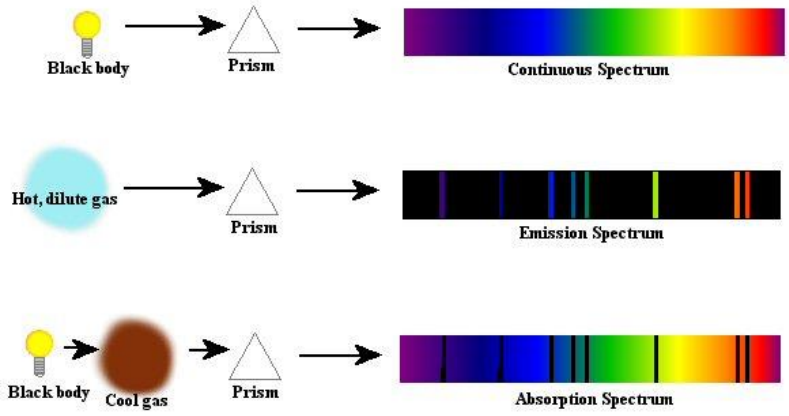

Figure 5 Different spectra and sources of generation: on the upper part of the image is represented the continuous spectrum, in the central part is represented the emission spectrum, in the bottom part is represented the absorption spectrum. Taken from [28].

Considering the absorption spectrum, which represents the spectrum obtained when part of the light is absorbed by the material, it is hence possible to introduce and define the absorbance spectroscopy. Absorbance spectroscopy is a type of molecular spectroscopy that identifies and quantifies specific substances exploiting the wavelength dependent absorption characteristics of the materials. [30] An example of absorption spectrum is reported in Figure 6. The absorption spectra are characterized by peaks that take the name of absorption bands or lines. [26]

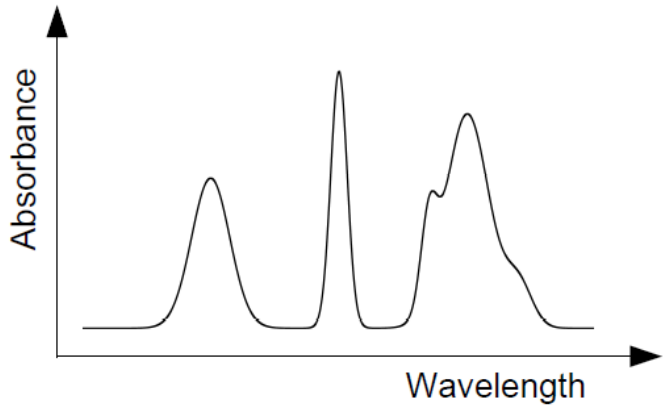

Figure 6 Example of absorption spectrum; on the x axis there is the wavelength, while on the y axis there is the absorbance. Taken from [26].

In consideration of the fact that hyperspectral imaging is a reflection spectroscopy technique [5], it is therefore necessary to introduce and define the reflectance spectrum and the reflection spectroscopy technique. The collection and the analysis of the reflected electromagnetic radiation as a function of wavelength is referred to as the reflectance spectrum. [22] The reflectance spectra are characterised by curves with pronounced downward deflections that denote the wavelength range in which the material has absorbed the incident light; these deflections are commonly referred to as absorption bands. [31] Also for the reflection, and specifically for the diffuse reflection, since the specular reflected light contains no to little information about the internal part of a medium, as already mentioned above, and it is not of interest for the aim of this work, it is hence possible to introduce and define the diffuse reflectance spectroscopy. Diffuse reflectance spectroscopy, also known as *elastic scattering spectroscopy*, is a spectroscopy technique that provides as an outcome the

reflectance spectrum. [32] Diffuse reflectance spectroscopy is a spectroscopy technique able to find out the regions of absorption of a sample under study, providing information about the energy, the width, and the intensity of the absorption regions. [33] In the diffuse reflectance spectroscopy, the incident light hit the sample, where it is reflected, scattered, and then transmitted; the detector recollects the back reflected, diffusely scattered light, where some of which has been absorbed by the sample itself. [24] As a consequence, the reflectance spectra obtained are made up of two different mechanisms: absorption and scattering. [32] Furthermore, the spectra obtained provide information about the structure of the medium and the optical properties of it. [32] Hence, in the case of diffuse reflectance spectroscopy there will be a combination of reflection, refraction, scattering and absorption of the incident light, since the samples used for reflectance spectroscopy are both scatterers and absorbers of electromagnetic radiations. [22]

2.3 THE LAMBERT-BEER LAW

The Lambert-Beer law is the fundamental law of spectroscopy, and it relates the attenuation of the light through a medium with the properties of the medium itself. [34] The absorbance of the substance is related to the transmittance, but also to the incident and transmitted intensities by means of the following equation, Equation 1:

$$A = -log_{10}\frac{I_0}{I} = log_{10}\frac{1}{T} \quad (1)$$

where A is the absorbance, T the transmittance, I_0 the incident intensity and I is the transmitted intensity. [34] Furthermore, it is important to underline that absorption represents the physical process, whereas absorbance is a quantity without unit that represents how much light is absorbed by the medium taken in consideration. [26] Considering now a solution, the Lambert-Beer law states that there is a linear relationship between the absorbance, the concentration, and the molar absorbance coefficient of a solution. [34] The previous mentioned linear relationship is represented in the following equation, Equation 2:

$$A = \varepsilon c l \quad (2)$$

where A is the absorbance, ε is the molar absorption, c is the molar concentration and l is the optical path length. Equation 2 is useful in the case in which it is important to determine the concentration of a solute in a solution, knowing the optical property of it. Of important interest is the fact that in the case of diffuse spectroscopy it is possible to approximate the Lambert-Beer law, specifically Equation 1; with this approximation it is possible to obtain the absorbance of the medium starting from the knowledge of the reflectance. In fact, most of the reflectance spectra is converted into apparent absorbance before performing other analysis, such as the statistical one. [22] This means that the Lambert-Beer law is still valid in case of the diffuse reflectance spectroscopy, specifically the one performed in the near-infrared waveband. [22] The approximation of the Lambert-Beer law for the diffuse reflectance spectroscopy is reported in the following equation, Equation 3:

$$A = log_{10} \frac{1}{R} \tag{3}$$

where A is again the absorbance and R is the reflectance, which is obtained as the ratio between the reflected light and the incident one. [31] Of course, since the Lambert-Beer law assumes that the reflectance and the scattering of the radiation is not significant, the use of this approximation results as a contradiction. [22] Nevertheless, it has been seen that the use of the Equation 3 to obtain the absorbance values works for quantitative interpretation of the data. [22]

2.4 HYPERSPECTRAL IMAGING IN FORENSIC SCIENCE

Hyperspectral imaging originates from remote sensing, and it was originally exploited for different purposes by NASA. [35] Nowadays, this technique has been applied in different areas and for different aims, like archaeology and art conservation, vegetation and water resource, food quality control, safety control, for example camouflage and plastic detection provides information about the presence of enemies' camp, medicine, for example it can help in the early detection of a disease, or it can be use in the identification of abnormal or diseased tissue, geology, for the searching of oil fields, and forensic science, which is the area on which this work has been focused. [35] [36] As previous mentioned, hyperspectral

imaging combines conventional imaging and spectroscopy, and in particular for the forensic applications, it allows to perform fast, non-invasive, and in-situ measurements, thus allowing the investigators to perform the analysis directly at the crime scene. [36] The spectral information is useful for identification, quantification, or age estimation purposes, giving information about the chemical composition of the sample under study, while the chance of viewing contemporaneously the spectral and the spatial information is useful in comparative research. [16] Furthermore, the use of the hyperspectral imaging system may reduce the workload of the laboratories, thus reducing the time necessary to link a suspect to a crime. [36] In forensic applications, hyperspectral imaging has been used to perform analyses on different traces of forensic interest other than bloodstains, including analysis of finger marks, drugs, hair, dentin, bruises, condoms and so on. [16] In forensic application, finger marks are principally detected, therefore the purpose of finger marks detection is to create contrast between the details of the finger marks and the background on which they are found. [16] Specifically, finger marks are a mixture of eccrine deposits from the finger and sebaceous deposits that are formed when the hands touch any part of the body, such as the face. [16] Moreover, the number of sebaceous deposits increases with the ageing while the chemistry of the finger marks changes among the subjects. [16] Several authors have studied the application of hyperspectral imaging for the detection and the enhancement of untreated finger marks as an alternative method respect the classical ones, which all involve the use of chemicals to enhance the contrast of the finger mark respect the background. [16] Bartick et al. [37] have been the first to apply near-infrared and infra-red hyperspectral imaging in the field of latent finger marks detection, successfully identifying finger marks present on aluminium coated microscope slides, followed then by Crane et al. [38] that have used infra-red hyperspectral imaging to detect unprocessed finger marks placed on different substrates, divided into porous and non-porous substrates. [16] Exline et al. [39] have compared the ability of hyperspectral imaging in the enhancement of contrast of treated finger marks with the traditional methods. [16] In general, it is not possible to obtain acceptable finger marks images using visible hyperspectral imaging when the finger marks are deposited on coloured, or patterned background, because in this situation there is a high influence of the background; [16] this problem can be solved using the near-infrared hyperspectral imaging, as demonstrated by Maynard et al. [40][16] Finally, according to the fact that the classical

methods used to detect finger marks are destructive and, since the finger marks could be mixed with different exogenous substances, such as abuse drugs, explosives traces and gunshot residue, the use of hyperspectral imaging may represent a solution for this problem [16]. In fact, when these substances are found in the finger marks of an individual, they can be directly related to the suspect. [16] Several authors have explored this area, like Grant et al. [41] that have used infrared hyperspectral imaging to identify microscopic particles of different materials present in the latent finger marks of volunteers. [16] Hyperspectral imaging has been also used in the determination of the presence of drug abuse in hair; [16] the first in doing this were Kalasinsky et al. [42]. Payne et al. [43] have demonstrated the possibility to differentiate blood with the one containing bilirubin using hyperspectral imaging; this is important specifically in the case of bruises analysis. [16] In fact, bruises, which gives important information in case of domestic abuse, is formed by blood, which presents haemoglobin that over time is degraded into different products, such as bilirubin, which present a spectrum with characteristic spectral features. [16] In the end, hyperspectral imaging could be applied for different purposes in forensic analysis, demonstrating to be an extremely versatile tool, which could be involved in the routinely analysis of forensic traces due to the advantages that could bring.

2.5 HYPERSPECTRAL IMAGING: DESCRIPTION OF THE TECHNIQUE

Hyperspectral imaging combines conventional imaging and spectroscopy, and the three-dimensional obtained data are referred to as *hyperspectral cube*. Hyperspectral imaging is a reflection spectroscopy technique, able to record not only the reflectance spectrum for each point of the sample under analysis, but also the transmission, the photoluminescence, or the Raman scattering, with a spectral resolution that resample the one of miniature spectrograph. [5][16] Furthermore, since it is a spectroscopy technique, it can be applied in different regions of the electromagnetic spectrum, like the ultraviolet, the visible, the near-infrared or the mid-infrared, and the resolution can be adapted to the different application, and it varies from microscopic to landscape. [16] Depending on the region of the electromagnetic

spectrum, different causes generate the spectral features found in the spectra. In the visible and ultraviolet wavebands, the spectral features are produced by electronic vibrational resonances, whereas in the infrared wavebands, the molecular vibrational resonances are responsible of the spectral features. [36] Moreover, hyperspectral imaging system operating in the visible/near-infrared wavebands, that ranges from 400 nm to 1000 nm, are useful in the identification of materials or gases such as atmospheric aerosols, vegetation, oxygen, and iron oxides, since they present optimal spectral features in this range. [36] Finally, the reflectance spectra obtained are the most flexible since they have been corrected for the illumination. [36]

2.5.1 HYPERSPECTRAL CUBE

As already mentioned, the data set obtained from the hyperspectral imaging system take the name of *hyperspectral cube*, and are three-dimensional data, containing two spatial dimension (x, y) and one wavelength dimension (λ). [16] The hyperspectral cube supplies images for each wavelength (λ_i), and from each individual pixel (x_j, y_k) is possible to obtain a spectrum. [16] Since the instruments can acquire two dimensions at time, it is not possible to have information in all the three dimensions of the cube simultaneously; for this reason, temporal scanning is required to make up the three-dimensional cube by piling in sequence the two-dimensional data. [16] Figure 7 represent the hyperspectral cube for a bloodstain.

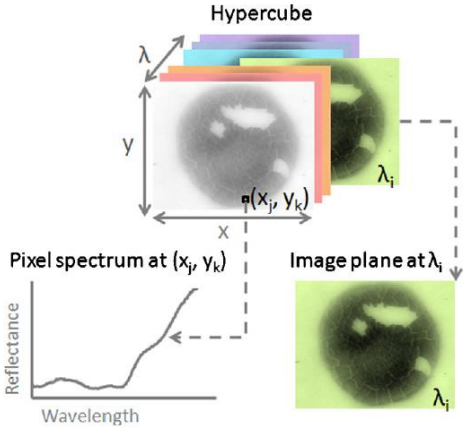

Figure 7 Hyperspectral cube of a bloodstain, with two spatial (x, y) and one wavelength (λ) dimension; taken from [16].

2.5.2 HYPERSPECTRAL CUBE ACQUISITION TECHNIQUES

Three different acquisition techniques for the hyperspectral cube exist, and are known as point scanning or *whiskbroom*, line scanning or *pushbroom*, and area scanning or *staredown*. [16] Furthermore, the assigned names derived from the hardware methodology used for the acquisition of the hyperspectral cube. [16] Figure 8 represents the three different acquisition techniques, previously mentioned.

Taken in consideration the point scanning, or *whiskbroom*, for each single point present in the field of view of the camera the complete spectrum is acquired. [16] In the objective lens, enters the light that is coming from the single point, and subsequently, the spectrometer separates the light into different wavelengths while a linear array detects it. [16] After the acquisition of the entire spectrum of a single point, with the same procedure, the spectrum of another point can be acquired. [16] In order to obtain a complete hyperspectral cube, the scanning must be performed in both the spatial directions.

For what concern the line scan, or the *pushbroom*, a simultaneous acquisition of the spectra of all the pixels contained in one image line is done. [16] In this scanning technique, light is dispersed on a two-dimensional charged coupled device detector, known as CCD detector; thus, a two-dimensional data matrix is acquired. [16] Hence, a two-dimensional data matrix is initially obtained. It is a two-dimensional matrix because it is made up of the spectral dimension and a spatial dimension; subsequently, in order to obtain the second spatial dimension of the cube, and therefore the complete cube, it is necessary to scan the sample surface perpendicular to the imaging line. [16] In this way, a relative movement between the sample and the camera is required; this could be achieved by moving the sample and keeping the camera in a fixed position, or vice versa, by moving the camera and keeping the sample in a fixed position. [16] The last scanning techniques, the area scanning or the or *staredown*, is also based on the acquisition of a two-dimensional data matrix, but contrary to the line scanning technique, the two-dimensional matrix is made up of two spatial dimensions, representing a more conventional image. [16] Then, to get the complete cube, thus, to get the spectral dimension, a sequence of these images is collected one wavelength band at time.

[16] In this scanning technique, a tuneable filter is typically used to modulate the wavelength of the incoming light. [16]

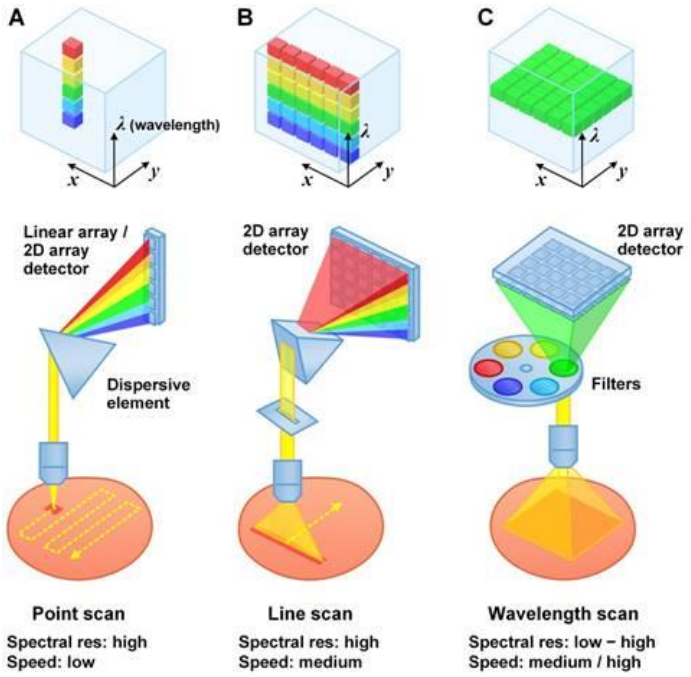

Figure 8 Acquisition techniques of the hyperspectral cube; a) the point scanning system, b) the line scanning system, c) the area scanning or the wavelength scanning system. Taken from [44].

2.6 HYPERSPECTRAL IMAGING: DESCRIPTION OF THE SYSTEM

The classical hyperspectral imaging system is formed by the objective lens, the wavelength modulator, the detector, the illumination, and the acquisition system. [16] Figure 9 is the schematic representation of the hyperspectral imaging system with all the elements listed before and the hyperspectral cube of the specimen. Since it is also an imaging system, different objective lenses can be used to get the desired spatial resolution, that for forensic applications could range from microscopic to landscape. [16] When dealing with a hyperspectral imaging system, it is important to pay attention to the choice of the illumination system source (halogen lamps, light emitting diode (LED), laser), the choice of the properties of the light (broadband or monochromatic, specular or diffuse), and the

arrangement of the illumination system. [16] In fact, all the choices mentioned above are crucial for a hyperspectral imaging system as they affect its performance and reliability. [16] Halogen lamps are broadband illumination sources commonly used in hyperspectral applications; they can be used to directly illuminate the sample or can be supplied by means of an optic fibre. [16] LED technology is of particular interest for the hyperspectral system, being inexpensive, robust, and reliable and, moreover, it is available on the market as a narrowband or a broadband light generator. [16] Laser could be suitable as light source for photoluminescence or Raman applications, being a powerful, directional, monochromatic light source. [16] Finally, the raw data in the hypercube are a consequence not only of the chemical composition of the sample, but also of the illumination intensity, the detector sensitivity, and the transmission of the optic, and for this reason a suitable calibration procedure is required. [16]

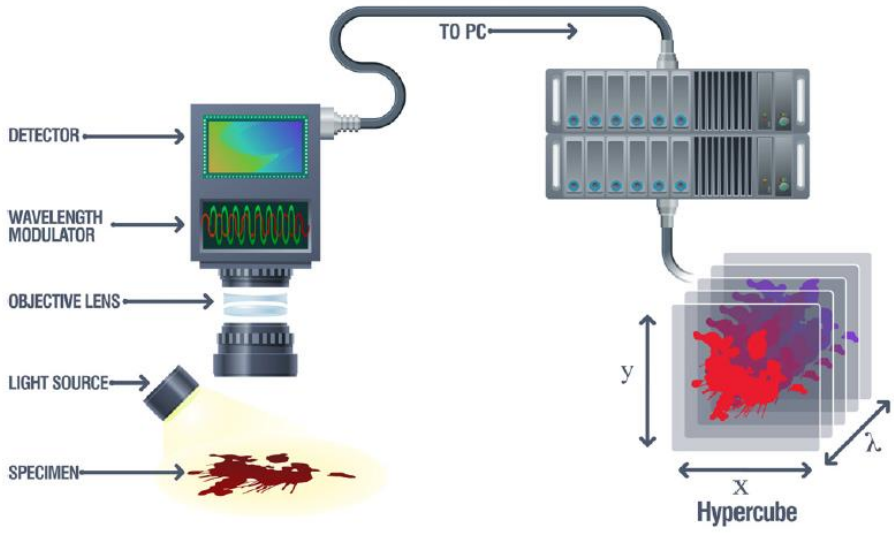

Figure 9 Schematic representation of the hyperspectral imaging system; taken from [16].

2.7 CALIBRATION PROCEDURE

Calibration procedure is required to compensate the fact that the raw data contained in the hyperspectral cube are the consequences not only of the chemical composition of the sample, but also of the illumination intensity, the detector sensitivity, and the optic transmission. [16]

Both spectral and spatial calibration procedures are required since the factors' influence is a function of the wavelength but could also show spatial variations. [16] Calibration procedure performed for reflectance acquisition is characterised by the acquisition of the dark response of the system, measured covering the lens, and the acquisition of the response of a high reflectance and uniform reference. [16] Calibration should be performed daily, because small changes in electrical power source, illumination, detector response and system alignment could evolve in variations in the acquired response. [16]

3. BLOOD

Blood, formed by a liquid and a cellular component, is characterized by the haemoglobin, a protein that gives blood the role of oxygen carrier. Haemoglobin reflectance spectrum dominates the visible spectrum of a bloodstain [11], and the changes occurring over time in haemoglobin are reflected in the changes occurring in the spectrum. For these reasons, in this section, after a summary of the main usages of blood in forensic practice, and a brief description of the anatomy and physiology of blood, an in deep description of the chemical changes occurring to the blood when is outside of the body, together with the spectral features of the blood, are reported.

3.1 BLOOD IN FORENSIC PRACTICE

In forensic practice, blood is the common biological evidence that is found in a crime scene, specifically in case of a violent crime scene. [11] It is an important information carrier [5], analysed for different purposes: the pattern of the bloodstains (in terms of size and shape) gives insight to the investigators about the motion of suspects and victims [8], the knowledge of time of bleeding (age estimation of the blood) helps the investigators to determine the moments in which the crime has been committed or to determine if the bloodstains are crime related or not [7], DNA analysis, performed on the bloodstains, helps the investigators in the identification of the suspects. [6] The first step when dealing with blood in forensic practice is blood identification, so see if the stains contain blood or not, in order then to perform the analysis on only the real bloodstains, thus reducing waste of time and resources. The identification is performed first using chemical based presumptive blood identification tests, followed then by confirmatory tests; all these tests have been already described in the first section of this work. In general, these tests are based on contact methods with blood, or require sample preparation and laboratory works, so they tend to destroy the biological samples, making them not suitable for further analysis. For these reasons, forensic science has been fascinated by new techniques, specifically hyperspectral imaging technique, which integrates conventional spectroscopy and imaging [7], thus providing both the spectral and the spatial information of all the elements present in the field of view. [7] Hyperspectral imaging technique can be used not only for the identification of blood in a stain but can be

also used for the age estimation of the bloodstains, that is the aim of the current work, based on the analysis of the temporal behaviour of the spectra of the blood, that highlights the chemical changes occurring in blood outside of the body. [16]

3.2 ANATOMY AND PHYSIOLOGY OF BLOOD

Blood is formed by a liquid portion, called plasma, and by a cellular component, which includes erythrocytes, leukocytes, and platelets (Figure 10). [45] In a normal healthy adult, the total volume of blood is approximately 5.5 litres, consisting, approximately, of 3 litres of plasma, 2.5 litres of erythrocytes, also including leukocytes and platelets. [45] The elements of blood present different densities, so when centrifuged or left bare in a tube, the different elements are separated based on their density: the erythrocytes are the denser elements, so they are found on the bottom of the tube, plasma is the least dense, so it remains on the top; between the two layers is found a thin layer, called the *buffy coat*, containing leukocytes and platelets. [45] The subdivision of blood elements, according to their densities, is shown in Figure 11.

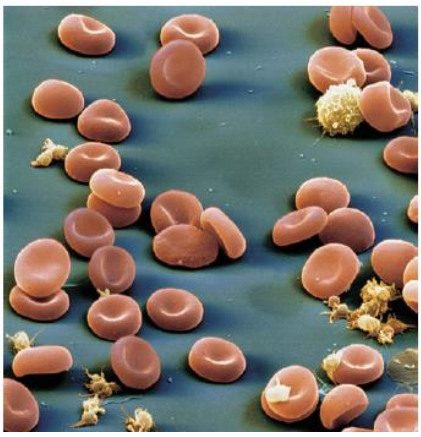

Figure 10 Cellular components of blood, taken from [45].

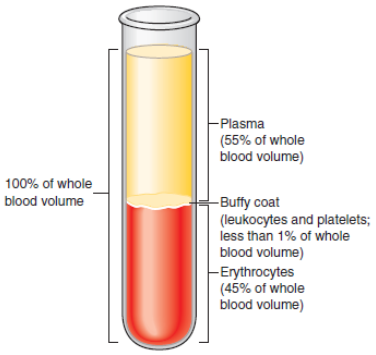

Figure 11 Distribution of the blood components according to their density in a tube, taken form [45].

In the following sections is given an in deep description of blood components, with special attention to the erythrocytes and the proteins contained in erythrocytes' plasma.

3.2.1 PLASMA

Plasma is the liquid portion of the blood, formed by an aqueous solution containing different solutes, which include proteins (categorized into albumins, globulins, and fibrinogen), nutrients (glucose, lipids, and amino acids), metabolic waste product (like urea and lactic acid), gases (oxygen, carbon dioxide and others) and electrolytes (like sodium and potassium). [45] Plasma, without fibrinogen and other clotting proteins, takes the name of serum. [45]

3.2.2 LEUKOCYTES

Leukocytes, also known as *white blood cells*, are nucleated cells and possess the normal cellular machinery, thus being the only fully functional cell in blood. [45] Leukocytes are normally found outside the bloodstream, specifically in other body tissues; their presence outside the blood vessels is due their mobility that allows them to squeeze through pores present in the capillaries and to move into other tissues. [45] This ability is related to their function that is to protect the organism against invading organism and/or other foreign materials. [45]

3.2.3 PLATELETS

Platelets are cell fragments without colour, arising from large bone-marrow cells; they are smaller than erythrocytes, and they are provided of smooth endoplasmic reticulum, cytoplasm granules, and mitochondria, but they are not provided of the nucleus. [45] Platelets are important in the formation of blood clots because they trigger the sequence of events that leads to blood clots formation. [45]

3.2.4 ERYTHROCYTES

Erythrocytes, or *red blood cells*, are the most abundant cells in blood, and they are characterized by a disk like shape, with a diameter of approximately 7.5 micrometres and a thickness of approximately 2 micrometres. [45] Figure 12 shows the typical disk shape of a red blood cell. The role of erythrocytes in the human body is oxygen and carbon dioxide transport; this function is important to carry oxygen from lungs to cells and, vice versa, to carry carbon dioxide from cells to lungs, in order then to eliminate carbon dioxide from the body. [45] Erythrocytes' plasma contains two proteins that makes high the capacity of erythrocytes to carry oxygen and carbon dioxide; these proteins are haemoglobin, which binds to oxygen and carbon dioxide, and carbonic anhydrase, which only transport carbon dioxide. [45]

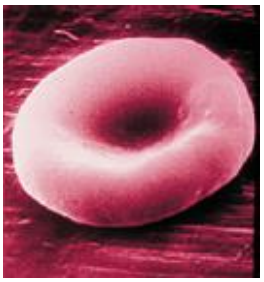

Figure 12 Normal red blood cell, taken from [45].

3.2.4.1 HAEMOGLOBIN

Haemoglobin has the role of transporting oxygen from lungs to the tissues and, vice versa, to transport carbon dioxide from tissue to lungs to facilitate the elimination of carbon

dioxide; for this reason, it can be considered a two-way respiratory carrier. [46] The affinity of haemoglobin to oxygen and carbon dioxide and to other compounds (organic phosphates, hydrogen, and chloride ions) depends on which part of the circulatory circuit is. [46] In the arterial circulation, haemoglobin shows high affinity for oxygen while low affinity for carbon dioxide and the other compounds, while in the venous circulation it shows a low affinity for oxygen while a high affinity for carbon dioxide and the other compounds. [46] Haemoglobin is formed by four polypeptide chains, present in two different types: two alpha chains and two beta chains; [45] moreover, the two polypeptide chains type have the same length but differ in the sequence of the amino-acids. [46] Each chain is comprised of an iron-containing structure with the form of a ring that takes the name of heme group; [45] moreover, the heme group represents the prosthetic group of the haemoglobin. [46] Haemoglobin represents the main blood chromophore, being the 97% of dry blood content; [47] specifically, the red colour is given by the iron present in the ferrous form in the heme group, that gives the typical red colour to the erythrocytes and thus to the whole blood. [45] Furthermore, iron represents the binding site for the oxygen; hence, since each haemoglobin contains four heme groups, where each heme group has an iron, haemoglobin can bind to a total of four oxygens. [45] Figure 13a represents the haemoglobin molecule with the four polypeptide chains and the four heme groups. Figure 13b represents the chemical structure of the heme group containing iron. The amino-acids, within the polypeptide chain, represent the binding sites for the carbon dioxide, where it binds reversible; nevertheless, carbon dioxide is transported less than oxygen by the haemoglobin. [45]

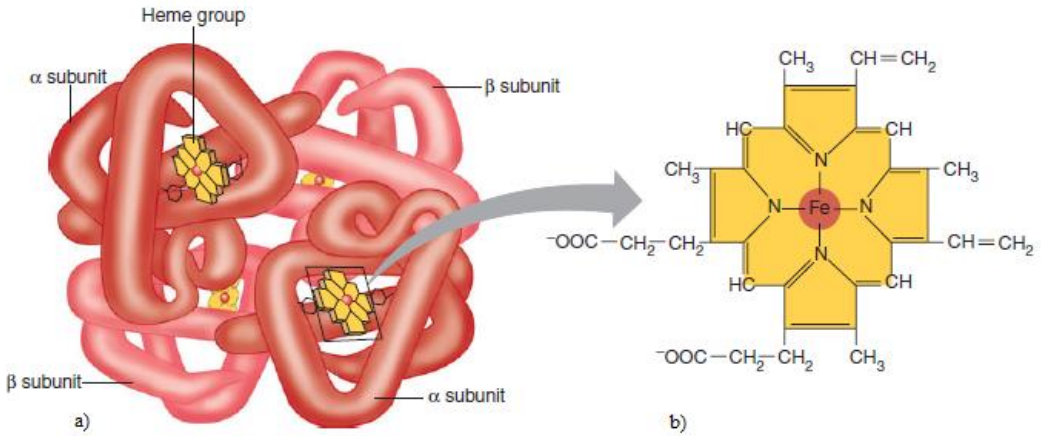

Figure 13 Haemoglobin structure. a) Is the haemoglobin structure, b) is the chemical structure of the heme group, taken from [45].

3.2.4.2 HAEMOGLOBIN BEHAVIOUR INSIDE AND OUTSIDE THE HUMAN BODY

Inside and outside the human body, haemoglobin can appear in different forms, called haemoglobin derivatives. [13] The behaviour of haemoglobin inside and outside the body changes drastically; since in forensic practice blood is found in the environment, so outside the body, it is important to understand the changes occurring to haemoglobin outside the body, because these changes are reflected in the spectral feature of blood over time. Inside a healthy human body, haemoglobin is found in two forms: de-oxyhaemoglobin, the one without oxygen, and oxy-haemoglobin, the one saturated with oxygen; a small part of the oxy-haemoglobin, indicatively the 1% of the oxy-haemoglobin, is auto-oxidized into met-haemoglobin, that is reduced back into deoxy-haemoglobin by a reductase protein, the cytochrome b5. [13] Outside the human body, so in the case of bloodstains, blood will completely saturate into oxy-haemoglobin when it meets oxygen; moreover, due to the decreasing availability of cytochrome b5, the conversion of oxy-haemoglobin into met-haemoglobin will be no more reversed. [13] Once the auto-oxidation of haemoglobin into met-haemoglobin has been taken, met-haemoglobin will denature into hemichrome, which is formed through changes of the conformation of the protein. [13] The conversion of haemoglobin, outside the body, into oxy-haemoglobin, met-haemoglobin and then into hemichrome, can be observed by a colour change of the blood, from deep red into dark brown; the colour change of the stain is explained by the fact that the absorption spectra of the haemoglobin derivatives are different from each other. [13] Figure 14 summarised the changes occurring to haemoglobin when outside or inside the human body.

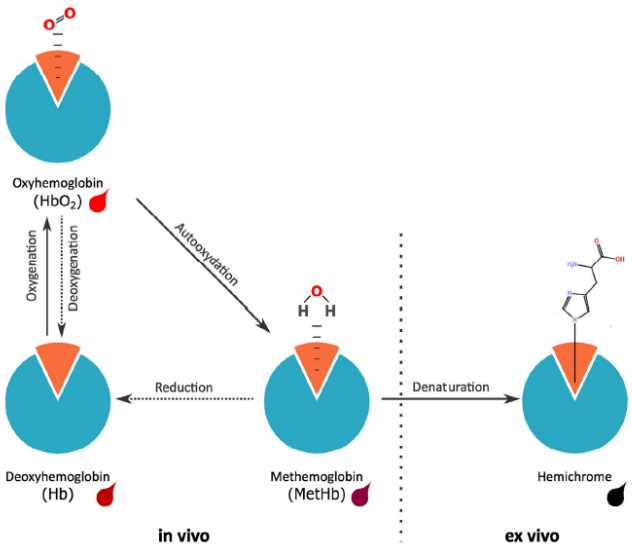

Figure 14 Schematic representation of haemoglobin behaviour inside the human body (in vivo) and outside the human body (ex vivo), taken from [8].

3.3 HAEMOGLOBIN AND HEMOGLOBIN DERIVATIVES SPECTRA

Haemoglobin reflectance spectrum dominates the visible region of bloodstains spectra. [11] Moreover, the changes occurring to the colour of the stains are the result of the variation in the haemoglobin concentration and its derivative (oxy-haemoglobin, met-haemoglobin and hemichrome) due to the previous described processes. [8] Since the variation of the concentration of haemoglobin and its derivative are time dependant, blood colour gives information about the age of the stain. [8] As previously mentioned, the different absorption spectra of the haemoglobin and its derivative determine the colour change of the stain. All the haemoglobin derivatives show a distinctive peak between 400 nm and 425 nm, the so called Soret peak. [8] In general the Soret peak is a strong narrow absorption band, mostly found at approximately 415 nm: this absorption peak gives the typical red colour to the stain, since it is found in the blue region of the spectrum. [13] The Soret absorption peak is due to the presence of haemoglobin; nevertheless, the detection of this peak depends on many factors, specifically the substrates and the lighting condition. [10] In the oxy-haemoglobin absorbance spectra two peaks, named as α and β peaks, are found; in general, these two weaker and broader peaks are found between 500 and 600 nm, respectively the α peaks is

found approximately at 577 nm, while the β peak is found at circa 540 nm. [6][13] Met-haemoglobin absorbance spectrum is characterized by two absorption peaks, one at 499 nm and the other at 626 nm, while hemichrome spectrum shows a typical absorption peak at 537 nm. [8] The variation in concentration of haemoglobin derivatives over time leads to spectral variation of the bloodstains, according to the autoxidation and denaturation processes occurring to the stain outside the body, thus the blood spectrum undergoes to different alterations during the ageing process. [8] Finally, the biggest changes occurring during the ageing of the bloodstains are found in the α and the β bands regions, due to the oxy-haemoglobin oxidation in met-haemoglobin and then into hemichrome. [14] Figure 15 represents the absorption spectra of haemoglobin and haemoglobin derivatives.

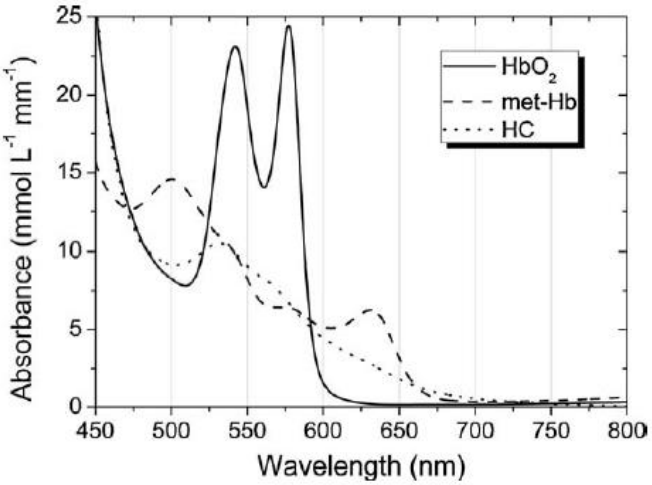

Figure 15 Haemoglobin's derivatives absorption spectra, taken from [13]

Moreover, the changes in the spectral features of blood depend on different factors other than time; examples of these factors are the thickness of the bloodstain, which changes the amount of light reflected, the temperature and the humidity. [14] Temperature could influence the spectral characteristics because, as all the chemical processes are temperature dependant, also the oxidation of oxy-haemoglobin into met-haemoglobin and then into hemichrome would be temperature dependant. [14]

4. MATERIALS AND METHODS

In the initial phase of this study, three different preliminary tests have been done, with the aim of finding the test bench and the sample preparation to use for the data collection for the temporal analysis. The preliminary tests, and thus the final test bench realised, have been defined in collaboration with Maria Teresa Pucarelli, that has used the same test bench and hence the same acquired data in her study "Hyperspectral Imaging System in Forensic Science: Background Correction via Neural Network". The three different preliminary tests use the same hyperspectral camera and blood type, while the illumination system and the samples used change according to the test considered. In the following section are going to be described first how the preliminary tests that have been realised, then the description of the test bench that has been defined and used, the sample preparation and the data collection are going to be reported, and finally the description of the temporal analysis on the acquired data, with the temporal parameter description and how the relation between the bloodstain age and the temporal parameter have been done, consequently with the definition of the curve expressing the previous relationship that could be used to perform age estimation of the bloodstains.

4.1 HYPERSPECTRAL CAMERA

The hyperspectral camera used for the acquisitions is the HinaLea 4250 (Figure 16), with a spatial resolution of 2.3 MP; the camera is characterised by a tuneable filter, placed in front of the sensor, that allow the sequential selection of the visible and the near-infrared spectral bands in an extended range between 400 nm and 1000 nm, with a step size of 2 nm. [48] Furthermore, the camera generates a hyper-spectral cube for each wavelength. The acquired images have been compensated from the white and dark response with a classical calibration procedure. The calibration procedure has been performed following the instruction present in the user manual of the camera: the dark reference image is recorded covering the lens of the camera by means of the lens cup, while the white reference is recorded with the camera looking vertically downward at a white standard of known reflectance. [48] Figure 17 shows the white reference used for the calibration of the white. After the calibration procedure, the

image is acquired; right before the acquisition of the image, auto-exposure command is done to correctly determine the amount of light reaching the sensor; hence, saturated images are avoided. TruScope Application Software, software release 1.0.9, is the software coming together with the camera, and it allows to acquire the image, to regulate the exposition, and to select the wavelength range to acquire. [48] Figure 18 is the screen of the acquisition page of TruScope application software. Moreover, TruScope also gives information about the temperature of the camera. TruScope application software can be used to performed different operations over the acquired hyperspectral cube, for example the spectral acquisition; in fact, using different areas offered by the software (rectangle, ellipse, circle) to select the region of interest, it is possible to obtain the spectral information as the average of all the spectral information contained in the selected area. [48] The spectral information can be then exported or imported. In this study, TruScope application software has been used to perform the calibration, set the exposition, and acquire the hyperspectral cube. In general, the time necessary to perform the exposure, the calibration of the system and the acquisition of the image is about three minutes.

Figure 16 HinaLea 4250, the hyperspectral camera used in this study.

Figure 17 White standard of known reflectance used for the calibration of the white.

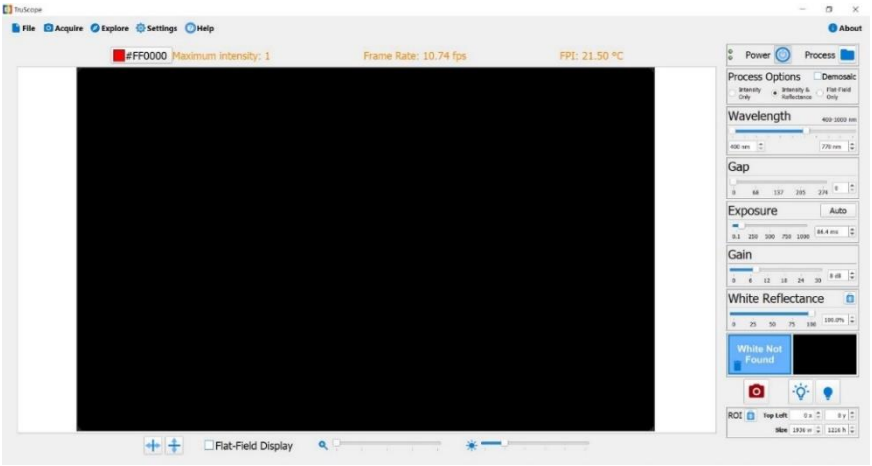

Figure 18 TruScope application software coming together with the hyperspectral camera; the image shows the acquisition interface, used to acquire the image, perform the calibration, regulate the exposition, and define the wavelength range to acquire.

4.2 SAMPLES PREPARATION: THE BLOOD USED FOR THE PRELIMINARY TESTS

Blood has been provided by a healthy female volunteer of 25 years old, and it has been recollected in an acid Vacutainer container (EDTA), obtaining, in this way, blood containing anti-coagulant. Then the blood has been placed directly over the different substrates through a pipette, in a way that the obtained drops present a similar dimension (about 1 cm) and a uniform blood quantity. Furthermore, according to the fact that the size of the blood droplet depends on the absorption features of each substrate, as a consequence, it is not possible to achieve the same size and the same quantity of blood for the drop over the different substrates. Therefore, each drop is characterized by a different quantity of pixel. The types and the number of substrates used vary according to the test considered, hence the detailed description of the substrates used is given in the relative paragraph. The substrates are chosen according to the fact that they have different colour and are characterised by different textures. Moreover, the samples have been kept at a constant laboratory temperature, approximately 22 ± 2 °C.

4.3 PRELIMINARY TESTS

The preliminary tests, developed in cooperation with Maria Teresa Pucarelli, are described in the following paragraphs. The first two tests have led to the definition of the test bench, but also to the optimization of the preparation of the sample, while, the third preliminary test performed, has been done to determine the optimal way in which the samples preparation has to be done. Moreover, in all the tests the camera has been placed at a high of 42 cm from the sample under analysis. Figure 19 is a schematic representation of the first and second preliminary tests done to define the final test bench.

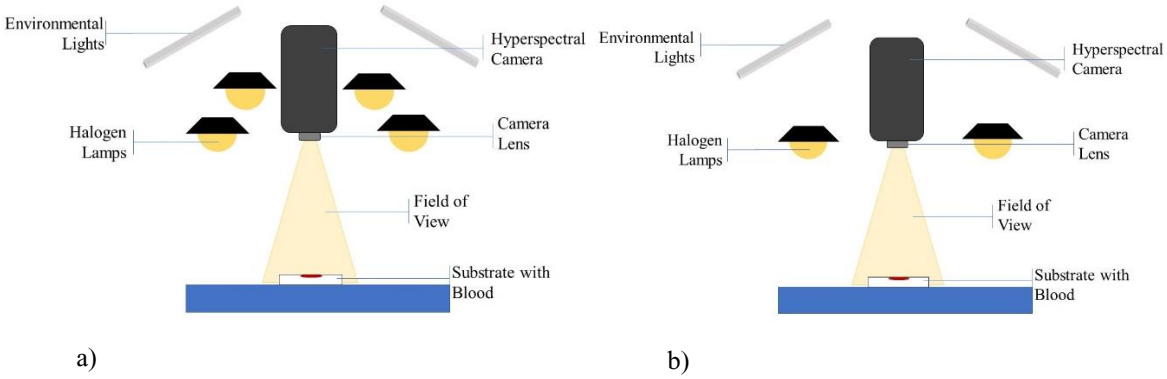

a) b)

Figure 19 Schematic representation of the first and second preliminary tests performed. a) schematic representation of the first preliminary test, which has the illumination system formed by four halogen lamps; the environmental lights are switched on. b) schematic representation of the second preliminary test; the illumination system is formed by two halogen lamps; the environmental lights are switched on

4.3.1 THE FIRST PRELIMINARY TEST

The first preliminary test has been performed using four halogen lamps as the illumination system for the camera, symmetrically mounted on the hyperspectral camera as to be perpendicular to the sample under analysis. In this test, the environmental lights, i.e., the fluorescent lamps, are switched on. The calibration of the system, in terms of the white and dark calibration, has been performed as previously described, and it has been executed only once for each day of acquisition; in detail, the calibration has been done at the beginning, before starting the acquisitions. For what concern the samples preparation, blood with EDTA

has been placed contemporaneously over a total of 23 substrates; after blood deposition, each sample has been acquired individually, at set times. Figure 20 and 21 shows the substrates used for the first preliminary test, before and after blood deposition. For the acquisition, the sample has been placed in the centre of the field of view of the camera and the spectral range acquired is the maximum one offered by the camera, from 400 nm to 1000 nm. The acquisitions of the blood samples, for the first preliminary test, have been scheduled to be carried out at set times; in detail, in the first day, the acquisitions are intended to be carried out with a high rate: after 30 minutes and then every hour, while a single acquisition is intended to be done in the following days. This preliminary test has not been successful, in fact the acquisitions of the spectral data have not continued and stopped during the first day due to problems encountered during the performing of it. Consequently, a second preliminary test has been performed.

Figure 20 Substrates used for the first preliminary test.

Figure 21 Substrates used for the first preliminary test, right after the deposition of the blood drop.

4.3.2 THE SECOND PRELIMINARY TEST

The second preliminary test has been performed with the illumination system formed by two halogen lamps symmetrically mounted on the hyperspectral camera as to be perpendicular to the sample under study. Also, in this case the environmental lights, i.e., fluorescent lamps, are switched on. As for the previous test, the dark and the white calibration has been done only once, at the beginning, before starting the acquisitions. In this test, the samples have been prepared placing the blood with EDTA over the centre of 15 substrates, waiting between each deposition 5 minutes; then the samples are acquired individually with respect set times. Figures 22 and 23 show the 15 substrates before the blood drop deposition (Figure 22) and after 24 hours the blood drop deposition (Figure 23). Each sample, during the acquisition, has been placed in the centre of the field of view of the camera and the spectral range acquired is the one that goes from 400 nm to 1000 nm. The acquisitions, for the second test, are intended to be done like the first one; in detail, in the first day, the acquisitions are intended to be done 30 minutes after the deposition and then every hour in the rest of the day, while a single acquisition has been scheduled for the days following the deposition of the blood. In the end, this test has not been successful, in fact the acquisitions have not continued and stopped after the second day.

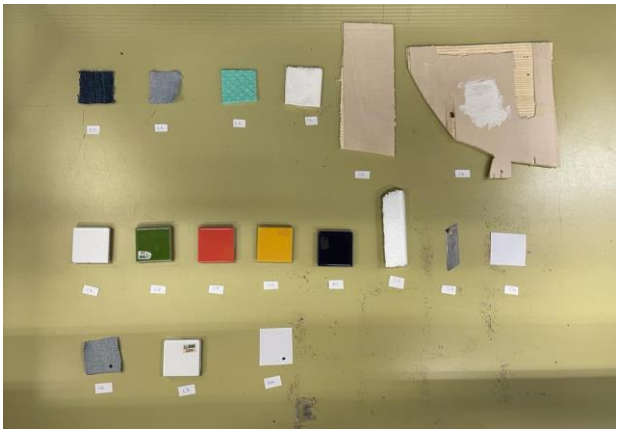

Figure 22 Substrates used for the second preliminary test.

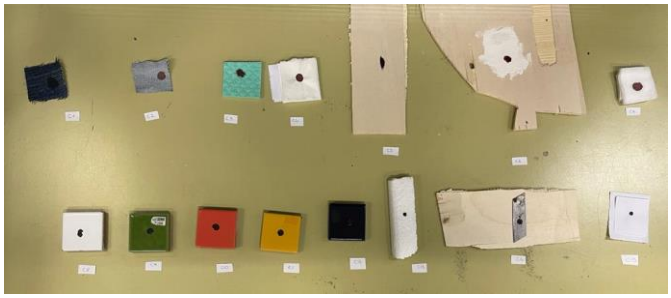

Figure 23 Substrates used for the second preliminary test after 24 hours the deposition of the blood drops.

4.3.3 THE THIRD PRELIMINARY TEST

A third and last preliminary test has been performed to determine the optimal preparation of the samples. In fact, following the failures of the previous two preliminary tests, it has been decided to arrange the substrate over a single support, specifically to place four substrates over a single support. For this reason, another test has been performed, with the aim of finding out the optimal area, i.e., the area where to deposit the blood over the substrate. Hence, two drops of blood have been placed over four different substrates (Wood, Light Jeans, Napkin, Dark Jeans), with a dimension of 5.25 cm x 3.25 cm, placed on a single support: one blood drop has been placed over the inner margin of the substrates, while the other blood drop has been placed on the external margin of the substrates. Three acquisitions, using as illumination system two halogen lamps mounted symmetrically on the camera, with the environmental light switched off, have been done at three different times: 20 minutes, 1.5 hours, and 2 hours. In this test, the calibration of the dark has been performed once, before starting the acquisitions, while the calibration of the white has been performed before each acquisition, at set times. Figure 24 shows the substrate chosen for the deposition of the two blood drops, with the aim of finding the region for the blood deposition. Finally, it has been chosen to deposit the blood drop on each substrate near the inner margin of the substrate.

Figure 24 Deposition of the two drops of blood over the four substrates.

4.4 TEST BENCH

The first and the second preliminary tests performed have led to the definition of the test bench that has been used for the acquisition of the data for the temporal analysis. Thus, the test bench realised is the first result obtained in the initial part of the study. The test bench realised is formed by the hyperspectral camera previously describe; moreover, the camera has been placed at a height of 42 cm from the plane where the samples to analysed are placed. The illumination system is formed by two halogen lamps, symmetrically mounted on the hyperspectral camera as to be perpendicular to the sample under study. The environmental lights are switched off. Figure 25 is the schematic presentation of the test bench used for the acquisition of the data.

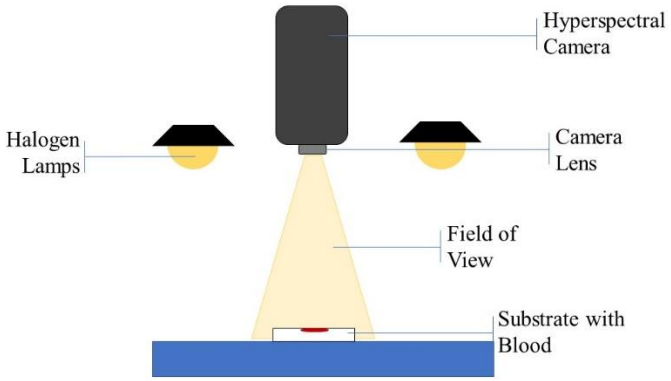

Figure 25 Schematic representation of the test bench used to acquire the data used for the temporal analysis.

4.5 SAMPLE PREPARATION: THE BLOOD USED FOR THE TEMPORAL ANLYSYS

As for the preliminary tests, blood has been provided by a healthy female volunteer of 25 years old, and it has been recollected in an acid Vacutainer container (EDTA). Then the blood has been placed directly over the different substrates through a pipette, in a way that the obtained drops present a similar dimension (about 1 cm) and a uniform blood quantity. The temporal analysis has been performed depositing the blood over 12 different substrates (black paper, white paper, yellow paper, red paper, white tile, sponge, red fabric, cardboard, light wood, light jeans, napkin, dark jeans); a specific ID has been associated to each substrate. Table 2 lists all the chosen substrates and the relative ID associated to it. The 12 substrates have been arranged to obtain the simultaneous acquisition of four samples at time. In fact, the samples have been subdivided in three groups of four and placed together on a single support. Each substrate has been cut as rectangle with a specific dimension: 5.25 cm x 3.25 cm. Figure 26 represents the three groups of four substrates placed on the relative support. The blood drop has been placed contemporaneously over the inner margin of four substrates of a single support, according to the results obtained with the third preliminary test done; the same procedure is performed on the remained two supports, with a time interval of five minutes between one deposition over the four substrates of a support and the

others. As for the samples used for the preliminary tests, also the samples used for the temporal analysis have been kept at a constant laboratory temperature of 22 ± 2 °C.

Table 2 Lists of the substrates and the associated ID

ID	Substrate
C_1	Black paper
C_2	White paper
C_3	Yellow paper
C_4	Red paper
C_5	White tile
C_6	Sponge (green)
C_7	Red fabric
C_8	Cardboard
C_9	Wood
C_{10}	Light jeans
C_{11}	Napkin
C_{12}	Dark jeans

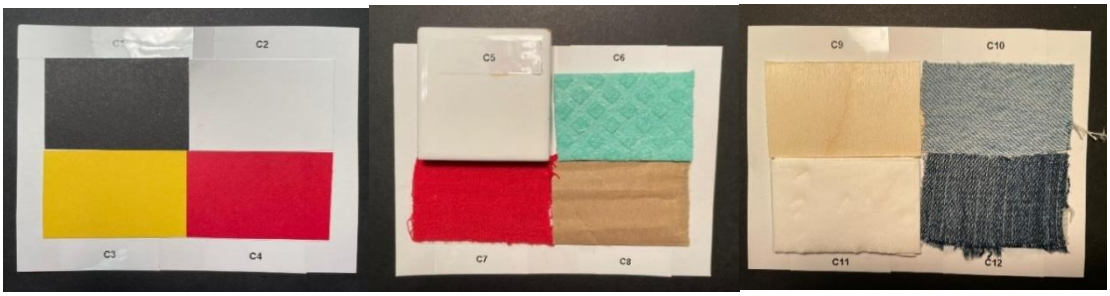

Figure 26 The 12 substrates subdivided in four group. Each substrate is associated to its specific ID and is cut with a determined dimension.

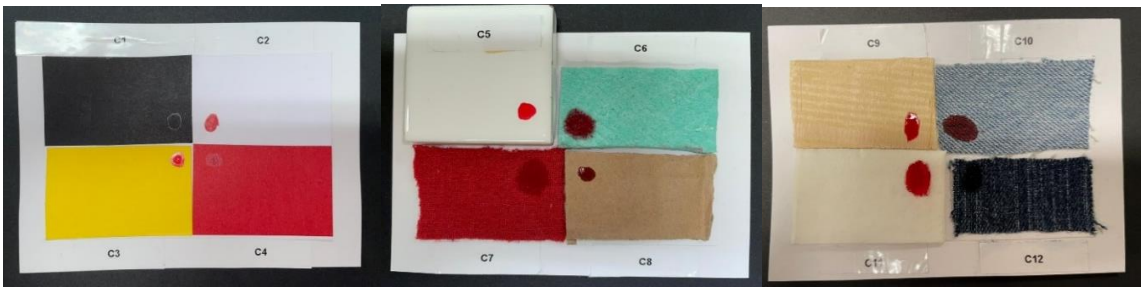

Figure 27 The 12 substrates, organised in three groups, right after the deposition of the blood drop. The drop has been placed over the inner margin of each substrate.

4.6 DATA COLLECTION

The spectral analysis is limited to the range that goes from 400 nm to 770 nm, with a step size of 2 nm (185 nominal spectral bands). The calibration of the dark has been performed once, before starting the acquisitions of the hyperspectral cube, while the calibration of the white has been performed before each acquisition. The hyperspectral cubes have been acquired for a total of 14 days. In the first day, the acquisitions have been done after 30 minutes the blood deposition on the substrates and then every hour, for a total of 8 hours; in the second day five acquisition have been done, where the first three have been performed with a temporal distance of one hour and the last two are performed with a temporal distance of two hours, followed by three acquisition in the third day, where the first two have been performed with a temporal distance of two hours, while the last one with a temporal distance of three hours, and then a single acquisition has been done daily until the 14th day. The hyperspectral cube, obtained from each acquisition, have been then pre-processed and analysed in custom-made Phyton and MATLAB® codes.

4.7 DATA ANALYSES

For each acquired image, it has been manually selected the area belonging to the bloodstain, thus obtaining reflectance spectra of the selected area, i.e., the spectra of the blood deposited over each substrate. The selection of the area has been done with a custom-made Python code; the code has been realised in manner that the selected area of interest for each substrate

has the same shape (circle) and covers the same area, thus comprises the same number of pixels. The spectra obtained from the manual selection of the area belonging to each stain are the average of all the pixels spectra found in the selected area. The temporal analysis, i.e., the extrapolation of a set of parameters that can be related with the blood age, has been performed initially only on the absorbance spectra obtained from the blood deposited over the White Tile, then applied to the other blood spectra, i.e., the spectra obtained from the deposition of the blood on different substrates, first without any background correction and subsequently for the corrected one. The correction of the background, which has been performed for all the blood deposited over all the substrate, except for the blood deposited on the White Tile, has been obtained by means of a neural network model, based on a Multi-Layer Perceptron (MLP) approach targeted to regression that involves predicting a real-valued quantity, which have been defined and used by Maria Teresa Pucarelli in her study "Hyperspectral Imaging System in Forensic Science: Background Correction via Neural Network". The model takes as input the bloodstain reflectance spectra on a substrate C_n at a time t_i, and the outputs are the spectra that it would have on a white reference substrate that is the substrate C_5 at the time t_i. The substrate C_5 at time t_i is given as ground truth (GT) to the model. More detailed description of the model and the results obtained can be found in the work of Maria Teresa Pucarelli. The data obtained, directly from the hyperspectral cube and as the output of the neural network, have been opened and analysed with a custom-made MATLAB® code.

4.7.1 PRE-PROCESSING OF THE DATA

The blood spectra obtained directly from the hyperspectral cube are named as *Input Spectra*, which comprises also the spectra of the blood deposited on the White Tile, while the spectra coming from the output of the neural network are named as *Predicted Spectra*. The blood spectra obtained directly from the hyperspectral cube, and the spectra coming from the output of the neural network, are reflectance spectra; in this study the temporal analysis has been performed considering the absorbance spectra of the bloodstain. Thus, the absorbance spectra have been obtained for each spectrum, from the reflectance ones, applying the Equation 3. Both the input and the predicted spectra have been pre-processed performing a

third order Savitzky-Golay filter. The Savitzky-Golay filters are smoothing polynomial filters usually used to smooth a noisy signal whose frequency span is large. [49] After the pre-processing, the temporal analysis has been conducted.

4.7.2 TEMPORAL ANALYSIS OF THE BLOOD DEPOSITED OVER THE WHITE TILE

The temporal analysis has been conducted with the definition and subsequently the extrapolation of a total of three parameters, named as *temporal parameters*, that can be related with the blood age. In details, the definition of the three parameters has performed observing the spectra obtained from the blood deposited over the White Tile, hence the analysis has been first conducted on the spectra of the blood deposited on the White Tile, and then extended to the other substrates.
The three parameters that have been extrapolated are:

- *Coefficient m*, which is the absolute value of the angular coefficient of the interpolating line to the blood absorbance spectrum, comprised between the α peak and the value of the blood spectrum corresponding to the wavelength value of 620 nm. The α peak has been found for each spectrum as the maximum value in the wavelength range from 570 nm to 620 nm.

- *Ratio*, defined as the ratio between the α peak and the relative valley value; the valley value is considered the value that the blood absorbance spectrum assumes at the wavelength value of 620 nm. Also in this case, the α peak has been found as the maximum value that the blood spectrum assumes in the range from 570 nm to 620 nm.

- *Inflection point*, which is the absolute value of the peak assumed by the first-order derivative of blood absorbance spectrum in the wavelength range defined between

572 nm and 620 nm. In this case, the first-order derivative of blood absorbance spectrum has been obtained by means of the *diff* command in MTLAB®.

After the determination of the parameters, a plot of the blood age has been performed in function of the parameters.

4.7.2 DETERMINATION OF THE RELATION BETWEEN THE TEMPORAL PARAMETERS AND THE BLOOD AGE FOR THE WHITE TILE

After the definition and the extrapolation of the three previously described parameters, the final step that has been performed is the determination of the relation between the temporal parameters, extracted from the blood deposited over the White Tile, and the age of the blood, hence, the determination of a curve able to represent the relationship between the temporal parameters and the age of the blood, which could be used for the aim of the study, that is the bloodstain age estimation. Observing the data, in order to find the curve that passes near the data considered and hence, to find the function able to describe the relationship between the temporal parameter and the blood age, it has been chosen to perform an exponential fitting over the values of the three parameters in function of the time. In general, with the word fitting is intended finding the curve that best approximate the trend of the data, thus adjusting the coefficients of a known function in a way that it best matches the data. [50] The curve has been obtained using the *fit* function in MATLAB®; the function chosen to express the relation has the form of an exponential with two terms, represented in the following equation, Equation 4:

$$y = ae^{bx} + ce^{dx} \tag{4}$$

where a, b, c, and d are the coefficients that have to be found, obtained performing the fitting over the values of the parameters, y is the age of the blood expressed in hours (Time) and x represents the value of the parameter chosen. To assess the goodness of the fitting, and therefore how much the curve can represent the relation between age and temporal

parameter, the root-mean-square error (RMSE) has been computed. RMSE is the square root of the variance of the residuals, where for residuals is intended a measure of how far the data are from the line. [51][52] RMSE represents the absolute fit of the curve to the data, specifically how close are the observed data to the values estimated; moreover, RMSE have the same unit as the response variable. [51] RMSE, in general, is computed as the root square of the square of the difference between the estimated values and the observed data. With the aim of understanding how much the curve found can estimate the dependent variable (blood age) from the knowledge of the independent variable (value of the temporal parameter), the R^2 has been taken in consideration. [53] Moreover, R^2 gives insight about the goodness of the fitting, since it evaluates how much the observed parameter is far from the curve, and its value will always range between 0 and 1, and it can also be express in percentage terms (0% to 100%). [53] In fact, when R^2 is equal to 1, it means that knowing the values of the independent variable it is possible to predict exactly the value assumed by the dependent variable, thus the values observed coincide exactly with the parameters estimated, and no error occurs. [53] The contrary occurs when it is equal to 0. [53] R^2, despite being used in a ubiquitous manner, it is in general used for linear relations, thus in case of non-linear relations, it only provides a crude indication of the goodness of the fitting. [54] In this case RMSE and the R^2 has been obtained directly from the *fit* function used to perform the fitting; in fact, the *fit* function, in addition to creating the fit of the data given as input with a model specified by the user, is able to provide the statistics related to the goodness of the fitting, as the RMSE and the R^2. [55] RMSE and R^2 values are therefore used to perform the uncertainty analysis of the results.

4.7.3 DETERMINATION OF THE RELATION BETWEEN THE TEMPORAL PARAMETERS AND THE AGE OF THE BLOOD DEPOSITED OVER DIFFERENT SUBSTRATES

After the conclusion of the temporal analysis and the determination of the curves, which express the relation between the temporal parameters and the blood age and could be used to perform the age estimation of the bloodstain deposited over the White Tile, the same

procedure has been extended to the bloodstain deposited over the other substrates. Initially, the temporal parameters have been extracted from the *Input* spectra of the bloodstain of all the substrates (except the White Tile), in the same manner that has been performed for the substrate C_5. Then, the exponential curve, expressing the relation between the parameters and the age of the blood, has been obtained in the same manner that has already been done for blood deposited on the White Tile. Initially, the curve has been obtained performing the fitting between the values of each temporal parameter, obtained from the spectra of the blood deposited over a single substrate, and the relative blood age, thus obtaining a single curve, for each substrate, expressing the relationship between the temporal parameter and the blood age. Subsequently, the same procedure has been performed without considering the substrates, i.e., a single curve has been realised for all the values of each temporal parameter, obtained from all the blood spectra deposited on each substrate, capable of expressing the relation between the parameter and the age of the blood, regardless from the substrate, hence not knowing it. In other words, all the values of a single temporal parameter, obtained from all the spectra of the blood deposited on substrates, have been considered all together, in order then to perform the fitting between the values extracted from all the blood spectra and blood age. In this manner, a general curve for all the substrates has been created for each temporal parameter. Subsequently, the same procedure has been performed over the *Predicted* spectra, or the spectra obtained after the application of the neural network. Thus, firstly the temporal analysis, with the extrapolation of the parameters from each corrected spectra, has been realised, then the exponential fitting has been performed. As for the *Input* spectra, the fitting has been first realised for the values of each temporal parameter obtained from the blood spectra deposited on each substrate, thus obtaining a single curve for each substrate. Subsequently, the fitting has been performed between all the values of a single temporal parameter obtained from all the spectra of the blood deposited on each substrate and the blood age, thus obtaining a single curve for each the temporal parameter for all the substrates, capable of expressing the relation between the parameter and the age of the blood, regardless from the substrate. As for the input spectra, this means that all the values of a single temporal parameter, obtained from all the spectra of the blood deposited on substrates, have been considered all together, in order then to perform the fitting between all the values extracted from the predicted spectra and the blood age. The curve obtained for the input and

the predicted spectra, are all intended to be used to estimate the age of the bloodstain over different substrates, knowing it and not knowing it. Also in this case, the RSME value has been taken in consideration as the parameter to assess the goodness of the fitting, together with the R^2 value.

5. RESULTS

In this section, are going to be reported first the results relative to the third preliminary tests, specifically, the test performed for the determination of the optimal area, and subsequently, the results relative to the temporal analysis and the determination of the relation between the temporal parameters and the blood age.

5.1 THIRD PRELIMINARY TEST RESULTS

The results, relative to the test performed with the aim of finding the point of deposition of the blood drop for four substrates arranged on a single support, are reported. The Figures 28, 29, 30, 31 show the comparison between the spectra of the two blood drops deposited in the two different positions, specifically over the inner and the external margin, of the four substrates chosen.

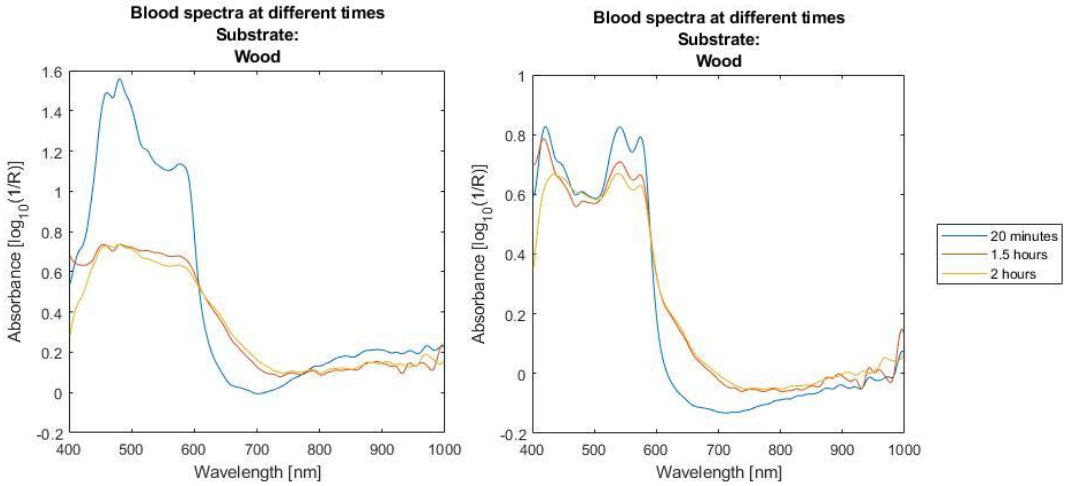

Figure 28 Comparison between the blood spectra over the same substrate (Wood) acquired at different times: on the left the spectra of the blood drop placed over the external margin, on the right the blood drop placed over the internal margin.

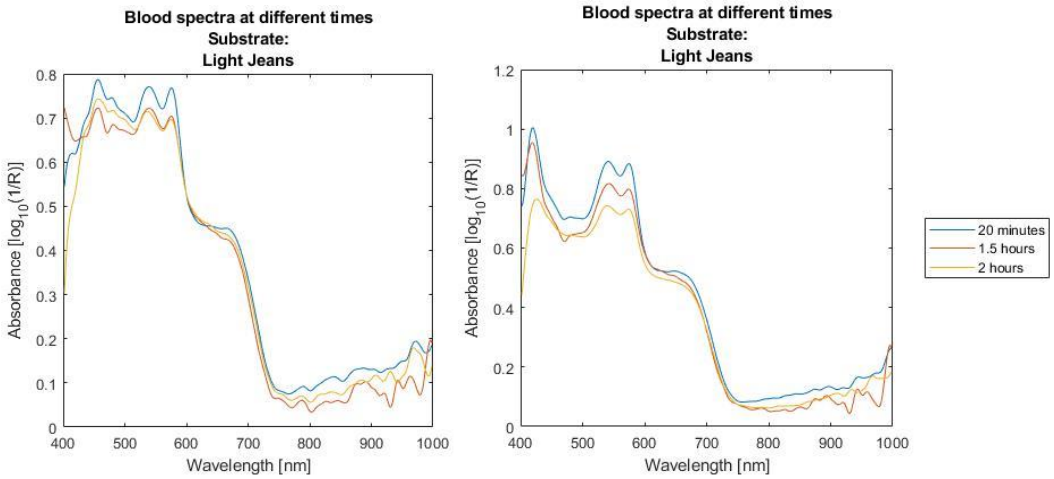

Figure 29 Comparison between the blood spectra over the same substrate (Light Jeans) acquired at different times: on the left the spectra of the blood drop placed over the external margin, on the right the blood drop placed over the internal margin.

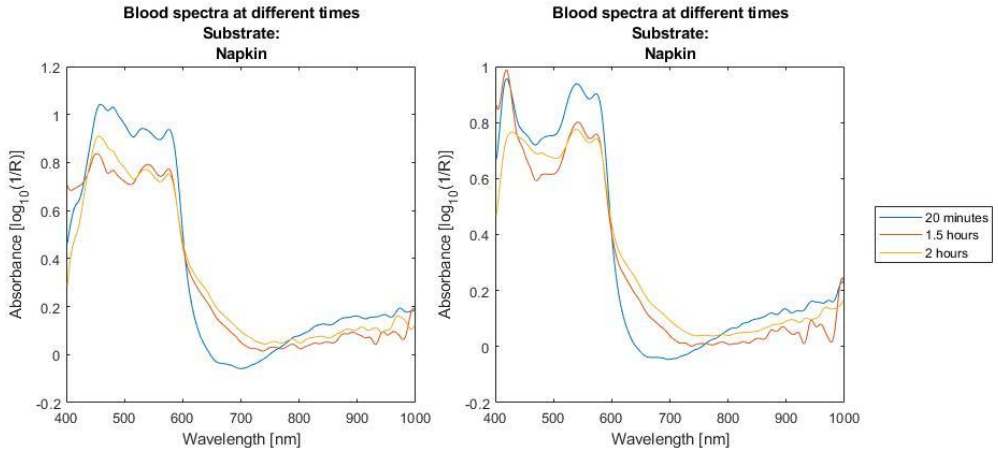

Figure 30 Comparison between the blood spectra over the same substrate (Napkin) acquired at different times: on the left the spectra of the blood drop placed over the external margin, on the right the blood drop placed over the internal margin.

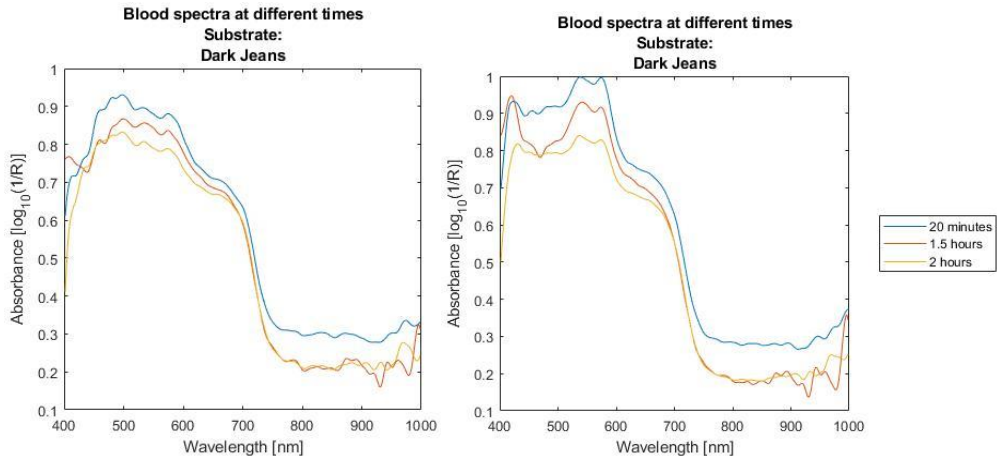

Figure 31 Comparison between the blood spectra over the same substrate (Dark Jeans) acquired at different times: on the left the spectra of the blood drop placed over the external margin, on the right the blood drop placed over the internal margin.

5.2 TEMPORAL ANALYSIS RESULTS: WHITE TILE

In this section are going to be reported the results relative to the temporal analysis performed over the White Tile, specifically the absorbance spectra of the blood at different times and subsequently the three parameters extrapolated from the spectra. Finally, the curve expressing the relation between the parameter and the blood age, together with the RMSE and the R^2 values obtained, are going to be reported. In Figure 32 are reported the blood absorbance spectra at different times that has been deposited over the White Tile (C_5).

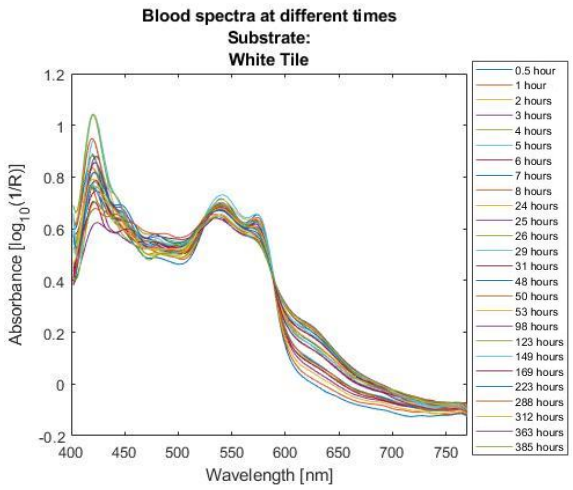

Figure 32 Blood absorbance spectra for the substrate C_5.

Figure 33 represents the temporal parameter, the *Coefficient m*, extrapolated from the absorbance spectra of the blood deposited over the White Tile. Figure 35 shows the interpolating line of the blood absorbance spectra, deposited over the C_5 substrate, in the wavelength range that goes from the α peak of the spectra to the value assumed by the spectra in the wavelength value of 620 nm; the blue dotted lines are the interpolating curves to the spectra in the defined range. The angular coefficient of the interpolating line (Figure 34) is the parameter *Coefficient m*.

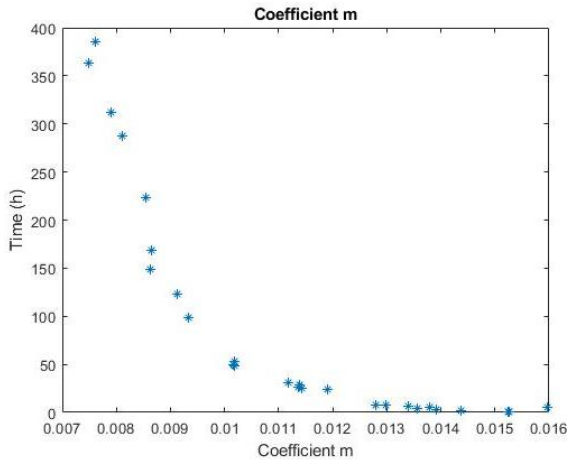

Figure 33 Coefficient m extrapolated from the absorbance spectra of the blood deposited over the substrate C_5.

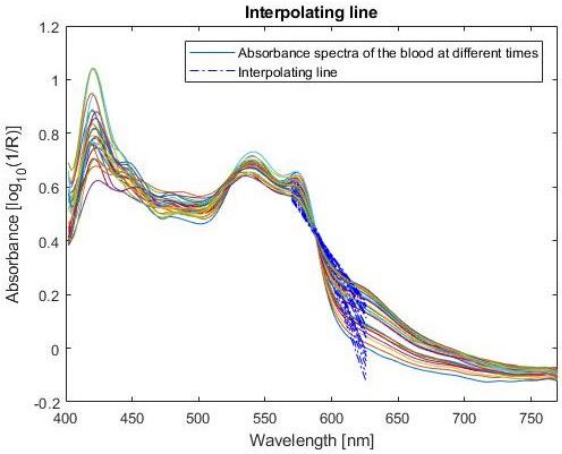

Figure 34 Interpolating line of the absorbance spectra of blood, deposited over the substrate C_5, in the range that goes from the alfa peak to the value of the spectra assumed at the wavelength 620 nm. The blue dotted line is the interpolating line to the spectrum in the defined range.

Figure 35 represents the temporal parameter *Ratio* extrapolated from the absorbance spectra of the blood deposited over the substrate C_5. Instead, Figure 36 shows the values used to obtain the parameter *Ratio*, respectively the blue star is the α peak while the red star is the value assumed by the absorbance spectra of the blood, in this case deposited over the White Tile, at the wavelength value of 620 nm.

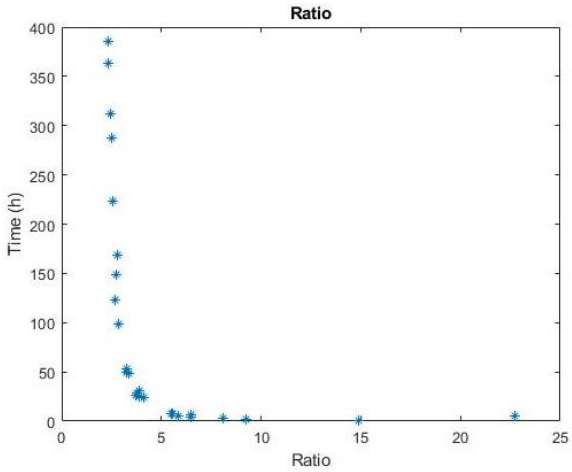

Figure 35 Ratio extrapolated from the absorbance spectra of the blood deposited over the substrate C_5.

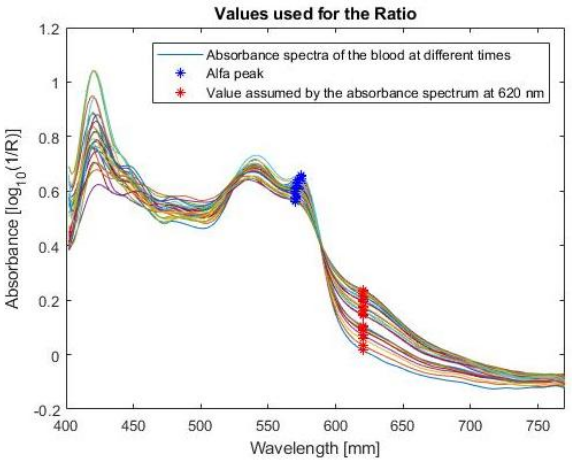

Figure 36 Values used for the determination of the parameter *Ratio*; the absorbance spectra are of the blood deposited over the White Tile.

In Figure 37 it is possible to see the parameter *Inflection Point* that has been extrapolated from the absorbance spectra of the blood deposited over the White Tile substrate. Figure 38, instead, represents the first derivative of blood absorbance spectra at different times, deposited over the substrate C_5, hence over the White Tile.

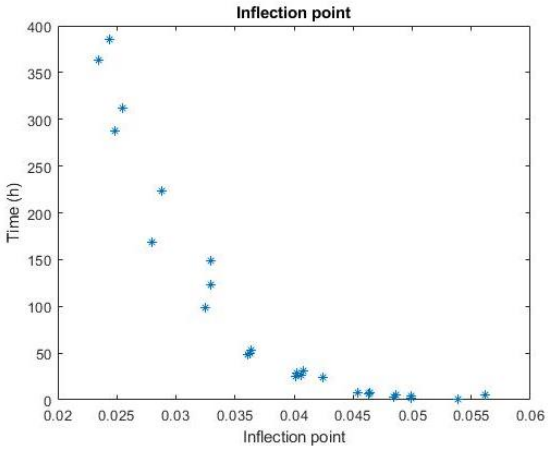

Figure 37 *Inflection point* calculated from the first derivative of the absorbance spectra of the blood deposited on the White Tile.

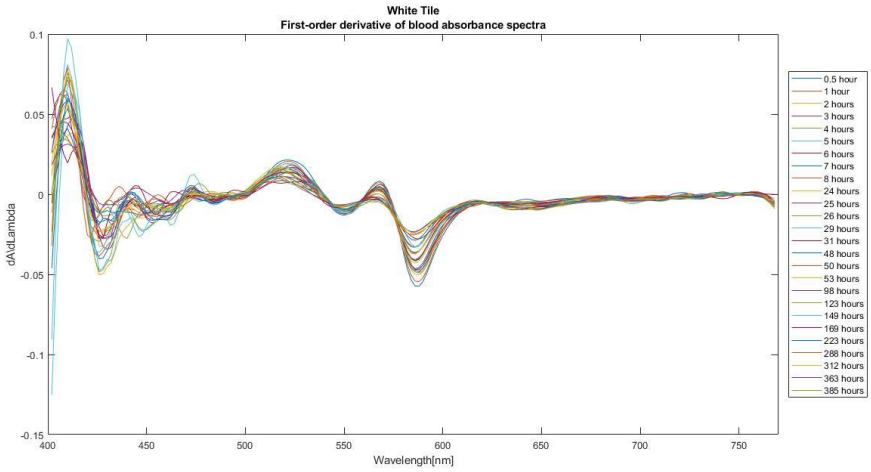

Figure 38 First-order derivative of the blood absorbance spectra, deposited over the White Tile.

Figure 39 shows the curve obtained performing the exponential fitting between the values of the *Coefficient m* obtained from the absorbance spectra of the blood deposited over the

substrate C_5 and blood age; the blue points are the values of the parameter in correspondence of the relative blood age, while the red curve represents the fitted curve. The RMSE value obtained is 14.26 hours, while the R^2 is 0.9860 (or 98.60%).

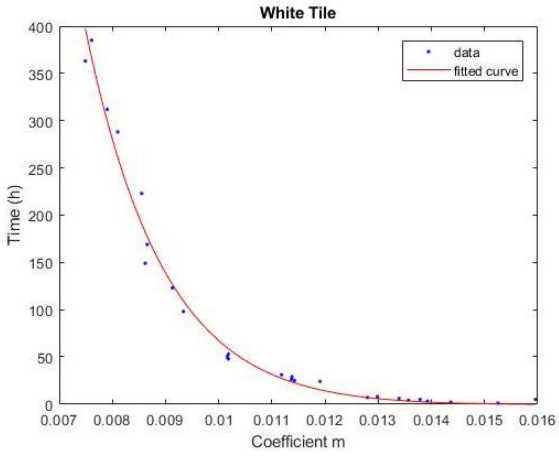

Figure 39 Exponential curve, which expresses the relation between the parameter and the age of the blood, obtained performing the fitting between the values of the *Coefficient m* obtained from the input spectra of blood deposited over the White Tile (C_5) and the blood age.

Figure 40 shows the curve obtained performing the exponential fitting between the values of the *Ratio*, obtained from the absorbance spectra of the blood deposited over the substrate C_5, and the blood age; as before, the blue points are the values of the parameter in correspondence of the relative blood age, while the red curve represents the fitted curve. The RMSE value obtained is 15.35 hours, while the R^2 is 0.9838 (98.38%).

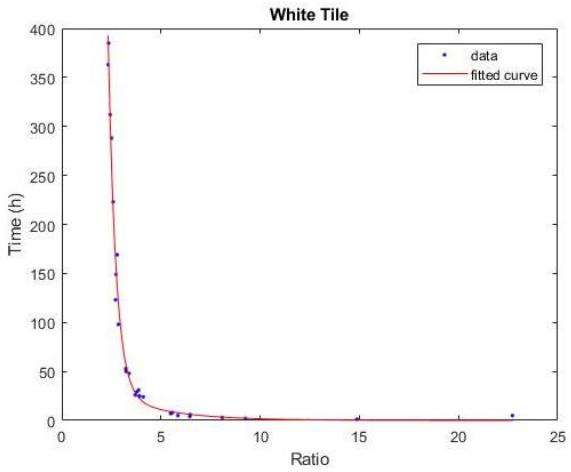

Figure 40 Exponential curve, which expresses the relation between the parameter and the age of the blood, obtained performing the fitting between the values of the *Ratio* obtained from the input spectra of blood deposited over the White Tile (C_5) and blood age.

Figure 41 shows the curve obtained performing the exponential fitting between the values of the *Inflection point*, obtained from the absorbance spectra of the blood deposited over the substrate C_5, and blood age; as before, the blue points are the values of the parameter in correspondence of the relative blood age, while the red curve represents the fitted curve. The RMSE value obtained is 19.50 hours, while the R^2 is 0.9738 (or 97.38%).

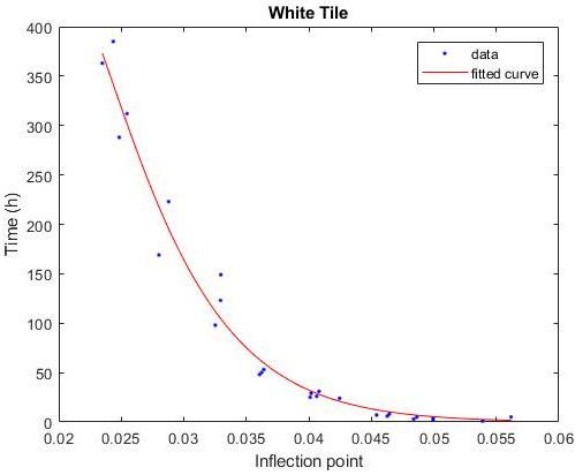

Figure 41 Exponential curve, which expresses the relation between the parameter and the age of the blood, obtained performing the fitting between the values of the *Inflection Point* obtained from the input spectra of blood deposited over the White Tile (C_5) and the blood age.

5.3 TEMPORAL ANALYSIS EXTENDED TO THE OTHER SUBSTRATES: RESULTS FOR THE INPUT SPECTRA

In this section are going to be reported the results related to the temporal analysis performed over the input absorbance spectra, i.e., the spectra not corrected for the background influence, of blood deposited over the other substrates.

5.3.1 Coefficient m

Figure 42 shows the curve obtained performing the exponential fitting between the values of the *Coefficient m*, obtained from the input absorbance spectra of the blood deposited over the substrate $C_{10,}$ and the blood age; the blue points are the values of the parameter in correspondence of the relative blood age, while the red curve represents the fitted curve. Figure 43, instead, shows the curve obtained performing the exponential fitting between the values of the *Coefficient m*, obtained from the absorbance spectra of the blood deposited over the Black Paper, and the blood age. Figure 44 represents the value of the RMSE of each curve associated to the substrate, obtained performing the exponential fitting between the values of the parameter *Coefficient m*, obtained from the input absorbance spectra of the blood deposited on each substrate, and the age of the blood, while Figure 45 represents the R^2 values associated to the curve of each substrate.

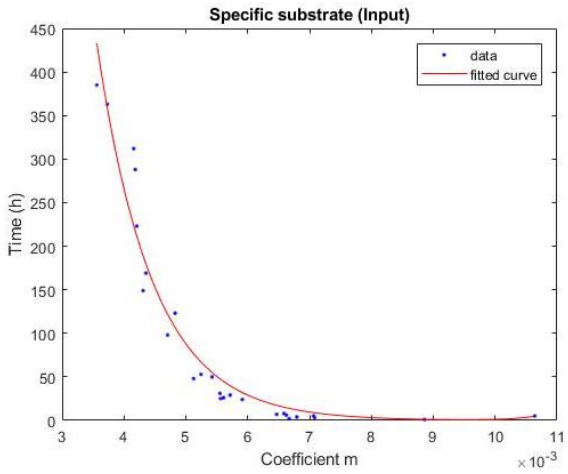

Figure 42 Exponential curve, which expresses the relation between the parameter and the age of the blood, obtained performing the fitting between the values of the *Coefficient m* obtained from the input spectra of blood deposited over the Light Jeans (C_{10}) and blood age.

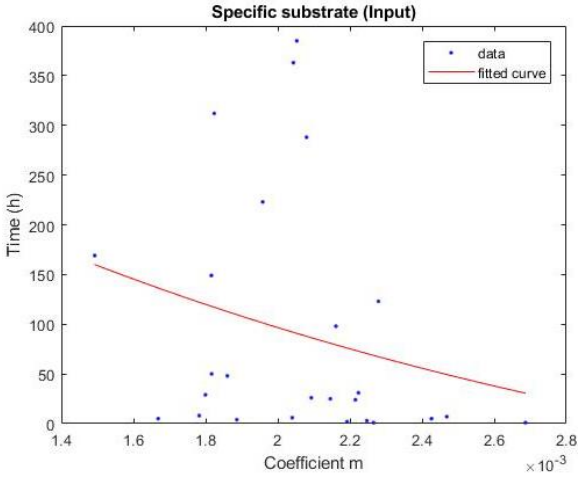

Figure 43 Exponential curve, which expresses the relation between the parameter and the age of the blood, obtained performing the fitting between the values of the *Coefficient m* obtained from the input spectra of blood deposited over the Black Paper (C_1) and blood age.

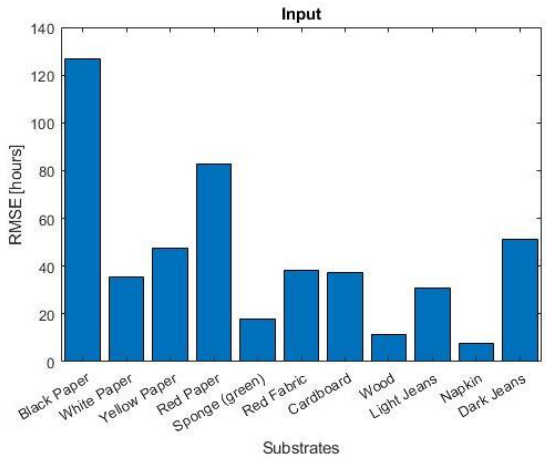

Figure 44 RMSE, of the curves associated to each substrate, obtained performing the fitting between the values of the parameter *Coefficient m* obtained from the input spectra of each substrate and the relative blood age.

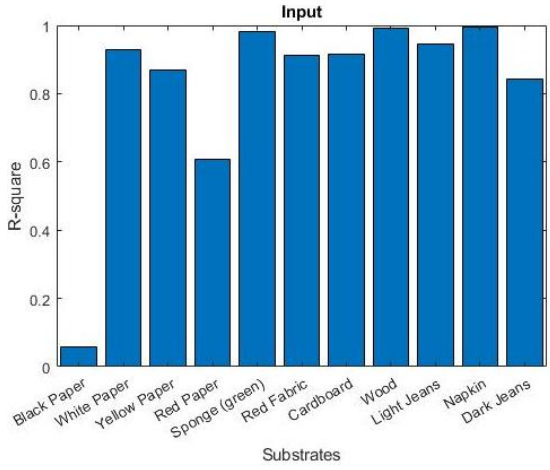

Figure 45 R^2 values, of the curves associated to each substrate, obtained performing the fitting between the values of the parameter *Coefficient m* obtained from the input spectra of each substrate and the relative blood age.

Figure 46 represents the curve obtained performing the fitting between all the values of the parameter *Coefficient m*, obtained from all the input spectra of the blood deposited on the substrates and the blood age, thus the curve expressing the relationship between the *Coefficient m* and the blood age, regardless the substrates; the blue dots are the values of the

parameter in correspondence of the relative blood age, while the red curve is the fitted curve. The R^2 value obtained is 0.0761 (7.61%), while the RMSE is 115.9 hours.

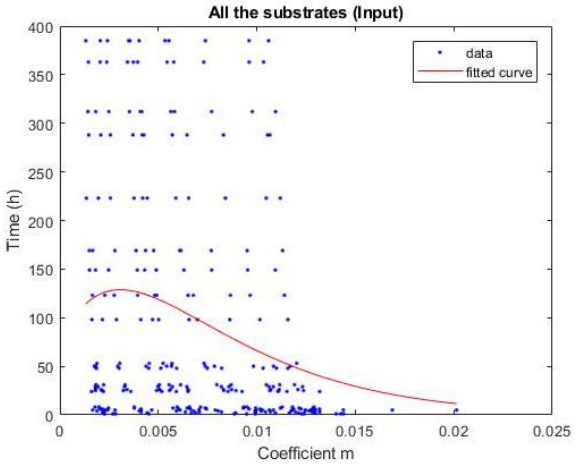

Figure 46 Curve which expresses the relation between the temporal parameter and the age of the blood, regardless from the substrate.

5.3.2 Ratio

Figure 47 shows the curve obtained performing the exponential fitting between the values of the *Ratio*, obtained from the input absorbance spectra of the blood deposited over the substrate C_{10} and the blood age; the blue points are the values of the parameter in correspondence of the relative blood age, while the red curve represents the fitted curve. Figure 48, instead, shows the curve obtained performing the exponential fitting between the values of the *Ratio*, obtained from the absorbance spectra of the blood deposited over the Black Paper and the blood age. Figure 49 represents the RMSE of each curve associated to the substrate, obtained performing the exponential fitting between the values of the parameter *Ratio* obtained from the input absorbance spectra of the blood on each substrate and the blood age, while Figure 50 represents the R^2 values associated to the curve of each substrate, obtained from the fitting performed between the values extracted from the spectra of the blood on each substrate and the relative age.

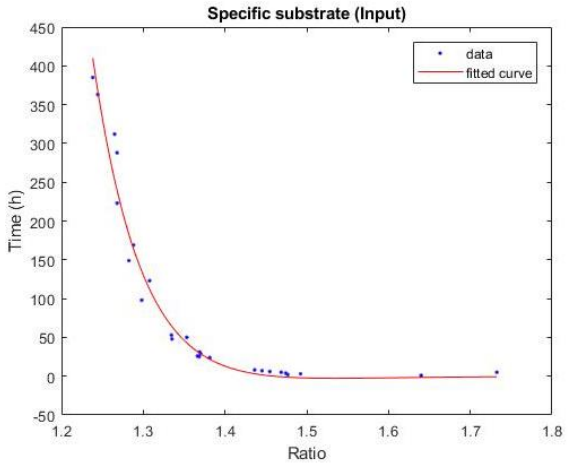

Figure 47 Exponential curve, which expresses the relation between the parameter and the age of the blood, obtained performing the fitting between the values of the *Ratio* obtained from the input spectra of blood deposited over the Light Jeans (C_{10}) and blood age.

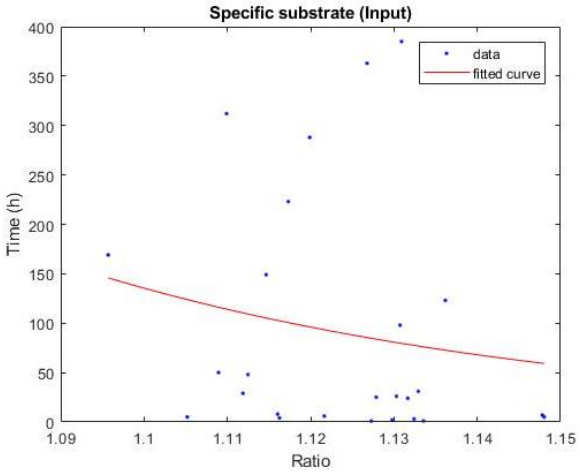

Figure 48 Exponential curve, which expresses the relation between the parameter and the age of the blood, obtained performing the fitting between the values of the *Ratio* obtained from the input spectra of blood deposited over the Black Paper (C_1) and blood age.

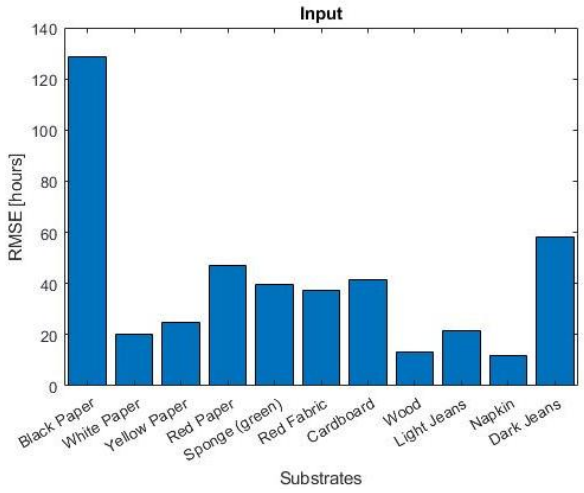

Figure 49 RMSE values, of the curves associated to each substrate, obtained performing the fitting between the values of the parameter *Ratio* obtained from the input spectra of each substrate and the relative blood age.

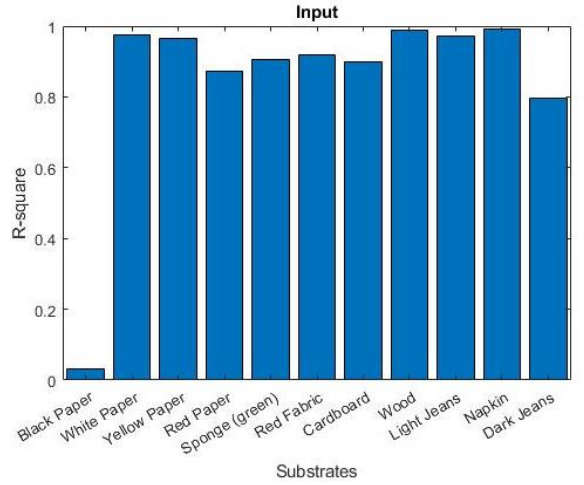

Figure 50 R^2 values, of the curves associated to each substrate, obtained performing the fitting between the values of the parameter *Ratio* obtained from the input spectra of each substrate and the relative blood age.

Figure 51 represents the curve obtained performing the fitting between all the values of the parameter *Ratio*, obtained from the all the input spectra of the blood deposited on each substrate and blood age, thus the curve expressing the relationship between the *Ratio* and the blood age, regardless the substrates; the blue dots are the values of the parameter in

correspondence of the relative blood age, while the red curve is the fitted curve. The R^2 value obtained is 0.0602 (6.02%), while the RMSE is 116.9 hours.

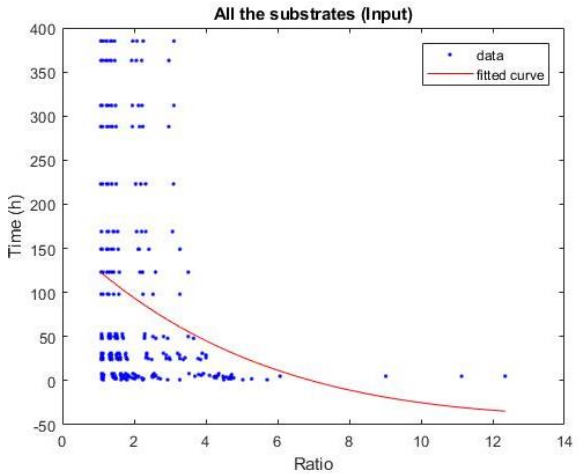

Figure 51 Curve which expresses the relation between the parameter and the age of the blood, regardless from the substrate.

5.3.2 Inflection point

Figure 52 shows the curve obtained performing the exponential fitting between the values of the *Inflection point*, obtained from the input absorbance spectra of the blood deposited over the substrate C_{10}, and the blood age; the blue points are the values of the parameter in correspondence of the relative blood age, while the red curve represents the fitted curve. Figure 53, instead, shows the curve obtained performing the exponential fitting between the values of the *Inflection point*, obtained from the absorbance spectra of the blood deposited over the Black Paper and the blood age. Figure 54 represents the value of the RMSE of each curve associated to the substrate, obtained performing the exponential fitting on the values of the parameter *Inflection point* obtained from the input absorbance spectra of the blood deposited on each substrate and the blood age, while Figure 55 represents the R^2 values associated to the curve of each substrate, obtained from the fitting performed between the values extracted from the spectra of the blood on each substrate and the relative age.

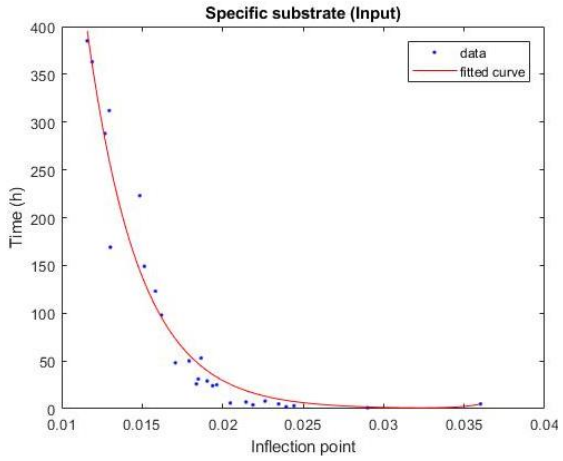

Figure 52 Exponential curve, which expresses the relation between the parameter and the age of the blood, obtained performing the fitting between the values of the *Inflection point* obtained from the input spectra of blood deposited over the Light Jeans (C_{10}) and blood age.

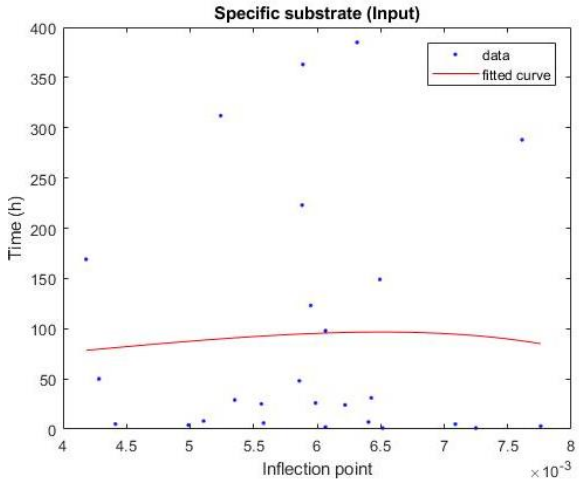

Figure 53 Exponential curve, which expresses the relation between the parameter and the age of the blood, obtained performing the fitting between the values of the *Inflection point* obtained from the input spectra of blood deposited over the Black Paper (C_1) and blood age.

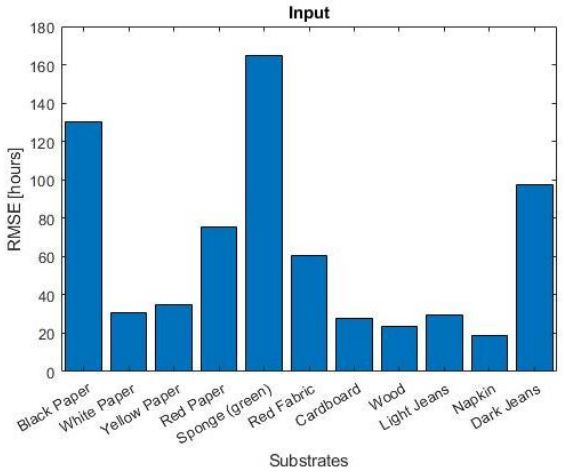

Figure 54 RMSE values, of the curves associated to each substrate, obtained performing the fitting between the values of the parameter *Inflection point* obtained from the input spectra of each substrate and the relative blood age.

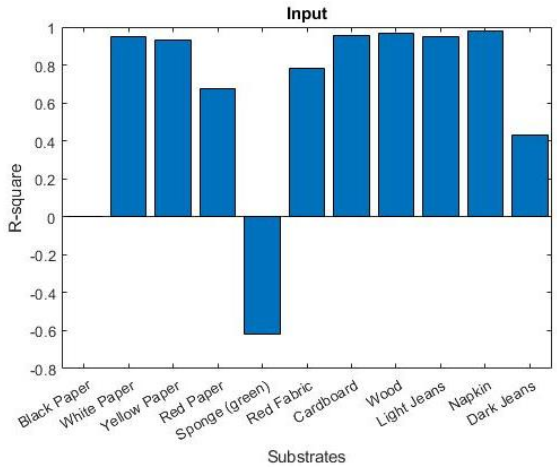

Figure 55 R^2 values, of the curves associated to each substrate, obtained performing the fitting between the values of the parameter *Inflection point* obtained from the input spectra of each substrate and the relative blood age.

Figure 56 represents the curve obtained performing the fitting between all the values of the parameter *Inflection point*, obtained from all the input spectra of the blood deposited on each substrate, and the blood age, thus the curve expressing the relationship between the *Inflection point* and the blood age, regardless the substrates; the blue dots are the values of the

parameter in correspondence of the relative blood age, while the red curve is the fitted curve. The R^2 value obtained is 0.1153 (11.53%), while the RMSE is 113.4 hours.

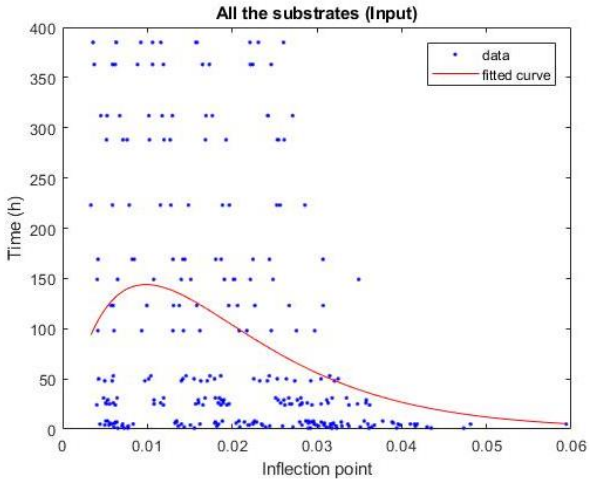

Figure 56 Curve which expresses the relation between the parameter and the age of the blood, regardless from the substrate.

5.4 TEMPORAL ANALYSIS EXTENDED TO THE OTHER SUBSTRATES: RESULTS FOR THE PREDICTED SPECTRA

In this section are going to be reported the results related to the temporal analysis performed over the predicted absorbance spectra, i.e., the spectra that have been corrected for the background influence by means of the neural network, of blood deposited over the other substrates.

5.4.1 Coefficient m

Figure 57 shows the curve obtained performing the exponential fitting between the values of the *Coefficient m*, obtained from the predicted absorbance spectra of the blood deposited over the substrate $C_{10,}$ and the blood age; the blue points are the values of the parameter in correspondence of the relative blood age, while the red curve represents the fitted curve.

Figure 58, instead, shows the curve obtained performing the exponential fitting between the values of the *Coefficient m*, obtained from the predicted absorbance spectra of the blood deposited over the Black Paper, and the blood age. Figure 59 represents the value of the RMSE of the curves for each substrate, obtained with the fitting performed between the values of the parameter *Coefficient m* obtained from the predicted absorbance spectra of the blood on each substrate and the blood age, while Figure 60 represents the R^2 values associated to each curve. Figure 61 represents the comparison of the RMSE of the curves associated to each substrate, obtained from the fitting performed between the values of *Coefficient m* extracted from the input, GT and predicted spectra, and the blood age.

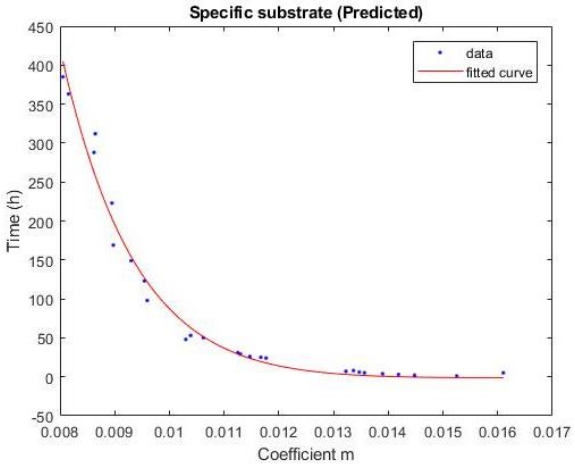

Figure 57 Exponential curve, which expresses the relation between the parameter and the age of the blood, obtained performing the fitting between the values of the *Coefficient m* obtained from the predicted spectra of blood deposited over the Light Jeans (C_{10}) and the blood age.

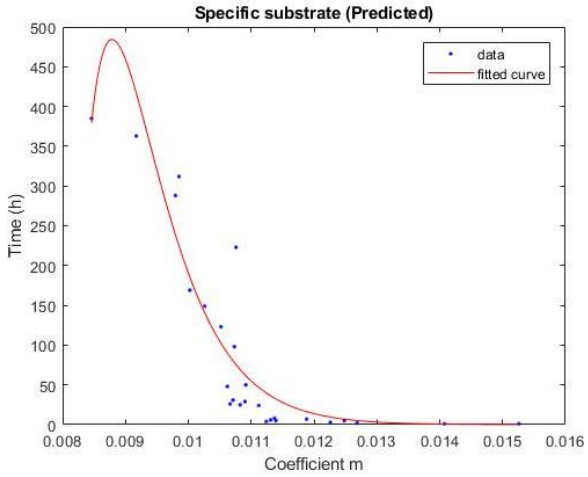

Figure 58 Exponential curve, which expresses the relation between the parameter and the age of the blood, obtained performing the fitting between the values of the *Coefficient m* obtained from the predicted spectra of blood deposited over the Black Paper (C_1) and the blood age.

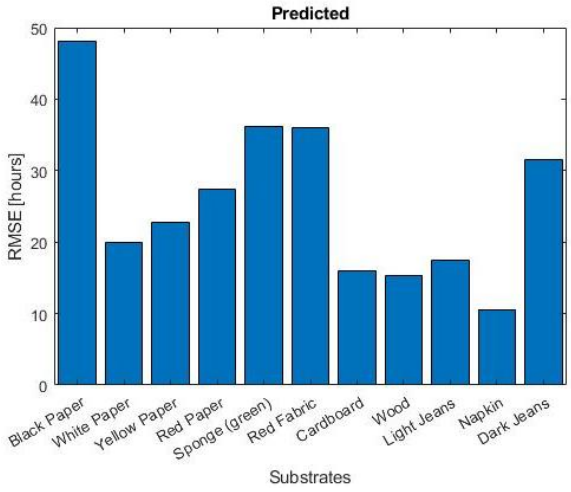

Figure 59 RMSE values, of the curves associated to each substrate, obtained performing the fitting between the values of the parameter *Coefficient m* obtained from the predicted spectra of each substrate and the relative blood age.

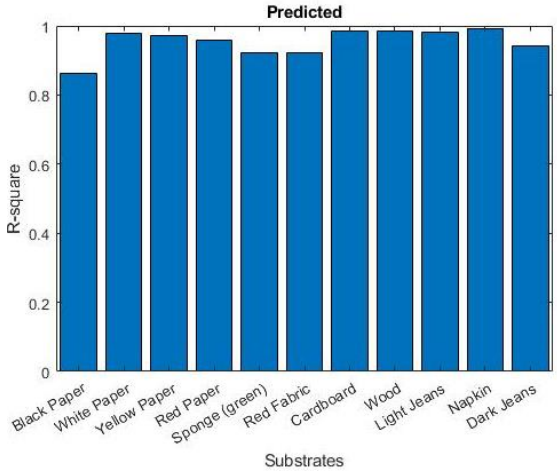

Figure 60 R^2 values, of the curves associated to each substrate, obtained performing the fitting between the values of the parameter *Coefficient m* obtained from the predicted spectra of each substrate and the relative blood age.

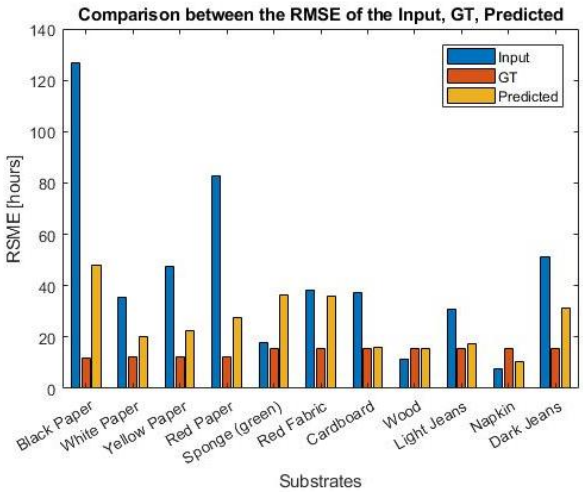

Figure 61 Comparison of the RMSE of the curves of each substrate, obtained with the fitting for the *Coefficient m* performed between the values obtained from the input, GT and predicted spectra of the blood, and the blood age.

Figure 62 represents the curve obtained performing the fitting between all the values of the parameter *Coefficient m*, obtained from all the predicted spectra of the blood deposited on each substrate and the blood age, thus the curve expressing the relationship between the

Coefficient m and the blood age, regardless the substrates; the blue dots are the values of the parameter in correspondence of the relative blood age, while the red curve is the fitted curve.

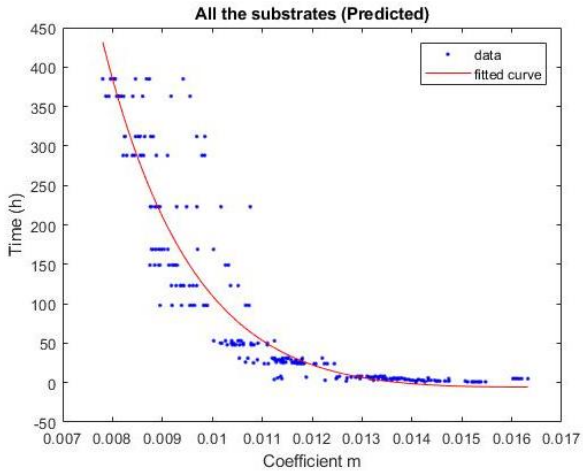

Figure 62 Curve which expresses the relation between the parameter and the age of the blood, regardless from the substrate.

Figure 63 is the comparison of the RMSE of the curves obtained performing the fitting between all the values of the *Coefficient m* extracted from the input (115.9 hours) and predicted spectra (45.46 hours) of the blood deposited on all the substrates and blood age, while Figure 64 is the comparison of the R^2 values of the curves obtained from the fitting of all the values of the *Coefficient m*, extracted from the input spectra (0.0762) and the predicted spectra (0.8580), with blood age.

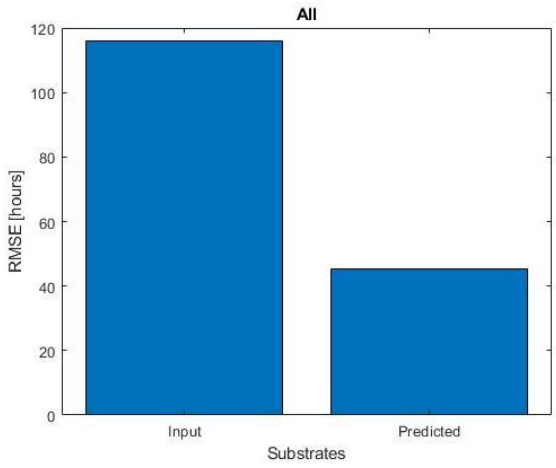

Figure 63 RMSE, of the curves of all the substrates, obtained performing the fitting between all the values obtained from the input and the predicted spectra of the blood and the blood age.

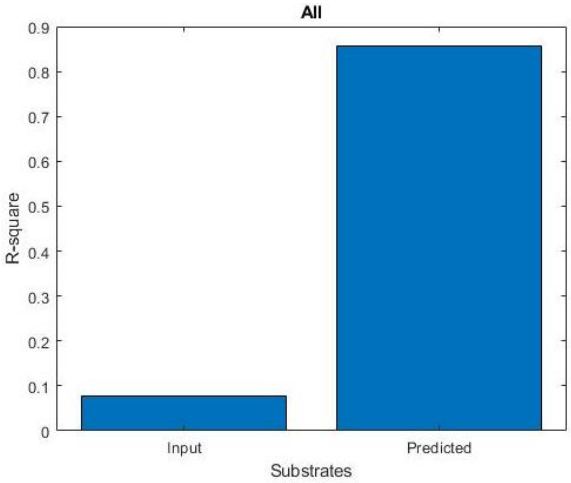

Figure 64 R^2 of the curves of all the substrates, obtained performing the fitting between all the values extracted from the input and the predicted spectra of the blood and the blood age.

5.4.2 Ratio

Figure 65 shows the curve obtained performing the exponential fitting between the values of the *Ratio*, obtained from the predicted absorbance spectra of the blood deposited over the substrate C_{10}, and the blood age; the blue points are the values of the parameter in correspondence of the relative blood age, while the red curve represents the fitted curve.

Figure 66, instead, shows the curve obtained performing the exponential fitting between the values of the *Ratio*, extracted from the predicted absorbance spectra of the blood deposited over the Black Paper, and the blood age. Figure 67 represents the value of the RMSE of the curves for each substrate, obtained with the fitting performed between the values of the parameter *Ratio* obtained from the predicted absorbance spectra of the blood deposited on each substrate and the blood age, while Figure 68 represents the R^2 values associated to each curve. Figure 69 represents the comparison of the RMSE of the curves associated to each substrate, obtained from the fitting performed between the values of *Ratio* extracted from the input, GT and predicted spectra of the blood, and the blood age.

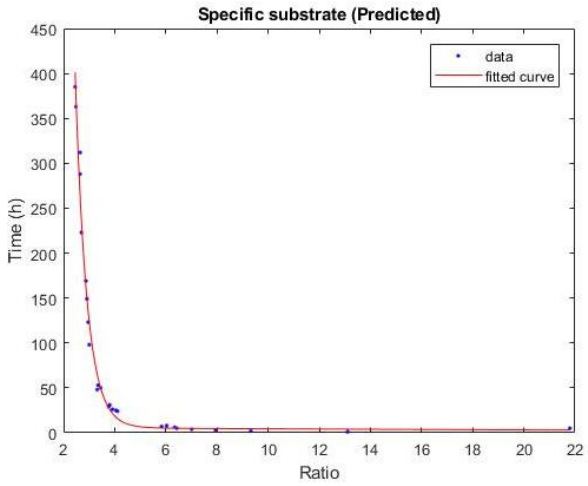

Figure 65 Exponential curve, which expresses the relation between the parameter and the age of the blood, obtained performing the fitting between the values of the *Ratio* obtained from the predicted spectra of blood deposited over the Light Jeans (C_{10}) and blood age.

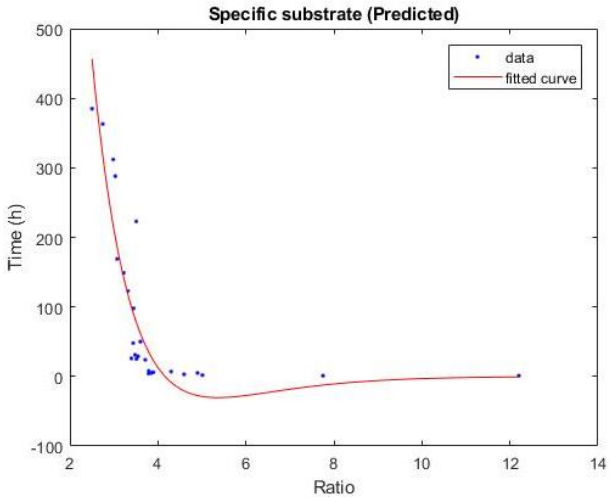

Figure 66 Exponential curve, which expresses the relation between the parameter and the age of the blood, obtained performing the fitting between the values of the *Ratio* obtained from the predicted spectra of blood deposited over the Black Paper (C_1) and blood age.

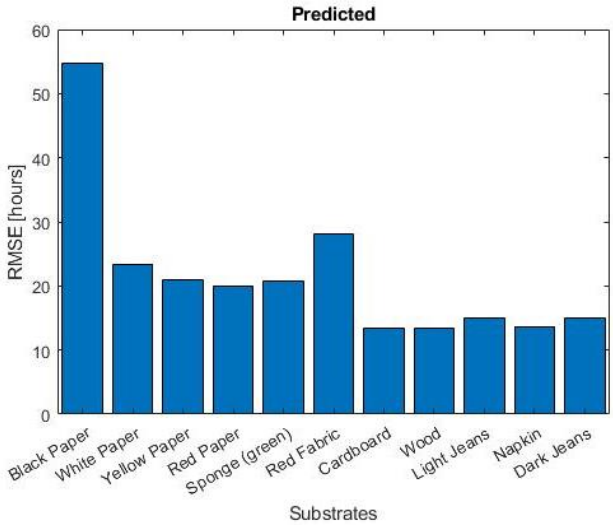

Figure 67 RMSE values, of the curves associated to each substrate, obtained performing the fitting between the values of the parameter *Ratio* obtained from the predicted spectra of each substrate and the relative blood age.

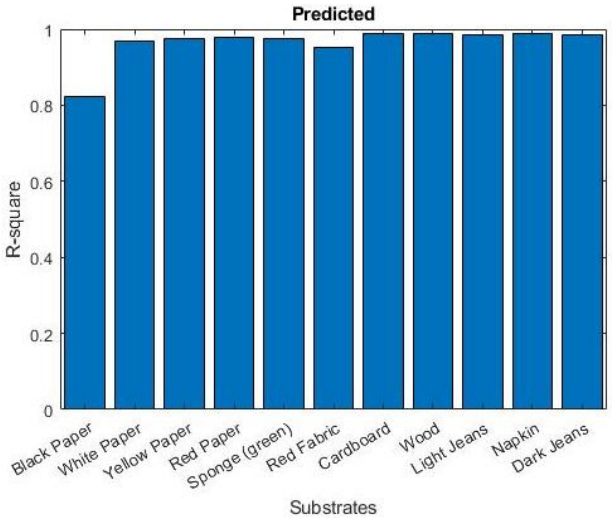

Figure 68 R^2 values, of the curves associated to each substrate, obtained performing the fitting between the values of the parameter *Ratio* obtained from the predicted spectra of each substrate and the relative blood age.

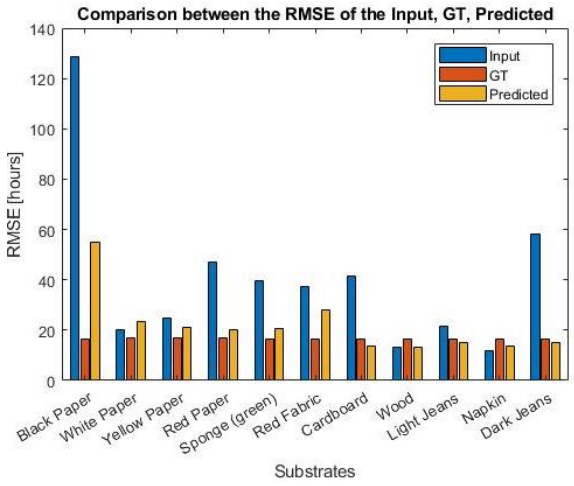

Figure 69 Comparison of the RMSE of the curves of each substrate, obtained with the fitting for the *Ratio* performed between the values obtained from the input, GT and predicted spectra of the blood, and the blood age.

Figure 70 represents the curve obtained performing the fitting between all the values of the parameter *Ratio*, obtained from all the predicted spectra of the blood deposited on each substrate, and the blood age, thus the curve expressing the relationship between the *Ratio*

and the blood age, regardless the substrates; the blue dots are the values of the parameter in correspondence of the relative blood age, while the red curve is the fitted curve.

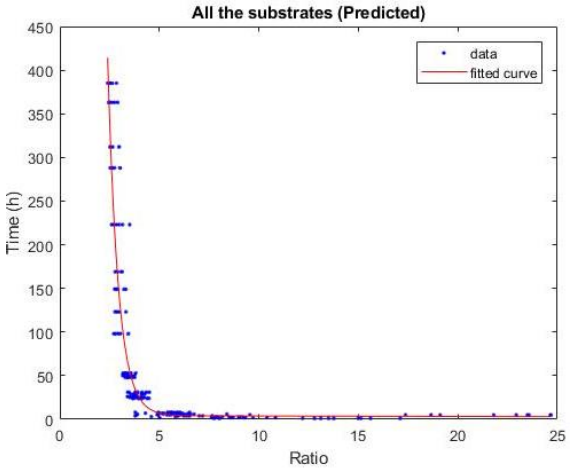

Figure 70 Curve which expresses the relation between the parameter and the age of the blood, regardless from the substrate.

Figure 71 is the comparison of the RMSE of the curves obtained performing the fitting between all the values of the *Ratio* obtained from the input (116.9 hours) and predicted spectra (41.32 hours) of the blood of all the substrates and the blood age, while Figure 72 is the comparison of the R^2 values of the curves obtained from the fitting of all the values of the *Ratio* for the input spectra (0.0602) and the predicted spectra (0.8830) and blood age.

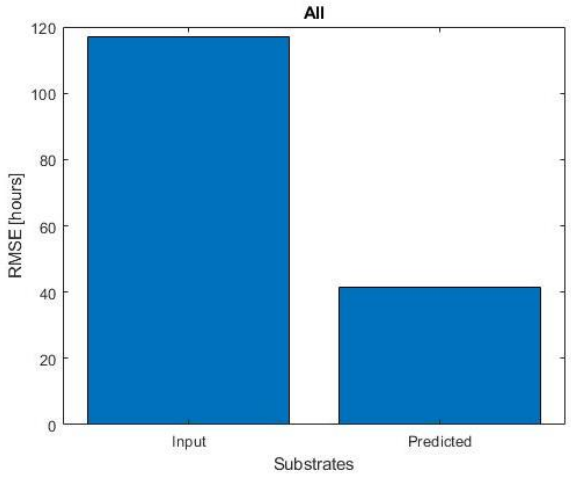

Figure 71 RMSE, of the curves of all the substrates, obtained performing the fitting between all the values obtained from the input and the predicted spectra of the blood and the blood age.

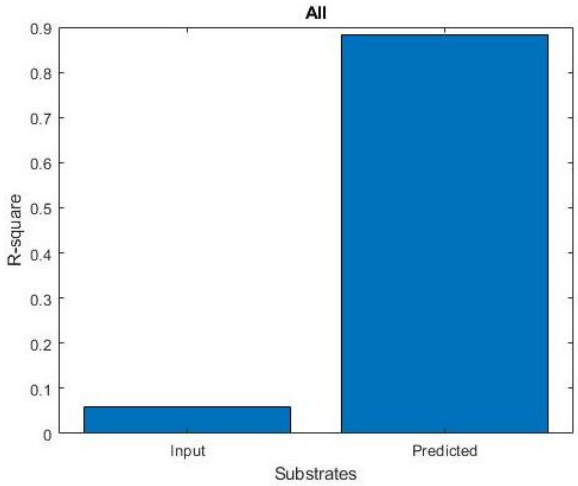

Figure 72 R^2 of the curves of all the substrates, obtained performing the fitting between all the values extracted from the input and the predicted spectra of the blood and the blood age.

5.4.3 Inflection point

Figure 73 shows the curve obtained performing the exponential fitting between the values of the *Inflection point*, obtained from the predicted absorbance spectra of the blood deposited over the substrate C_{10}, and the blood age; the blue points are the values of the parameter in correspondence of the relative blood age, while the red curve represents the fitted curve.

Figure 74, instead, shows the curve obtained performing the exponential fitting between the values of the *Inflection point*, obtained from the predicted absorbance spectra of the blood deposited over the Black Paper, and the blood age. Figure 75 represents the value of the RMSE of the curves for each substrate, obtained with the fitting performed between the values of the parameter *Inflection point* obtained from the predicted absorbance spectra of the blood deposited on each substrate and the blood age, while Figure 76 represents the R^2 values associated to each curve. Figure 77 represents the comparison of the RMSE of the curves associated to each substrate, obtained from the fitting performed between the values of *Inflection point* extracted from the input, GT and predicted spectra of the blood and the blood age.

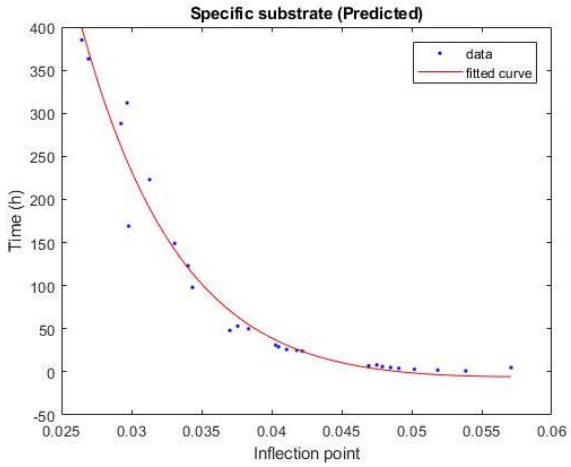

Figure 73 Exponential curve, which expresses the relation between the parameter and the age of the blood, obtained performing the fitting between the values of the *Inflection point* obtained from the predicted spectra of blood deposited over the Light Jeans (C_{10}) and blood age.

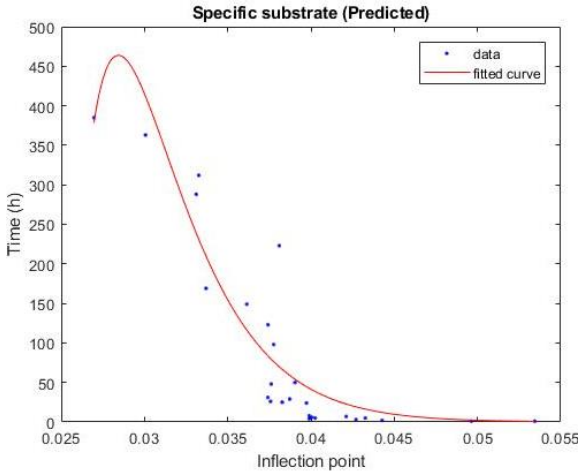

Figure 74 Exponential curve, which expresses the relation between the parameter and the age of the blood, obtained performing the fitting between the values of the *Inflection point* obtained from the predicted spectra of blood deposited over the Black Paper (C_1) and blood age.

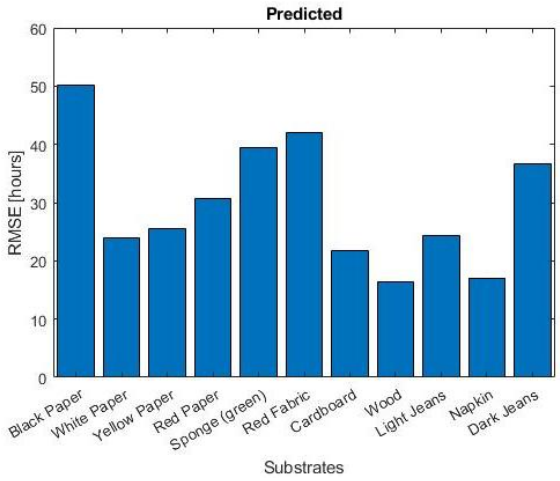

Figure 75 RMSE values, of the curves associated to each substrate, obtained performing the fitting between the values of the parameter *Inflection point* obtained from the predicted spectra of each substrate and the relative blood age.

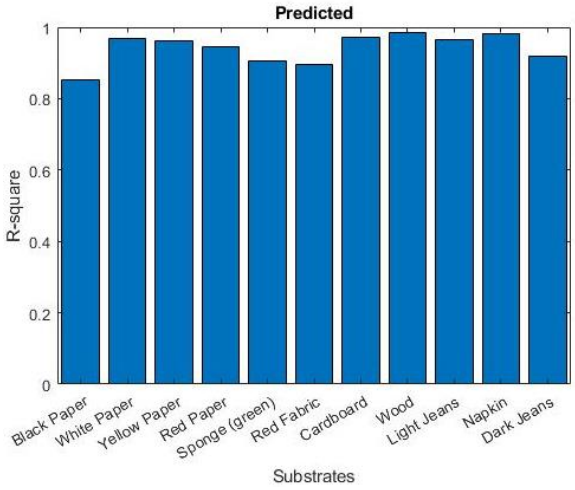

Figure 76 R^2 values, of the curves associated to each substrate, obtained performing the fitting between the values of the parameter *Inflection point* obtained from the predicted spectra of each substrate and the relative blood age.

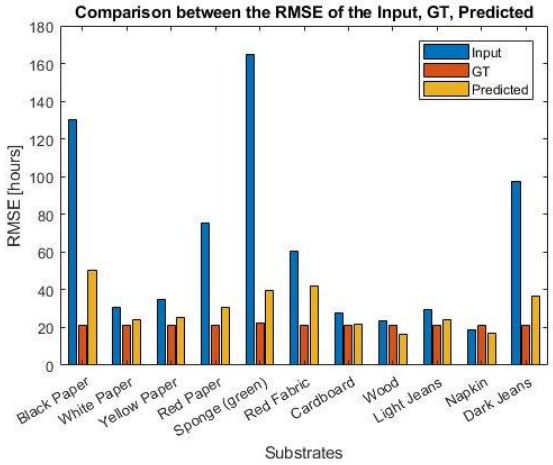

Figure 77 Comparison of the RMSE of the curves of each substrate, obtained with the fitting for the *Inflection point* performed between the values obtained from the input, GT and predicted spectra of the blood, and the blood age.

Figure 78 represents the curve obtained performing the fitting between all the values of the parameter *Inflection point*, obtained from all the predicted spectra of the blood deposited on each substrate, and the blood age, thus the curve expressing the relationship between the

Inflection point and the blood age, regardless the substrates; the blue dots are the values of the parameter in correspondence of the relative blood age, while the red curve is the fitted curve. Figure 79 is the comparison of the RMSE of the curves obtained performing the fitting between all the values of the *Inflection point* obtained from the input (113.4 hours) and predicted spectra (42.87 hours) of the blood of all the substrates and the blood age, while Figure 80 is the comparison of the R^2 values of the curves obtained from the fitting of all the values of the *Inflection point* for the input spectra (0.1150) and the predicted spectra (0.8736) and the blood age.

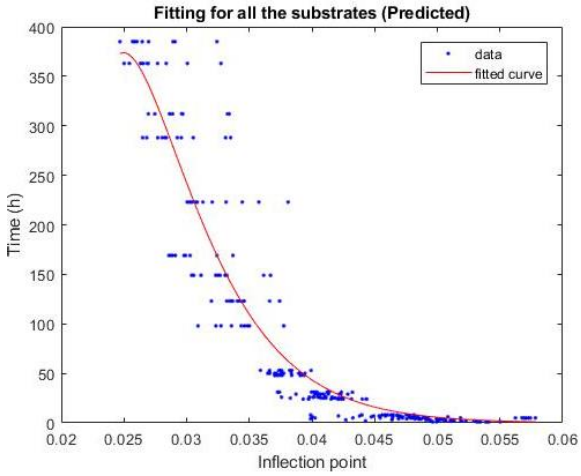

Figure 78 Curve which expresses the relation between the parameter and the age of the blood, regardless from the substrate.

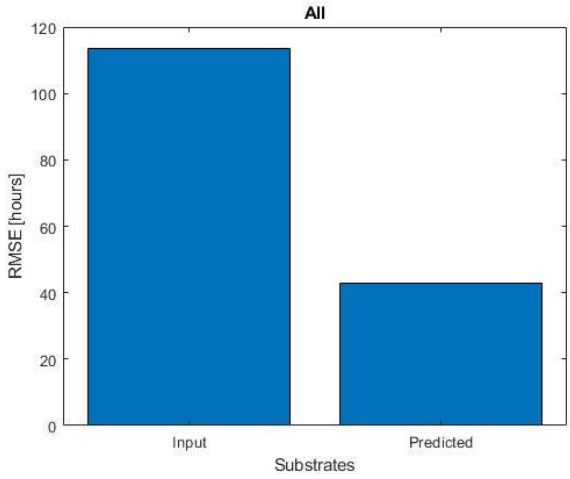

Figure 79 RMSE, of the curves of all the substrates, obtained performing the fitting between all the values obtained from the input and the predicted spectra of the blood and the blood age.

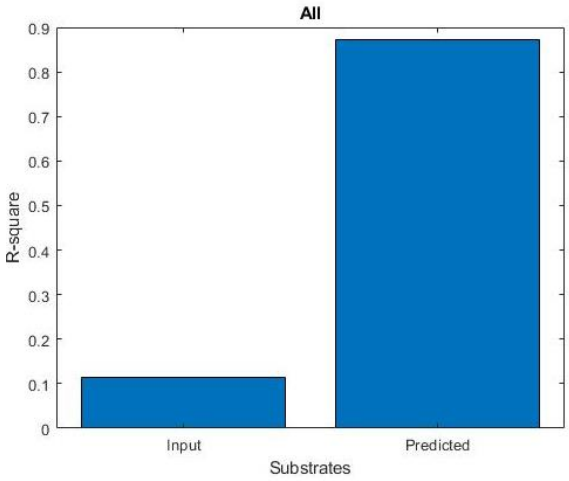

Figure 80 R^2 of the curves of all the substrates, obtained performing the fitting between all the values extracted from the input and the predicted spectra of the blood and the blood age.

6. DISCUSSION

The aim of the present study is the age estimation of bloodstains and to obtain this the temporal analysis of the bloodstain spectra has been performed. In detail, the temporal analysis of the blood absorbance spectra has been performed in a qualitative way, thus observing the blood absorbance spectra changes over time, but also in a quantitative manner, hence with the definition of a set of temporal parameters related to the temporal changes that occurred to the bloodstain. The final step has been the definition of the relationship existing between the defined temporal parameters and the age of the blood, with the final aim of obtaining a curve, expressing the relationship between them, to be used for the estimation of the bloodstains' age. The analysis has first been performed on blood deposited on the White Tile, and then extended to the other substrates, to determine a single curve for each substrate, which could be used to estimate the age of the bloodstain when the substrate is known. Subsequently, a single curve for each temporal parameter and for all the substrates is determined, which could instead be used to estimate the age of the bloodstain when the substrate is not known, hence regardless of the substrate. The first step that has been considered, has been the definition of the test bench to be used in order to have optimal data, for instance, spectra, to be used for the temporal analysis, or more in general, for different purposes. In fact, the first thing that has been performed has been the definition of the test bench, together with a proper preparation of the samples, in order to have a simplify and optimized acquisition of a high number of samples. Thus, the realization of the test bench marks the first step in every study, representing the basis of it, since good results can be achieved starting from good data on which to perform the analysis. Moreover, the study has been conducted with human blood coming from a healthy female volunteer, and recollected in tubes containing EDTA, which is an anti-coagulant. It has been decided to collect the blood in this container because it is simpler to perform the study. In fact, blood without the addition of anti-coagulant coagulates within two hours, thus making it unsuitable to perform further tests days after the collection of the blood in the tube. The tubes with EDTA can be stored in the fridge or can be maintained at room temperature for 24 hours, because the anti-coagulant maintains stable the erythrocytes, the leucocytes, and the thrombocytes, in this way avoiding the coagulation. [56]

When dealing with a hyperspectral camera, several things must be taken into consideration, starting from the illumination system, which represents one of the fundamental elements of the hyperspectral imaging technique. In this study, the choice of the illumination system has been extremely important since it can affect the performances and the reliability of the hyperspectral system. In this study, it has been decided to use the halogen lamps as the source of the illumination system, since they are easy to be found and able to provide a quite broadband and a uniform illumination. Halogen lamps are like the conventional incandescent light, for what concerns the presence of a tungsten filament placed in a gas-filled and light-transmitting envelope, but they differ from them, since the halogen lamps present traces of halogen vapor in the inert fill gas, and the gas pressure (7-8 ATM) together with the bulb temperature (from 250 °C to 600 °C) are much higher than the conventional incandescent light. [57] Hence, these lamps are extremely dangerous since high temperatures are reached; in fact, objects around them can catch fire and people can burn themselves if they eventually touch them. [58] The fact that high temperatures are reached by the halogen lamps raises the question of how many lamps must be used to prevent that the produced heat can ruin the biological sample. This question has been answered with the execution of the first and the second preliminary tests. The first test, in fact, has highlighted the problem connected to the number of halogen lamps to be used as an illumination system for the test bench. In fact, in the first test, a total of four lamps, symmetrically mounted on the hyperspectral camera as to be perpendicular to the sample under analysis, have been used. The choice of using four halogen lamps has generated a faster aging process of the blood due to the high temperatures reached; this means that the temporal analyses cannot be performed on this data since they were not truly representative of the blood aging process. In fact, the four halogen lamps have *"cooked"* the blood over the substrate, thus accelerating the aging process. For this reason, the first test, characterized by the use of four halogen lamps and a total of 23 different substrates, has been immediately interrupted in the first day of acquisition because the sudden colour change of the blood deposited over the substrates has been noticed. This is indicative of an aging process caused by the high temperature reached and it is not representative of a real aging process. Thus, after the interruption of the first test, it was necessary to reduce the number of halogen lamps to be used. Furthermore, in this test, the high number of substrates chosen have caused problems during the acquisition; in fact, it has

not been possible to do the precise acquisition of the spectral data at the set times. In addition, the single acquisition of 23 samples have resulted to be time consuming and difficult to perform. Moreover, when the first preliminary test has been performed, it was not known the time necessary by the camera to perform a single acquisition, which is approximately three minutes, thus the contemporaneous deposition of the blood drops over the different substrates has represented another problem. In fact, in this way it is not possible to acquire the data, i.e., blood spectra, at the set times; for example, the last sample would not be acquired at the set time, but it would be acquired at the set time plus the time necessary to perform the acquisition of 23 samples. These errors lead to the execution of a second preliminary test, which has been performed with an illumination system formed by two halogen lamps, mounted symmetrically on the hyperspectral camera, and considering a total of 15 different substrates. The number of lamps in the second test has been reduced according to the fact that four halogen lamps resulted to be dangerous for the biological sample under analysis. As the first test, the second has been performed with the environmental light, i.e., fluorescent lamps, on. The principal aim of the second test has been to verify if two halogen lamps as an illumination system is the correct number of lamps to use, in order to reduce the effect of the temperature increment, hence reducing the effect that heating has on the aging process of the blood. This test has been realised with a reduced number of samples to simplify the acquisition; furthermore, the blood has been deposited with a temporal distance of 5 minutes in order to be more precise in performing the acquisition at the set times. Moreover, the temporal distance of 5 minutes between each blood deposition has been chosen because it is approximately the time necessary to take the sample, perform the acquisition and switch to the next sample. In performing the second test, using two halogen lamps, the aging process of the blood, deposited over the substrates, has not be influenced by the heating effect, which has been significantly reduced. Thus, it has been decided to use, for the realization of the test bench, two halogen lamps since they do not interfere with the aging process of the blood. Nevertheless, also the second test has been prematurely stopped, specifically after the second day of acquisition. The second test has highlighted another problem, that is the influence of the environmental light, i.e., fluorescent lamps in this case, over the blood spectra acquired. In fact, this problem has been encountered since the second test has been carried out for a longer time than the first one that was suddenly stopped in the

first day of acquisition due to the influence of the high temperature reached. In fact, analysing the spectral data it has been possible to see the influence of the fluorescent lamps over the blood spectra acquired. Figure 81 shows the blood absorbance spectra at different times of the blood drop deposited over the Light Jeans; the acquisitions have been done using two halogen lamps as illumination system with the environmental lights on. From the figure (Figure 81) it is possible to see the influence of the environmental lights on blood absorbance spectra; in detail, it is possible to see the presence of sharp peaks at approximately 542 nm and 572 nm, corresponding to the α and β peaks of the blood, characterised by a high prominence, which over time decrease only in intensity. According to literature, the aging process of the bloodstain determines the decrement in the prominence of the two peaks, which become broader joining in a single band. [6][17] Thus, the high prominence of the peaks and the fact that they do not become broader joining in a single band as the time passes, is due to the influence of the environmental lights. Therefore, these spectra are not representative of the aging process of the bloodstain. In fact, fluorescent lamps intensity spectra are characterised by sharp emission lines and present a high variability spectrum, [59] which influences the overall behaviour of the blood spectra, as it is possible to see from Figure 81. Consequently, the blood absorbance spectra, obtained with the environmental light switched on, are characterised by sharps peaks provoked by the sharp emission lines of the fluorescent lamps, and they are also noisier with respect to the one acquired with the environmental lights switched off, due to the high variability intensity spectrum of the fluorescent lamps. Figures 82 and 83 are respectively the intensity spectrum of two halogen lamps plus the environmental lights and the intensity spectrum of two halogen lamps without the influence of the environmental lights. Making the comparison between the two intensity spectra (Figure 82 and 83), it is possible to see that the main difference between the two is caused by the presence of fine lines of emission, typical of the fluorescent lamp, that provoke the presence of different peaks in the intensity spectrum of the halogen lamps, specifically at 544 nm, 580 nm, and 611 nm, which instead is continuous (Figure 83). The presence of fine emission lines at 544 nm and 580 nm, in the intensity spectrum of the halogen lamps with the environmental light switched on, determines the high prominence of the β an α peaks presents over time in the blood spectra, contrary to what is reported in the literature. As a consequence, the second test shows how the environmental lights influence the blood

spectra and underlines the fact that in a real forensic application of the hyperspectral camera would be necessary to switch off the environmental lights and, more in general, to perform the acquisitions without the presence of illumination sources different from the illumination system used to acquire the data with the hyperspectral camera. Thus, one limiting factor of the hyperspectral camera is the fact that to use it would be necessary to guarantee the absence of other illumination sources that could influence the blood spectral features.

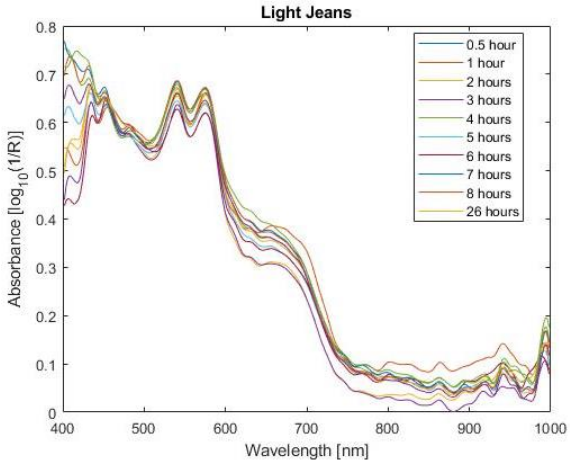

Figure 81 Absorbance spectra at different times of the blood deposited on the Light Jeans; the illumination system is formed by two halogen lamps and the environmental lights are switched on. The blood spectra are obtained from the second preliminary test.

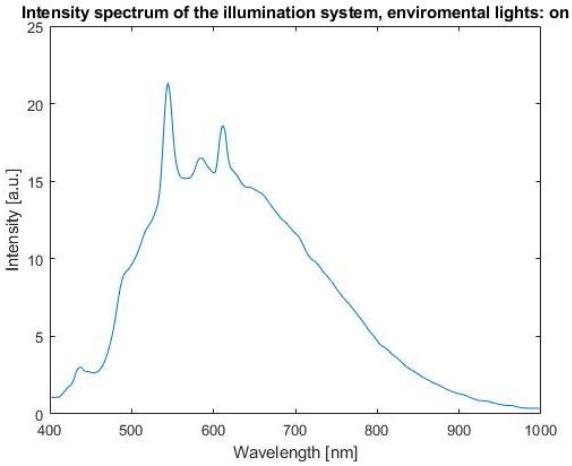

Figure 82 Intensity spectrum of two halogen lamps and the influence of the environmental light.

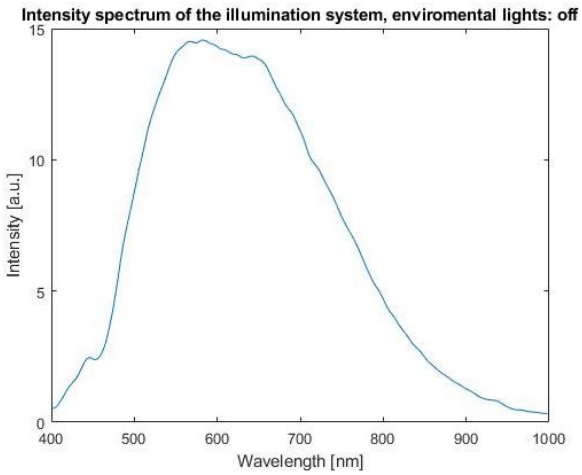

Figure 83 Intensity spectrum of the illumination system formed by two halogen lamps. The environmental lights are switched off.

The performing of the second preliminary test has confirmed the use of two halogen lamps as illumination system, since they do not interfere with the aging process of the blood, but it also demonstrated the influence of the environmental lights over the blood spectra. In fact, from these results, it has been clear that the final test bench will be characterised by the environmental lights switched off, to avoid spectral peaks and flickering disorder over the spectra acquired. The third preliminary test has been performed with the aim of finding the optimal region where to deposit the blood over four samples arranged on a single support. In fact, the previous two tests have been performed acquiring individually the samples, hence the single substrate has been placed approximately in the centre of the field of view of the camera, under the camera lens. In the first and second preliminary tests have been used a high number of substrates, respectively 23 and 15, and they have been acquired individually at the set times; this, in fact, led to the onset of complexity in the execution phase of the acquisition. Hence, the substrates have been arranged over a single support with the aim of optimizing the acquisition of a high number of samples, thus, to simplify the acquisition and to be more precise in performing the acquisition at the set times. As it has been decided to organise the samples in this way, it has been necessary to understand where to deposit the blood over the four substrates, arranged over a single support. To better understand where to place the blood, two blood drops have been deposited over the inner and the external

margin of four substrates, characterised by a dimension of 5.25 cm x 3.25 cm. Furthermore, the substrates have been cut with that specific dimension in a way to completely cover the field of view of the camera. This test has been performed only on four substrates (Wood, Light Jeans, Napkin, Dark Jeans), placed over a single support; there was no special reason on why these substrates have been chosen. The results of this test are reported in Figures 28, 29, 30 and 31, which shows a comparison of the absorbance spectra obtained for the blood drop placed in the two different areas of the substrates. From these figures, it is possible to see how the spectra of the blood drops, placed over the inner margin of the substrates, are affected by less noise with respect to the spectra of the blood drops deposited over the external margin. In details, for all the spectra of the blood drops deposited in the inner margin of the substrates, it is always possible to observe the presence of the Soret peak and the lower wavelengths are characterised by lower noise, and the peaks α and β are more visible, specifically for the Dark Jeans and the Wood. An explanation for the better spectra obtained for the blood deposited over the inner margin could be that the blood is exactly under the lens of the camera thus affected by less distortion and noise. Therefore, after performing this test, it has been chosen to deposit the blood over the inner margin of each substrate for the acquisition of the spectra data to use for the temporal analysis. Moreover, during the performing of this test, it has been decided to perform the calibration differently in respect to the first and second preliminary tests. In fact, it has been decided to perform the calibration of the white before each acquisition, while maintaining the dark calibration at the beginning, thus right after the switching on of the camera. The calibration of the white has been performed before each acquisition, in order to compensate the errors that could arise from the calibration of the sensor and in order to reduce the thermal noise (instrumental or sensor noise) occurring due to the prolonged used of the camera. [60][61]. The thermal error, together with other instrumental (or sensor) error, can cause noise over the spectral bands, thus lowering the efficiency of the hyperspectral system in performing the analysis. [61] This calibration procedure has been also adopted for the acquisition performed with the defined test bench. Finally, after the performing of the preliminary tests, it has been possible to define the test bench that has been used for the acquisition of the data used for the temporal analysis. Moreover, the previous described tests also show the way in which the samples should be prepared for the acquisition and how the calibration procedure should be performed. In fact,

the disposition of the substrates over a single support allows to obtain precise data, i.e., data acquired precisely at the set times and to simplify the acquisition of a high number of samples, allowing the optimization of it, and the calibration procedure, tested in the third preliminary test, allows to obtain spectral data little corrupted by the noise. Thus, to summarise, the test bench realised and then used for the acquisitions of the data is formed by:

- The hyperspectral camera, the Hinalea 4250.
- Two halogen lamps mounted symmetrically on the camera as to be perpendicular to the sample under analysis.
- The environmental lights, i.e., fluorescent lamps, switched off.

Thus, the 12 substrates, used for the data collection for the temporal analysis, have been organised in three groups of four to optimize the acquisition of a high number of samples, and the blood has been deposited over the inner margin of each substrate of a single support, according to the results obtained from the third preliminary test, with a temporal distance of 5 minutes between the substrates of one support and the other. Moreover, the calibration procedure performed for the data collection, is characterised by the execution of the dark calibration at the beginning, when the camera is switched on, and the calibration of the white performed before each acquisition, always according to the results obtained from the third preliminary test. For the collection of the data for the temporal analysis, it has been decided to acquire only the spectral range from 400 nm to 770 nm since it is the range in which the blood features are found, and in this manner the acquisition of a single sample is also faster than acquiring the entire range offered by the camera, which goes from 400 nm to 1000 nm. Figures 84 represent the blood absorbance spectra deposited over the Light Jeans obtained after the definition of the test bench, thus the spectral data used for the temporal analyses. Comparing Figures 81 and 84, it is possible to see how the data used for the temporal analysis, obtained from the test bench definition, are characterised by lower noise and less sharp β and α peaks, since there is no influence of the environmental light; moreover, the performing of the white calibration before each acquisition, guarantees the presence of the Soret peak that instead is not possible to see in the spectra obtained from the second preliminary test. This comparison shows how the first and second preliminary tests

performed lead to the definition of the test bench, from which it is possible to obtain spectra representative of the temporal changes occurring to blood over time and less affected by noise or interferences.

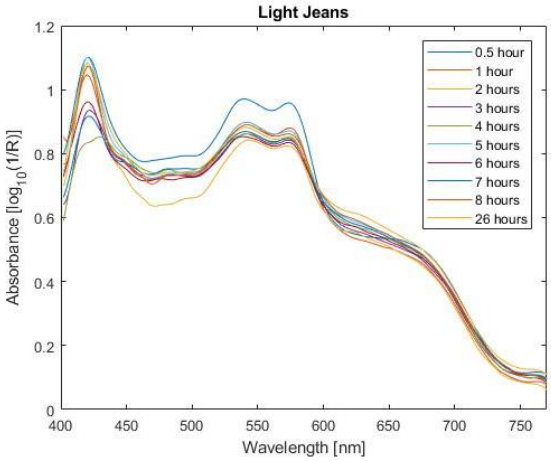

Figure 84 Blood absorbance spectra at different times; blood deposited over the substrates Light Jeans. Spectra obtained from the defined test bench.

After the definition of the test bench and the sample preparation, the data have been collected and subsequently, the temporal analysis has been performed. The first acquisition of the sample has been performed after 30 minutes its deposition, leaving the samples to dry at the room temperature; this has been performed because it is impossible in a real forensic case work to deal with a bloodstain that has just been deposited. Moreover, letting the blood dry becomes important when performing a near-infrared analysis, since in the first minutes, blood absorbance spectrum is dominated by the absorption peaks of water. [9] Then the acquisitions have been performed with a high rate in the first day of acquisition, acquiring every hour, then slowly reducing the acquisitions, which have been reduced to a single acquisition a day after the third day from the initial deposition. Initially, the acquisitions have been performed with a high rate with the purpose of estimating the dynamic spectral changes due to haemoglobin oxidation, while the prolonged acquisitions have been realised in order to see the spectral variations caused by the aging process of blood. [62] Initially, the temporal analysis, that is the extrapolation of a set of parameters able to describe the temporal changes occurring to the blood spectra, has been performed only on the White Tile,

since the light colour of the tile allows the optimal visualization of the bloodstains without any interference of the colour of the substrate. Figure 32 shows the absorbance spectra in function of time of the blood deposited over the White Tile. From this figure it is possible to see the main characteristics of the bloodstain spectra, which in the visible region is dominated by the haemoglobin absorbance spectrum and its derivatives. [13] First of all, in the blood spectrum a t = 0.5 hours, are visible the Soret peak due to the presence of haemoglobin, at approximately 414 nm, and the two distinctive absorption peaks, the β and the α peaks, respectively at 542 nm and 572 nm, given by the oxy-haemoglobin. The spectrum presents also a very steep slope in the wavelength range between 600 nm and 650 nm, according to the fact that no met-haemoglobin and hemichrome are found. Considering now the spectra over time, it is possible to observe the temporal changes occurring to the blood spectra, corresponding to the autoxidation and denaturation processes occurring to haemoglobin outside the human body, described in the third chapter of this work. The intensity of the two oxy-haemoglobin absorption peaks (β and α) decreases over time and the two peaks tend to collapse into one, as it is possible to see from the figure (Figure 32). This meets what is found in literature. In fact, with the increment in age of the bloodstain, the β and the α peaks decrease in intensity, becoming broader and joining in a single band. [17] The decrement of the β and the α peaks are due to the decrement of the amount of oxy-haemoglobin that undergoes into an autoxidation process, with the consequently formation of the met-haemoglobin and hemichrome. [13] Always from Figure 32, another change of the spectrum over time can be seen. In fact, the steepness of the curve between 600 nm and 650 nm changes, specifically it decreases. This also is found in literature since the decrement of the steepness in the curve between 600 nm and 650 nm are due to hemichrome and met-haemoglobin formation. [6] From the Figure 33, it is also possible to see, over time, the appearance of another peak, at 620 nm. This peak is the absorption peak of the met-haemoglobin, which in fact, as found in literature, absorbs at indicatively 626 nm. [8] In the end, the changes found in the blood absorbance spectra all agree with the previous studies performed. Starting from the changes occurring over time to the spectra of the blood deposited over the White Tile, three temporal parameters have been considered, to quantify the temporal changes occurring to blood and representative of the autoxidation and denaturation processes to which haemoglobin in a bloodstain is subjected. The first, the

Coefficient m, is the absolute value of the angular coefficient of the interpolating line to the blood absorbance spectra between the range that goes from the α peak, and the value assumed by the spectra at 620 nm. In fact, this parameter has been chosen in order to represent the changes occurring to the blood spectra in the range that goes from 570 nm to 620 nm, thus comprising the changes occurring to blood absorbance spectra due to the decrement of the intensity of the α peak and the appearance of the met-haemoglobin peak at 620 nm. The decrement of the intensity of the α peak and the appearance of the met-haemoglobin peak, determine a change in the slope of the interpolating line of the spectra in the pre-mentioned range. In fact, as it is possible to see in the Figure 35, the interpolating line is characterized by a slope whose steepness changes over time; moreover, since the line presents a negative angular coefficient, it has been considered its absolute value. The second parameter considered, the *Ratio,* is obtained as the ratio between the α peak and the value assumed by the absorbance spectrum at 620 nm. The idea of the realization of this parameter has come from the fact that several studies have already used a similar parameter to quantify the temporal changes occurring in the blood spectra, as performed by Li et al. [14] that have used the ratio of two values assumed by the spectra to perform the kinetics analysis of the aging process of a bloodstain, or in the original study of Kind et al. [63] that have performed, for the temporal analysis, the measurements at 560 nm for the α peak, which have been standardised performing the ratio of the peak with the value assumed by the spectrum in the adjacent valley. For both the previous two parameters (*Coefficient m* and *Ratio*), the value of 620 nm has been chosen since it is the absorption band of met-haemoglobin; in fact, met-haemoglobin gives an absorption peak at approximately 626 nm. [8] Figure 36, shows the values used to perform the ratio, specifically the red stars are the α peak, which changes over time, while the blue star is the value of the absorbance spectrum at the wavelength value of 620 nm. The last parameter, the *Inflection point*, has been realised observing the first order derivative of the blood absorbance spectrum. The derivative has been taken into consideration according to the fact that it makes the dips and the peaks of the aged blood spectrum more evident. [6] In general, the derivative of the absorbance spectrum is performed since it can remove the baseline shifts, which are unwanted effects that could be generated by lamp or detector instabilities and shows specific characteristics that can be used to discriminate two absorbance spectra that are similar. [64] Moreover, the first order

derivative of an absorbance spectrum presents typical features, and it is defined as the rate of change of the absorbance with respect the wavelength. [64] The first order derivative passes through zero in correspondence of the wavelength of the maximum absorbance peak, and at either side of this point, there are positive and negative bands, where the relative maximum and minimum are at the same wavelengths of the inflection points of the absorbance spectrum, as it is possible to see from Figure 38. [64] Hence, observing the first-order derivative spectra of the blood (Figure 38), it has been taken in consideration, as a potential temporal parameter, the absolute value of the peak that the derivative assumes in the wavelength range from 572 nm to 620 nm. Therefore, the *Inflection point* corresponds to the variation of the angular coefficient of the tangent line at the inflection point of the absorbance spectrum, which therefore changes over time. Since the parameter is defined in the range that goes from 572 nm to 620 nm, it is possible to hypothesise that its changes are due to the autoxidation and denaturation processes that lead to the formation of met-haemoglobin and hemichrome, which lead to changes in bloodstain spectra in the wavelength range that goes from 600 nm to 650 nm. After the extrapolation of the parameters from the blood absorbance spectra deposited over the White Tile, the plot of the values obtained in function of time has been performed. Figures 33, 35 and 37 represent respectively the plot of the *Coefficient m*, the *Ratio*, and the *Inflection point* in function of time. As it is possible to see in all the three figures, the parameters present a decreasing exponential trend, thus characterised by a fast and distinctive decay, specifically in the first hours of acquisition, followed then by a slow decay, in the extended acquisitions. Moreover, from the comparison of the *Coefficient m* and the *Inflection point* with the parameter *Ratio*, it seems that the *Ratio*, over time, tends to assume more or less the same value, thus it seems that it is more stable over the long period, while the *Coefficient m* and the *Inflection point* vary more. Moreover, both the *Coefficient m* and the *Inflection point* present the fast decay up to the 50^{th} hour, while the *Ratio* starts to be more stable after 24 hours from the blood deposition. Nevertheless, all the parameters present a decreasing exponential trend, which is consistent with the literature [14], that suggests the presence of two kinetics processes with different time scales, corresponding to the changes occurring to haemoglobin over time. In detail, the fast decay, found in the first hours after blood deposition, subsequently followed by the slow decay, are due to the transition rate of oxy-haemoglobin into met-haemoglobin

and hemichrome, which at first is rapid (fast decay), but then decreases as the stain ages (slow decay). [13] Since the aim of the study is the age estimation of the bloodstain, it is therefore necessary to determine the relation existing between the parameters found and the age of the blood, in order then to obtain a curve, expressing the relation, that could be used to perform the age estimation of the bloodstain, starting from the measuring of the value of the temporal parameter. Therefore, from the observation of the obtained data and supported from the literature (decreasing exponential representative of the autoxidation and denaturation processes of the haemoglobin), it has been decided to perform an exponential fitting of the obtained data. The fitting has been performed using an exponential formed by two terms (Equation 5), since the changes occurring to haemoglobin are first fast while slow as the stain ages. In fact, the exponential with two terms is used when the outcomes are the result of the sum of a fast and slow exponential decay. [65] The fitting has been done, since for fitting procedure it is intended to adjust the coefficient of a known function in a way that best matches the data, hence, to obtain a curve that best approximates the trend of the data, able to represent the relation existing between the data. [50] Thus, three curves have been obtained (Figures 39, 40, 41), one for each parameter extracted from the blood spectra, and the value of the RMSE together with the value of R^2 have been evaluated to assess the goodness of the fitting. Therefore, the RMSE and the R^2 have been used to perform the uncertainty analysis of the results. In all the fittings performed, the time has been considered as the dependent variable (y), while the temporal parameter has been considered as the independent variable (x), since the goal is the determination of a curve, i.e., a function, able to represent the relationship between blood age and the parameter, with the aim of estimate blood age starting from the knowledge of the value of the temporal parameter that can be extracted from the blood spectrum. The first fitting performed, Figure 39, represents the exponential fitting performed over the obtained value of the *Coefficient m* and the time (blood age) expressed in hours. The RMSE obtained is 14.26 hours, representing an absolute error measure of 14.26 hours over the entire range of time considered, which is of 385 hours. This means that the curve fits well the data and can represent the relationship between the two variables considered. The value of R^2 is 0.9860 and it is near to 1, which means that knowing the value of the independent variable, that in this case is the value of the parameter *Coefficient m*, it is possible to estimate, with high capacity, the value of the dependent

variable, that is the age of the blood, and the error of the estimate is extremely low. The second fitting, Figure 40, has been performed between the values of the *Ratio* and the time, in the same manner of the *Coefficient m*. The RMSE obtained is 15.35 hours; also, in this case the curve fits well the data and can represent the relationship between the two variables. The R^2 is 0.9838, thus also in this case it is possible to estimate the age of the blood extrapolating the value of the *Ratio* from blood spectrum. Furthermore, the fact that the curve obtained for the *Ratio* becomes stable after the 24^{th} hour makes the curve less sensible. The last fitting, Figure 41, is the fitting performed between the *Inflection point* and the time. The RMSE value obtained is 19.50 hours; respect to the previous two RMSE values obtained, it is the worst one, but still indicative of a good fitting over the data. For what concerns the value of R^2, it is 0.9738, also in this case near to 1 and indicative of a high estimate capacity. Hence, the three temporal parameters obtained present a relation with the blood age, and the relationship existing between them can be represented with a decreasing exponential. From the values of RMSE and R^2, the most promising parameter is represented by the *Coefficient m*. Nevertheless, the exponential curves obtained for each temporal parameter can be used to perform the estimate of the bloodstain age deposited over the White Tile, hence over a white and reference substrate, starting from the knowledge of the temporal parameter, according to the high R^2 values that have been obtained. After these findings, the same analysis has been extended over the blood deposited on the other substrates, different from the White Tile. The other substrates chosen present different colours but also different textures. Although the Coefficient *m* presents the best RMSE and R^2 values, all the three defined temporal parameters have been taken in consideration. Hence, the three temporal parameters have been extracted from the input spectra, i.e., the spectra without any background correction, of the blood deposited over the substrates, then the fitting procedure has been performed, in order to obtain a single curve representing the relation between the parameter and the blood age with respect to a single substrate, that is the obtaining of the function expressing the relationship between the temporal parameter and the blood age that could be used to estimate the age of the blood, knowing the substrate. In general, the RMSE values associated to the curves (Figures 44, 49, 54) are quite good for the majority part of the substrates, thus demonstrating again that the decreasing exponential represents in a good manner the relation between the parameters and the age of the bloodstain. The values of R^2

are also quite good for the majority part of the curves of each substrate, as it is possible to see in Figures 45, 50 and 55. The best results are reached for those samples where the influence of the substrate does not interfere too much with blood spectra, specifically the light-coloured substrates, as the Light Jeans. In fact, Figures 42, 47 and 52, represent the exponential curves of each temporal parameters of the Light Jeans; furthermore, also the RMSE and the R^2 values are quite good for all the curves of each temporal parameters (Figures 44, 49 and 54 and Figure 40, 50 and 55). For instance, the curves, which expresses the relation between the values of the temporal parameters extracted from the blood spectra deposited over the Light Jeans and the age of the blood, are characterised by an RMSE value of 30.61 hours for the *Coefficient m*, 21.46 hours for the *Ratio* and 29.72 hours for the *Inflection point*, with a R^2 value of 0.9441 for the *Coefficient m*, 0.9725 for the *Ratio* and 0.9473 for the *Inflection point.* On the contrary, especially for some substrates, as the Black Paper and the Red Paper for the *Coefficient m*, the Black Paper for the Ratio, and the Black Paper, the Sponge, and the Dark Jeans for the *Inflection point*, the RMSE values associated to the curves are high, thus not representing a good fitting, and thus, the impossibility to have a curve able to represent the relation between the parameters and the age of the blood deposited on those specific substrates. The same is reflected over the R^2 value, in fact for the curve, obtained fitting the values of the temporal parameters from the spectra of the blood deposited on the same previously mentioned substrates, the worst R^2 values are found, thus representing the impossibility to use the curve to estimate the age of the blood that has been deposited over these substrates. Furthermore, for the curve associated to the Sponge a negative R^2 value is obtained since the curve does not follow the trend of the data; in fact, the fit is worse that fitting a horizontal line. [66] In particular, the worst RMSE and R^2 values are obtained for the curves that expresses the relation between the values of each temporal parameter extracted from the spectra of the blood deposited on the Black Paper and the blood age, since the black colour of the substrate interferes with blood absorbance spectra, completely covering it. In fact, as it is possible to see in Figure 85, the blood absorbance spectra differ completely from the blood absorbance spectra found when the blood is deposited on a white substrate, as the White Tile (Figure 32).

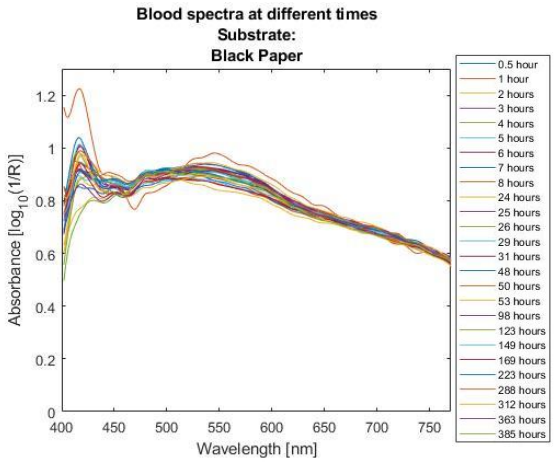

Figure 85 Absorbance spectra of the blood deposited over the Black Paper at different times.

Specifically, an RMSE value of 126.9 hours for the *Coefficient m*, 128.5 hours for the *Ratio* and 130.5 hours for the *Inflection point*, while a R^2 value of 0.0570 (5.70%), 0.0321 (3.21%), and 0.0025 (0.25%) have been respectively obtained for the curves of the *Coefficient m*, the *Ratio,* and the *Inflection point*. These values of RMSE and R^2 have been obtained because the values of each temporal parameter, Figure 43, 48 and 53, do not present any exponential distribution, but they are randomly distributed. Things become worst when a single curve is researched to express the relation between all the values of a temporal parameter, obtained from the blood spectra deposited on all the substrates, and the blood age. In fact, for all the three parameters, it is not possible to obtain a single curve for all the substrates, as it is possible to see from the Figures 46, 51, and 56. From these figures (Figure 46, 51, 56) it is possible to see how the curve is not able to fit all the values, and moreover, it is possible to see a total of 11 distinctive exponential distribution of the values, where each one is associated to a specific substrate. The RMSE values associated to the curves, respectively of 115.9 hours, 116.9 hours, and 113.4 hours, confirm the bad fitting, hence the impossibility to determine a single curve representative of the relation between the temporal parameters and the blood age that can be used to perform the age estimation of the blood, regardless of the substrate. Moreover, the curves of all the three parameters, are characterised by bad R^2 values, respectively of 0.0761 (7.61%) for the *Coefficient m*, 0.0602 (6.02%) for the *Ratio*, and 0.1150 (11.50%) for the *Inflection point*, confirming the impossibility to use the curve

to make estimation about the age of the blood, regardless the substrate. From these results, it is understandable how the colour of the substrate and its texture can influence blood spectra; in fact, the substrate influences the behaviour of the blood spectra, hence the relative values of the temporal parameters extracted from the blood spectra differ from each other, and especially for the blood deposited on the Black Paper, the values obtained do not present any exponential trend. Indeed, the coloured background, absorbing the visible light, disturb the measure of the reflectance spectra of the bloodstain, [67] hence the acquired reflectance spectra differ from the typical blood reflectance spectrum, and this is, of course, also reflected in the absorbance spectrum, and this is the reason why the values of the temporal parameters differ from each other and in some cases do not present any exponential trend. For this reason, it has been decided to perform the same procedure over the predicted spectra, thus on the blood spectra that have been corrected from the contribution of the substrate, i.e., the influence that the colour of the substrate has on the blood spectrum. The correction has been performed using the neural network model defined and used by Maria Teresa Pucarelli in her thesis "Hyperspectral Imaging System in Forensic Science: Background Correction via Neural Network". After the background correction, for the *Coefficient m*, as it is possible to see in Figure 59, good RMSE values are obtained, together with good R^2 values, for each fitting procedure performed between the values of the temporal parameter extracted from the blood spectra and the age of the blood deposited on each the substrate. In particular, the curves obtained for the substrates Black Paper and Red Paper, which before the correction presented high RMSE values, show a reduction of the RMSE. In fact, as it is possible to see in Figure 61, in which a comparison of the RMSE values of the curves, obtained for the input spectra and the predicted spectra of the blood, is performed, there is a high decrement of the RMSE values associated to the curves of the Black Paper and the Red Paper after the correction. Moreover, also the R^2 values, obtained with the interpolation of the values of the *Coefficient m* after the correction with the blood age, are good; in fact, as it is possible to see from Figure 60, specifically for the curves of the Black Paper and the Red Paper, there is an increment in the R^2, particularly visible for the Black Paper. Hence, this demonstrates not only that the curves obtained are able to express the relationship between the temporal parameter and the age of the blood and can be used to perform the estimate of the age of the blood knowing the substrate, but also the necessity of the removal of the substrate colour

contribution that can completely influenced the behaviour of the blood spectrum. In fact, as it is possible to see from Figure 58, which represents the interpolating curve obtained for the blood deposited on the Black Paper after the correction, the values present an exponential trend, thus the fitting procedure produces an exponential curve with a lowered RMSE value (48.16 hours) and a R^2 of 0.8641. Moreover, the background correction has also produced better results for the curve expressing the relation between the *Coefficient m* and the age of the blood deposited on the Light Jeans, as it is possible to see from Figure 59 and 60, with an RMSE value of 17.55 hours and an R^2 of 0.9816. Consequently, the background correction works well, and it is hence possible to obtain a single exponential curve, expressing the relation between the temporal parameter and the blood age, for each substrate analysed, and could be potentially used to perform the age estimation, knowing the substrate, and measuring the temporal parameter (*Coefficient m*). The final step has been the realization of a single exponential curve expressing the relationship between the temporal parameter (*Coefficient m*) and the blood age, regardless from the substrates, as has been performed for the input spectra. After the background correction, indeed, it has been possible to obtain a single exponential curve, Figure 62, with a good RMSE value (45.46 hours), which indicates that the curve fits well the data and it is able to represents the relation between the parameter and blood age. Moreover, the R^2 value obtained are extremely good, in fact it has increased from 0.0761 to 0.858, meaning that the curve presents a high capacity to estimate the age of the blood knowing the value of the *Coefficient m*. Figure 63 shows the comparison between the RMSE values obtained with the fitting procedure in case of the input spectra and the predicted spectra, when the fitting has been done in order to obtain a single curve regardless from the substrates. Figure 64 shows the comparison between the values of R^2 obtained for the input spectra and the predicted spectra. Both the figures (Figure 63 and 64), show the effects of the background correction, reflected over the better values of RMSE and R^2 associated to the curve. As for the *Coefficient m*, comparable results have been obtained for the *Ratio*. In fact, from Figure 67, it is possible to observe the RMSE values obtained after the application of the correction, where good RMSE values, associated to the curves, have been obtained for all the substrates, and in particular for the Black Paper, where a marked decrement of the RMSE value is observed. In fact, from the comparison of the RMSE values obtained from the input spectra and the predicted spectra, Figure 69, it is possible to see the

overall ameliorating of the RMSE values associated to the curves, specifically for the curve obtained for the Black Paper, which has now, after the correction, an RMSE value of 54.74 hours. In fact, from Figure 66, the values for the *Ratio* parameter obtained after the background correction of the blood spectra deposited on the Black Paper, present an exponential trend, different from the highly dispersed values observable before the correction (Figure 48). Moreover, as it is possible to see from Figure 68, also the values of R^2 are better with respect to the values obtained without the correction, in particular for the curve associated to the Black Paper. In fact, the curve obtained for the Black Paper present a R^2 value of 0.8244, extremely different from the value of 0.0321 obtained without the correction, demonstrating that the exponential curve, obtained after the background correction, can be used to estimate the age of the blood deposited over the Black Paper. As for the *Coefficient m*, the background correction has also produced better results for the curve expressing the relation between the *Ratio* and the age of the blood deposited on the Light Jeans, as it is possible to see from Figure 69 and 68, with an RMSE value of 15 hours and an R^2 of 0.9866. Hence, also in this case, a single exponential curve, expressing the relation between the temporal parameter (*Ratio*) and the blood age, for each substrate can be obtained, which could be used to estimate the age of the bloodstain over a particular substrate. After the correction, also for the *Ratio* a single exponential curve, regardless from the substrate, is obtained, Figure 70. As it is possible to see from the figure (Figure 70) a single exponential curve is obtained; moreover, the RMSE value is also good, representing an overall error of 41.32 hours, while the R^2 is of 0.8830. Also in this case, the background correction works well, as it is possible to see from the comparison of the RMSE values in Figure 71 and from the comparison of the R^2 values in Figure 72, and, consequently, it is possible to obtain a single exponential curve expressing the relation between the temporal parameter and the blood age, which could be used to estimate bloodstain age, regardless form the substrate, with an absolute error measure (RMSE) of 41.32 hours and with an estimate capacity of 88.03%. The same procedure has been performed in case of the *Inflection point*. The single exponential curves, obtained for the blood deposited on each substrate, present an ameliorating RMSE value, in particular the curves obtained for the substrates Black Paper (50.09 hours), Dark Jeans (36.66 hours) and Sponge (39.49 hours), as it is possible to see in Figure 75 and, in particular, in Figure 77, where a comparison of

the RMSE values for each curve, obtained from the fitting procedure performed between the values of the temporal parameters extracted from the input and the predicted spectra of the blood and the blood age, is done. Moreover, also the values of R^2 are better for the curves of the same previously mentioned substrates after the correction with respect to the temporal analysis performed with the input spectra; in fact, they respectively assume R^2 values after the correction of 0.8530, 0.9198 and 0.9069, as it is possible to see from Figure 76. Moreover, the background correction has also produced better results for the curve expressing the relation between the *Inflection point* and the age of the blood deposited on the Light Jeans, as it is possible to see from Figure 77 and 76, with an RMSE value of 24.41 hours and an R^2 of 0.9644. Also in this case, it is possible to obtain a single exponential curve for each substrate, which could be used to estimate the blood age depending on the substrate where the stain is deposited, with good RMSE and R^2 values. Moreover, after the correction, also for the *Inflection point,* it is possible to obtain a single exponential curve regardless from the substrate, as can be seen in Figure 78, characterised by a RMSE value of 42.87 hours and R^2 of 0.8736. Hence, also in this case, the correction has worked well, as it possible to see from the comparison of the RMSE values in Figure 79, and for the better R^2 values obtained, Figure 80. Consequently, it is possible to obtain a single exponential curve expressing the relation between the temporal parameter (*Inflection point*) and the blood age regardless from the substrate, which could be used for the estimation of the blood age, with a RMSE of 42.87 hours and a R^2 of 0.8736.

7. CONCLUSION

Hyperspectral imaging system is a very promising technique, which finds application in different fields, from the medical field, passing to the art and conservation fields, reaching the forensic science field. In this study, it has been seen the application of the hyperspectral imaging in the forensic field application, with the performing the temporal analysis, in qualitative and quantitative manner, of bloodstains deposited over different substrates, with the aim of the estimate of the age of the bloodstain deposited over different substrates. Before the performing of the temporal analysis, the definition of the test bench resulted to be important, to obtain optimal data to use for different purposes analyses, that in this case has been the temporal analysis. Consequently, after the definition of the test bench, which has also led to the determination of the sample preparation and acquisition procedure, and the obtaining of the spectral data, the first thing done has been to study the changes occurring to blood absorbance spectrum caused by the aging process, hence performing the temporal analysis in a qualitative way, thus directly observing the spectral changes over time, which indeed, are caused by the different autoxidation and denaturation processes occurring to the haemoglobin in the stain. According to the fact that the colour of the substrate can influence the behaviour of the spectrum of the blood deposited over it, the temporal analysis has first been performed on the blood deposited over the White Tile, and then extended to the blood deposited over the different substrates. Subsequently, a total of three parameters have been defined and extracted from the blood over the White Tile, which are able to express in a quantitative way the processes leading to the spectral changes of the bloodstains. Thus, observing the data and supported from the literature, an exponential fitting has been performed over the values obtained for the three temporal parameters, to determine the curve expressing the relationship between the temporal parameter and the bloodstain age. The low values of the RMSE with the consequently high value of R^2, have suggested that the curves are able to represent the relationship, thus it can be used to perform the age estimation of the bloodstain deposited over the White Tile. Moreover, the *Coefficient m*, due to the lowest value of RMSE and the highest value of R^2, have resulted to be the most promising parameter for the White Tile. Supported from these results, the temporal analysis has been extended to the other samples, hence the same procedure performed for the White Tile has been performed for the remaining 11 substrates, with the aim of finding a single curve for each

parameter for each substrate, which could be used to estimate the age of the bloodstain knowing the substrate, and in the end, finding a single curve for all the values of each parameter obtained from the different samples, which could be used to estimate the age of the bloodstain regardless from the substrate, hence not knowing the substrate. The RMSE values and the R^2 obtained are quite good for the majority part of curves associated to each substrate, which could be used in the age estimation of the bloodstain knowing the substrate; nevertheless, problems have been encountered when dealing with substrates as the Black Paper, whose colour completely changes the absorbance spectrum of the blood, and, consequently, also the temporal parameter extracted from the spectra present no exponential trend, causing high RMSE values and low R^2. When the single curve, regardless from the substrate, has been searched, the value of the RMSE and R^2 are quite bad, demonstrating the impossibility to find a single curve that could be used in the age estimation of the bloodstain not knowing the substrate. The reason why the values of RMSE and R^2 are quite bad, is due to the fact that the values of the temporal parameters change according to the substrate colour influence, hence suggesting the necessity to perform a background correction of the blood spectra. For this reason, the neural network model defined in the thesis of Maria Teresa Pucarelli, has been used. Finally, the same procedure has been performed over the so-called predicted spectra, which are the blood spectra that have been corrected from the background influence with the neural network model. The same procedure has been performed over the corrected spectra for all the temporal parameters, first considering the blood deposited on the single substrate, then considering obtaining a single curve for all the substrates, hence a curve able to estimate the bloodstain age regardless the substrate. The values of RMSE and R^2 obtained for the curves, are all good, also for those substrates, as the Black Paper which have been problematic before the correction. Moreover, also the RMSE and R^2 obtained in case of a single curve for all the substrates are good for all the temporal parameter considered, suggesting that the curves can be used to perform the age estimation of the bloodstains deposited over different substrates. This means that the defined curves for all the substrates could be used for the estimate of the age of the bloodstain, without knowing the substrates, hence in this way it is possible to directly used them to obtain an estimate of the bloodstain without considering the use of the curve relative to the substrate, since the curves obtained are characterised by a low RMSE and high R^2. In the end, all the three parameters

found are related with the blood age, with a relationship expressed by a decreasing exponential. Moreover, the defined curve present similar RMSE and R^2 values, which are optimal when the background correction is performed. Although this, the optimal RMSE and R^2 values are obtained after the correction for the *Inflection point.* Hence, this demonstrates not only that the obtained curve could be used to perform the age estimation of the bloodstain knowing the substrate, and not knowing it, but also the importance of the background correction, that is necessary when dealing with bloodstains analysis performed with hyperspectral imaging system. Although the values of RMSE and R^2 are optimal for the *Inflection point*, it is not possible to say which is the optimal temporal parameter to use to perform the age estimation of a bloodstain since, for all the temporal parameters, the exponential curves obtained after the background correction present similar RMSE and R^2 values. Moreover, since for the White Tile the optimal results have been obtained for the *Coefficient m*, this shows that the correction via Neural Network creates something of uncontrollable, and this is the reason why that all the three parameters have been taken in consideration when the temporal analysis has been extended to the other substrates. In conclusion, this work leads to the definition of the test bench to use to obtain optimal data with the hyperspectral imaging system. Moreover, this work lead also to the application of the background correction via a Neural Network model. The results obtained are consistent with the literature, showing also the importance of performing the background correction when dealing with blood deposited over different substrates, and suggesting that the defined temporal parameters are related with bloodstain age, and the curves, expressing the relationship, could be used to perform the age estimation of bloodstain deposited over different substrates, in case in which the substrate is known, hence using the curve defined for each substrate, and regardless from the substrate, hence when it is not known, using the more general curve defined for all the substrates.

REFERENCES

[1] Siegel, Jay A. "Forensic Science". *Encyclopedia Britannica*, 1 Jun. 2020, https://www.britannica.com/science/forensic-science.

[2] Dictionary of Forensic Science - Oxford Reference: https://www.oxfordreference.com/view/10.1093/acref/9780199594009.001.0001/acref-9780199594009

[3] Definition of Forensic Science (all-about-forensic-science.com): https://www.all-about-forensic-science.com/#:~:text=Forensic%20science%20is%20the%20scientific,evidence%20suitable%20for%20legal%20proceedings.&text=Forensic%20scientists%20determine%20scientific%20facts,courts%20or%20other%20legal%20proceedings.

[4] What is Forensic Science? - Definition, History & Types - Video & Lesson Transcript | Study.com: https://study.com/academy/lesson/what-is-forensic-science-definition-history-types.html

[5] A. Majda, R. Wietecha-Posłuszny, A. Mendys, A. Wójtowicz, and B. Łydżba-Kopczyńska, "Hyperspectral imaging and multivariate analysis in the dried blood spots investigations," *Appl. Phys. A Mater. Sci. Process.*, vol. 124, no. 4, pp. 1–8, 2018, doi: 10.1007/s00339-018-1739-6.

[6] M. Zulfiqar, M. Ahmad, A. Sohaib, M. Mazzara, and S. Distefano, "Hyperspectral imaging for bloodstain identification," *Sensors*, vol. 21, no. 9, pp. 1–20, 2021, doi: 10.3390/s21093045.

[7] G. Edelman, T. G. van Leeuwen, and M. C. G. Aalders, "Hyperspectral imaging for the age estimation of blood stains at the crime scene," *Forensic Sci. Int.*, vol. 223, no. 1–3, pp. 72–77, 2012, doi: 10.1016/j.forsciint.2012.08.003.

[8] T. Bergmann, F. Heinke, and D. Labudde, "Towards substrate-independent age estimation of blood stains based on dimensionality reduction and k-nearest neighbor classification of absorbance spectroscopic data," *Forensic Sci. Int.*, vol. 278, pp. 1–

8, 2017, , doi: 10.1016/j.forsciint.2017.05.023.

[9] G. Edelman, V. Manti, S. M. Van Ruth, T. Van Leeuwen, and M. Aalders, "Identification and age estimation of blood stains on colored backgrounds by near infrared spectroscopy," *Forensic Sci. Int.*, vol. 220, no. 1–3, pp. 239–244, 2012, doi: 10.1016/j.forsciint.2012.03.009.

[10] J. Yang, "Crime Scene Blood Evidence Detection Using Spectral Imaging", Rochester Institute of Technology, 2019.

[11] S. Cadd, B. Li, P. Beveridge, W. T. O'Hare, and M. Islam, "Age determination of blood-stained fingerprints using visible wavelength reflectance hyperspectral imaging," *J. Imaging*, vol. 4, no. 12, pp. 5–13, 2018, doi: 10.3390/jimaging4120141.

[12] H. Lin, Y. Zhang, Q. Wang, B. Li, P. Huang, and Z. Wang, "Estimation of the age of human bloodstains under the simulated indoor and outdoor crime scene conditions by ATR-FTIR spectroscopy," *Sci. Rep.*, vol. 7, no. 1, pp. 1–9, 2017, doi: 10.1038/s41598-017-13725-1.

[13] R. H. Bremmer, A. Nadort, T. G. van Leeuwen, M. J. C. van Gemert, and M. C. G. Aalders, "Age estimation of blood stains by hemoglobin derivative determination using reflectance spectroscopy," *Forensic Science International*, vol. 206, no. 1–3, pp. 166–171, 2011, doi: 10.1016/j.forsciint.2010.07.034.

[14] B. Li, P. Beveridge, W. T. O'Hare, and M. Islam, "The age estimation of blood stains up to 30 days old using visible wavelength hyperspectral image analysis and linear discriminant analysis," *Science and the Justice*, vol. 53, no. 3, pp. 270–277, 2013.

[15] Imaging system | definition of Imaging system by Medical dictionary (thefreedictionary.com): https://medical-dictionary.thefreedictionary.com/Imaging+system

[16] G. J. Edelman, E. Gaston, T. G. van Leeuwen, P. J. Cullen, and M. C. G. Aalders, "Hyperspectral imaging for non-contact analysis of forensic traces," *Forensic Science International*, vol. 223, no. 1–3, pp. 28–39, 2012, doi: 10.1016/j.forsciint.2012.09.012.

[17] B. Li, P. Beveridge, W. T. O'Hare, and M. Islam, "The estimation of the age of a blood stain using reflectance spectroscopy with a microspectrophotometer, spectral pre-processing and linear discriminant analysis," *Forensic Science International*, vol. 212, no. 1–3, pp. 198–204, 2011, doi:10.1016/j.forsciint.2011.05.031.

[18] B. Li, P. Beveridge, W. T. O'Hare, M. Islam, "The application of visible wavelength reflectance hyperspectral imaging for the detection and identification of blood stains", *Sci. Justice*, no. 54, pp. 432-438, 2014, doi: 10.1016/j.scijus.2014.05.003.

[19] J. Zwinkels, "Light, Electromagnetic Spectrum," *Encycl. Color Sci. Technol.*, pp. 1–8, 2015, doi: 10.1007/978-3-642-27851-8_204-1.

[20] G. J. J. Verhoeven, "The reflection of two fields – Electromagnetic radiation and its role in (aerial) imaging", *AARGnews*, no. 55, pp. 10–18, 2018, doi: 10.5281/zenodo.3534245.

[21] R. D. Overheim, D. L. Wagne, "Light and Color", United States of America, Wiley, 1992. ISBN: 0-471-08348-8.

[22] F. M. Mirabella, "Modern Techniques in Applied Molecular Spectroscopy", United States of America, Wiley, 1998. ISBN: 0-471-12359-5.

[23] Considerations for Diffuse Reflection Spectroscopy | American Laboratory: https://www.americanlaboratory.com/914-Application-Notes/190743-Considerations-for-Diffuse-Reflection-Spectroscopy/

[24] PIKE_Diffuse-Reflectance-Theory-Applications.pdf (piketech.com): https://www.piketech.com/files/pdfs/PIKE_Diffuse-Reflectance-Theory-Applications.pdf

[25] Absorption of Light | Facts, Summary & Definition | Chemistry Revision (alevelchemistry.co.uk):https://alevelchemistry.co.uk/definition/absorption-of-light/

[26] Introduction to Spectroscopy.pdf (su.se): https://www.su.se/polopoly_fs/1.521101.1602178917!/menu/standard/file/Introduction%20to%20Spectroscopy.pdf

[27] SPETTROSCOPIO in "Enciclopedia Italiana" (treccani.it): https://www.treccani.it/enciclopedia/spettroscopio_%28Enciclopedia-Italiana%29/

[28] Spectrum | Search Results | EIU Astro (wordpress.com): https://jcconwell.wordpress.com/?s=spectrum&searchbutton=go%21

[29] OP-TEC, "Basics of Spectroscopy: Photonics-Enabled Technologies", University of Central Florida, 2008. ISBN: 1-57837-501-0.

[30] Absorption Spectroscopy - What is Absorption Spectroscopy (ibsen.com): https://ibsen.com/technologies/absorption-spectroscopy/#:~:text=Absorption%20spectroscopy%20is%20a%20molecular,of%20the%20optical%20beam%20increases

[31] R. B. Smith, "Introduction to Spectroscopy", 2012, MicroImages, Inc., 1999-2012. https://microimages.com/documentation/Tutorials/hyprspec.pdf

[32] Diffuse Reflectance Spectroscopy (DRS) | Division of Atomic Physics (lu.se): https://www.atomic.physics.lu.se/research/biophotonics/facilities-and-equipment/diffuse-reflectance-spectroscopy-drs/

[33] B. J. Wood and R. G. J. Strens, "Diffuse reflectance spectra and optical properties of some sulphides and related minerals," *Mineral. Mag.*, vol. 43, no. 328, pp. 509–518, 1979, doi:10.1180/minmag.1979.043.328.11.

[34] Beer Lambert Law | Transmittance & Absorbance | Edinburgh Instruments (edinst.com): https://www.edinst.com/us/blog/the-beer-lambert-law/

[35] G. Lu and B. Fei, "Medical hyperspectral imaging: a review," *J. Biomed. Opt.*, vol. 19, no. 1, p. 010901, 2014, doi: 10.1117/1.jbo.19.1.010901.

[36] M. West, J. Grossmann, and C. Galvan, "Commercial Snapshot Spectral Imaging: The Art of the Possible," Mitre Technical Report, The Mitre Corporation, September 2018.

[37] E. Bartick, R. Schwartz, R. Bhargava, M. Schaeberle, D. Fernandez, and I. Levin, "Spectrochemical analysis and hyperspectral imaging of latent fingerprints", *16th Meeting of the International Association of Forensic Sciences*, 2002.

[38] N.J. Crane, E.G. Bartick, R.S. Perlman, and S. Huffman, "Infrared spectroscopic imaging for noninvasive detection of latent fingerprints", *J Forensic Sci*, no. 52, pp. 48-53, 2007. doi: 10.1111/j.1556-4029.2006.00330.x.

[39] D.L. Exline, C. Wallace, C. Roux, C. Lennard, M.P. Nelson, and P.J. Treado, "Forensic applications of chemical imaging: latent fingerprint detection using visible absorption and luminescence", *Journal of Forensic Science*, vol. 5, no. 48, pp. 1047-1053, 2003, PMID: 14535667.

[40] P. Maynard, J. Jenkins, C. Edey, G. Payne, C. Lennard, A. McDonagh, and C. Roux, "Near infrared imaging for the improved detection of fingermarks on difficult surfaces", *Australian Journal of Forensic Science*, vol. 1, no. 41, pp. 43-62, 2009, doi: 10.1080/00450610802172248.

[41] A. Grant, T.J. Wilkinson, D.R. Holman, and M.C. Martin, "Identification of recently handled materials by analysis of latent human fingerprints using infrared spectromicroscopy", *Applied Spectroscopy*, vol. 9, no. 59, pp. 1182-1187, 2005, doi: 10.1366/0003702055012618.

[42] K.S. Kalasinsky, J. Magluilo Jr., and T. Schaefer, "Hair analysis by infrared microscopy for drugs of abuse", *Forensic Science International*, no. 63, pp. 253-260, 1993, doi: 10.1016/0379-0738(93)90278-i.

[43] G. Payne, N. Langlois, C. Lennard, and C. Roux, "Applying visible hyperspectral (chemical) imaging to estimate the age of bruises", *Medicine Science and the Law*, vol. 3, no 47, pp.225-232, 2007, doi: 10.1258/rsmmsl.47.3.225.

[44] Y. W. Wang, N. P. Reder, S. Kang, A. K. Glaser, and J. T. C. Liu, "Multiplexed optical imaging of tumor-directed nanoparticles: A review of imaging systems and approaches," *Nanotheranostics*, vol. 1, no. 4, pp. 369–388, 2017, doi: 10.7150/ntno.21136.

[45] C. L. Stanfield, “Principles of Human Physiology”, San Francisco, Pearson Benjamin Cummings, 5th edition, 2012, ISBN: 0-321-81934-9.

[46] A. J. Marengo-Rowe, “Structure-Function Relations of Human Hemoglobins,” *Baylor Univ. Med. Cent. Proc.*, vol. 19, no. 3, pp. 239–245, 2006, doi: 10.1080/08998280.2006.11928171.

[47] R. H. Bremmer, D. M. de Bruin, M. de Joode, W. J. Buma, T. G. van Leeuwen, and M. C. G. Aalders, “Biphasic oxidation of Oxy-Hemoglobin in bloodstains,” *PLoS One*, vol. 6, no. 7, pp. 1–6, 2011, doi:10.1371/journal.pone.0021845.

[48] HinaLea Imaging, “User Manual: Model 4250 VNIR 4250 System Technical Specifications”.
URL: https://hinaleaimaging.com/wp-content/uploads/2021/10/VNIR-4250-Intelligent-Imaging-System-0720-F2.pdf

[49] Savitzky-Golay filtering - MATLAB sgolayfilt - MathWorks Italia: https://it.mathworks.com/help/signal/ref/sgolayfilt.html#description

[50] http://herschel.esac.esa.int/hcss-doc-15.0/load/sg/html/ch05.fitter.html

[51] Assessing the Fit of Regression Models - The Analysis Factor: https://www.theanalysisfactor.com/assessing-the-fit-of-regression-models/

[52] RMSE: Root Mean Square Error - Statistics How To: https://www.statisticshowto.com/probability-and-statistics/regression-analysis/rmse-root-mean-square-error/

[53] Coefficiente di determinazione R quadro - Paola Pozzolo: https://paolapozzolo.it/coefficiente-determinazione-r-quadro/

[54] Capitolo 14 La regressione non-lineare | Metodologia sperimentale per le scienze agrarie (statforbiology.com): https://www.statforbiology.com/_statbook/la-regressione-non-lineare.html#coefficienti-di-determinazione

[55] Fit curve or surface to data - MATLAB fit - MathWorks Italia: https://it.mathworks.com/help/curvefit/fit.html#bto2vuv-1-gof

[56] Provette per campioni ematici: tipologie e ordine di riempimento (nurse24.it): https://www.nurse24.it/studenti/standard/provette-campione-ematico.html#:~:text=Le%20provette%20con%20EDTA%20sono,stabili%20fino%20a%2024%20ore.

[57] HALOGEN LAMPS - How They Work (mgaguru.com): https://mgaguru.com/mgtech/universal/ut130.htm

[58] Temperature of a Halogen Light Bulb - The Physics Factbook (hypertextbook.com): https://hypertextbook.com/facts/2003/ElaineDevora.shtml

[59] C. D. Elvidge, D. M. Keith, B. T. Tuttle, and K. E. Baugh, "Spectral identification of lighting type and character," *Sensors*, vol. 10, no. 4, pp. 3961–3988, 2010, doi:10.3390/s100403961.

[60] W. J. Moses, J. H. Bowles, R. L. Lucke, and M. R. Corson, "Impact of signal-to-noise ratio in hyperspectral sensor on the accuracy of biophysical parameter estimation in case II waters", *Optics Express*, vol. 20, no. 4, 2012, doi: 10.1364/OE.20.004309.

[61] B. Rasti, P. Scheunders, P. Ghamisi, G. Licciardi, and J. Chanussot, "Noise reduction in hyperspectral imagery: Overview and application," *Remote Sens.*, vol. 10, no. 3, pp. 1–28, 2018, doi:10.3390/rs10030482.

[62] M. Romaszewski, P. G lomb, A. Sochan, M. Cholewa, "A dataset for evaluating blood detection in hyperspectral images", *Forensic Science International*, no. 320, 2021. doi: 10.1016/j.forsciint.2021.110701.

[63] S.S. Kind, D. Patterson, and G.W. Owen, "Estimation of the age of dried blood stains by a spectrophotometric method", *Forensic Science 1*, vol. 1, pp. 27-54, 1972, doi.org/10.1016/0300-9432(72)90146-X.

[64] A. J. Owen, "Uses of Derivative Spectroscopy," *Spectroscopy*, p. 8, 1995.

[65] GraphPad Prism 9 Curve Fitting Guide - Equation: Two phase decay: https://www.graphpad.com/guides/prism/latest/curve-

fitting/reg_exponential_decay_2phase.htm

[66] Evaluating Goodness of Fit - MATLAB & Simulink - MathWorks Italia: https://it.mathworks.com/help/curvefit/evaluating-goodness-of-fit.html

[67] G. Edelman, “Spectral analysis of blood stains at the crime scene”, University of Amsterdam, 2014.